Experimental Investigation of Corrosion Causes on AISI 304 SS Alloy in 3.5% $NaCl_2$ Solution within Steam Autoclave Chamber and Room Temperature

Fikru Alemayehu Desta

A Thesis Summited to Department of Mechanical Engineering
School of Mechanical, Chemical and Material Engineering

Presented in Partial Fulfillment of the Requirement for the Degree of Master's in Manufacturing Engineering

Office of Graduate Studies
Adama Science and Technology University

July,2024

Adama, Ethiopia

Experimental Investigation of Corrosion Causes on AISI 304 SS Alloy in 3.5% $NaCl_2$ Solution within Steam Autoclave Chamber and Room Temperature

Fikru Alemayehu Desta

Advisor: - Dr.Moera Gutu Jiru (Associate Professor)

A Thesis Submitted to Department of Mechanical Engineering
School of Mechanical, Chemical and Material Engineering.

Presented in Partial Fulfillment of the Requirement for the Degree of Master's in Manufacturing Engineering

Office of Graduate Studies
Adama Science and Technology University

July,2024
Adama, Ethiopia

APPROVAL

I, the advisors of the thesis entitled "Experimental Investigation of Corrosion Causes on AISI 304 SS Alloy in 3.5% $NaCl_2$ Solution within Steam Autoclave Chamber and Room Temperature**"** and developed by Fikru Alemayehu Desta, hereby certifies that the recommendation and suggestions made by the board of examiners are appropriately incorporated into the final version of the thesis.

Advisor	Signature	Date

We, the undersigned, members of the Board of Examiners of the thesis by Fikru Alemayehu Desta have read and evaluated the thesis entitled "Experimental Investigation of Corrosion Causes on AISI 304 SS Alloy in 3.5% $NaCl_2$ Solution within Steam Autoclave Chamber and Room Temperature" and examined the candidate during open defense. This is, therefore, to certify that the thesis is accepted for partial fulfillment of the requirement of the degree of Master of Science in Manufacturing Engineering.

Chairperson	Signature	Date
Internal Examiner	Signature	Date
External Examiner	Signature	Date

Final approval and acceptance of the thesis is contingent upon submission of its final copy to the Office of Postgraduate Studies (OPGS) through the Department Graduate Council (DGC) and School Graduate Committee (SGC).

Department Head	Signature	Date
School Dean	Signature	Date
Office of Postgraduate Studies, Dean	Signature	Date

DECLARATION

I hereby declare that this Master Thesis entitled “Experimental Investigation of Corrosion Causes on AISI 304 SS Alloy in 3.5%$NaCl_2$ Solution within Steam Autoclave Chamber and Room Temperature” is my original work. That is, it has not been submitted for the award of any academic degree, diploma or certificate in any other university. All sources of materials that are used for this thesis have been duly acknowledged through citation

_____	_____	_____
Name of the student	Signature	Date

RECOMMENDATION

I, the advisor of this thesis, hereby certify that I have read the revised version of the thesis entitled “Experimental Investigation of Corrosion Causes on AISI 304 SS Alloy in 3.5% $NaCl_2$ Solution within Steam Autoclave Chamber and Room Temperature " prepared under my guidance by Fikru Alemayehu Desta submitted in partial fulfillment of the requirements for the degree of Masters of Science in Manufacturing Engineering. Therefore, I recommend the submission of a revised version of the thesis to the department following the applicable procedures.

_____ _____ _____

Main Advisor Signature Date

ACKNOWLEDGMENTS

First of all, I would like to thank God for this special day and next I would like to express my sincere gratitude to everyone who supported and contributed to the completion of this thesis.

In addition, I am deeply thankful to my supervisor, Dr. Moera Gutu Jiru, for his invaluable guidance, encouragement, and insightful feedback throughout the course of this research. His expertise and unwavering support were instrumental in shaping this study. In addition, I would like to say thank you to my friend Deribe Mangistu, Dabalu Ashetu, and Habtemichael Wude for your invaluable support in everything.

I am grateful to the National Veterinary Institute for providing the necessary facilities and resources for conducting the experiments and analyses presented in this thesis. Special thanks to the engineering maintenance team, production and quality control team for their assistance with sample preparation and experimental setup. I am indebted to my colleagues and fellow researchers at ASTU, whose discussions and feedback enriched my understanding and enhanced the quality of this research. I would also like to thank my family for their love, patience, and encouragement throughout my academic journey. Their unwavering support has been a constant source of strength.

Finally, I extend my heartfelt thanks to all my friends who supported me and provided moral support during the ups and downs of this research endeavor

TABLE OF CONTENT

LIST OF TABLES

LIST OF FIGURES

LIST OF ABBREVIATIONS

$(CH_3)_2CO$	Acetone
AISI	American Iron and Steel Institute
AOD	Argon-Oxygen Decarburization
ASTM G3	Standard for Laboratory Immersion Corrosion Testing
BCC	Body Centered Cubic
BCT	Body Centered Tetragonal
C_{eq}	Chromium Equivalent
cGMPs	Current Good Manufacturing practices
Cl^-	Chloride Ions
DO	Dissolved Oxygen
DSS	Duplex Stainless Steel
ECM	Electrochemical Machining.
FCC	Face-Centered Cubic
g	gram
GMP-	Good Manufacturing Practice
H_2S	Hydrogen Sulfide
HCO_3	Hydrogen Carbonate
HCP	Hexagonal-Close Packed
HPASS	High-Performance Austenite Stainless Steel
kgf	Kilogram Force
mg	Milligram
$NaCl_2$	Sodium Chloride Solution
NH4+	Ammonium Ion
NO^{3-}	Nitrate Ion
NVI	National Veterinary Institute
^oC	Degree Centigrade
OM	Optical Microscopy
PH	Precipitation Hardenable
PREN	Pitting Corrosion Resistance Equivalent Number
PRE*w*	Pitting Resistance Equivalent of Tungsten Involvement
SCC	Stress Corrosion Cracking
SC-CO_2	Supercritical Carbon Dioxide

SCWR	Supercritical Water Reactor
SDSS	Super Duplex Stainless Steel
SEM	Scanning Electron Microscopy
SO_4^-	Sulphite Ion
SS	Stainless Steel
UNS	Unified Numbering System
VOD	Vacuum-Oxygen Decarburization
WHO	World Health Organization
XRD	X-ray Diffraction

LIST OF ACRONYMS

α	Ferrite Phase
δ	Sigma Phase
ϒ	Austenite Phase

ABSTRACT

Stainless steel is material widely used in industry because of their good mechanical and corrosion resistance properties. Although this material is corrosive resistance, when exposed to highly aggressive environment, corrosion affects performance of materials. The objective of this research is to identify the primary causes of corrosion initiation and progression in SS304 within a steam autoclave, with a focus on available machine at National Veterinary Institute (NVI). The methodology involved immersion tests of SS304 samples in pure water, hard water, and sodium chloride ($NaCl_2$) solutions at room temperature and in steam autoclave temperature for 72 hours, 120hurs and 168hours exposure time. Additionally, analysis of corrosion products from samples cut out of the autoclave chamber was performed to study corrosion oxide composition. Analytical techniques such as weight loss measurements, SEM, XRD, and optical microscopy were employed to investigate the corrosion mechanisms. Results indicated that type of solution, its condition, and the duration of exposure all have a significant impact on the corrosion rate and weight loss of SS304. Higher salinity, such as in a 3.5% $NaCl_2$ solution, results in increased susceptibility, with a corrosion rate of 0.0256872 mm/year and a weight loss of 4.32333 mg. On the contrary, soft water and distilled water exhibit lower corrosion rates, indicating higher resistance. Exposure to steam autoclaves notably speeds up corrosion rates, while the length of exposure influences the pattern, initially increasing rates before reaching a stable point. SEM analysis revealed localized pitting corrosion initiation on SS304 samples immersed in 3.5% NaCl solution. XRD analysis identified chloride ions in corrosion products, emphasizing their role in destabilizing the passive film and accelerating corrosion. Samples from the autoclave chamber displayed evidence of pitting and underlining the vulnerability of autoclave components to chloride-induced corrosion. Mitigation strategies include minimizing chloride-containing solutions during sterilization, implementing regular cleaning and maintenance, and considering alternative materials resistant to chloride-induced corrosion for autoclave construction and also offering valuable guidance for enhancing steam autoclave system reliability and longevity in industrial applications like the NVI.

***Keywords**: Steam, Oxidation, pitting corrosion, Corrosion type, Sterilization, Electrolytes, stainless steel*

CHAPTER ONE:

1. INTRODUCTION

1.1 Background of the Research

The continuous evolution of technology has played a vital role of transformative changes in applications of metals and their alloys. Stainless steel, in particular, has gained widespread use due to its admirable corrosion resistance and mechanical strength properties (Gardner, 2019). Notably, AISI 304 stainless steel stands out for its good corrosion resistance, making it a cornerstone material in vital sectors such as pharmaceuticals, food processing machineries, laboratory equipment's, materials in hospitals, and various chemical processing machineries.

Stainless steel is an iron-based alloy material that typically incorporates; chromium, manganese, sulfur, phosphorus, nitrogen, and molybdenum as base constituents, with iron as the balancing element. This alloying process imparts a range of beneficial properties to stainless steel, rendering it versatile for diverse applications across various environmental conditions (Zaffora *et al*., 2021). The strategic combination of different elements with iron enhances materials mechanical and chemical attributes. One of the key advantages of alloyed stainless steel lies in its ability to combine the stiffness characteristic of non-metal elements with the robust strength inherent in iron-based steels (McGuire, 2008). The classification of stainless-steel alloys based on their crystal structure leading to four primary categories; Austenite, Ferrite, Martensitic, and Duplex (Gardner, 2019). Each classification possesses distinct properties that cater to specific engineering requirements.

Commercially stainless steel is available in numerous grades; SS304, SS310, SS316, and SS318 being prominent examples. These grades find extensive application, particularly in the pharmaceutical and food industries, where the unique properties of stainless steel are required to meet regulatory quality and hygiene standards. The following experiment delves into corrosion behavior of a specific grade, AISI 304, within the confines of a steam autoclave chamber, addressing the critical need to compromise and mitigate potential corrosion-related challenges in industrial settings.

AISI 304 stands as a frequently employed stainless steel alloy within steam autoclave chambers owing to its remarkable resistance to corrosion and high temperatures. Comprising 18-20% chromium, 8-10% nickel, and small amounts of molybdenum and nitrogen, this alloy exhibits good corrosion resistance across diverse environments, including those with some concentration of chloride ions (Marcus, 2002). Despite the inherent corrosive resistance of AISI 304 stainless steels, they remain susceptible to corrosion when exposed to

specific environments, such as autoclave chambers. The impact of corrosion on the stainless-steel surface extends beyond mere aesthetic consequences, affecting surface chemical composition, thermal properties, and mechanical attributes, thereby causing the material to operate below its intended capacity (Singh, 2020).

Steam autoclave machines play a pivotal role in various industries such as pharmaceuticals, healthcare and research laboratories in ensuring the sterility of instruments, equipment and materials. It is also known as the heart of biological laboratories for its vital function in sterilizing biological laboratory equipment and solutions. The autoclave utilizes high-pressure steam to achieve sterilization, thereby preventing the spread of harmful microorganisms. Among the materials commonly employed in the construction of steam autoclave chambers, AISI 304 and AISI 316 stainless steel stands out for their renowned corrosion resistance properties. However, despite its widespread use, instances of corrosion on SS304 within steam autoclave environments have been showed, raising concerns about equipment reliability, longevity, and operational safety.

Corrosion constitutes the deterioration of materials over their service life due to oxidation and reduction reactions occurring on the metal surface in corrosive conditions. The consequence of corrosion extends to the structural integrity of materials, overall productivity, product quality, and the economic well-being of nations (Schweitzer,2013; Aslani and Dehestani, 2020; Harsimran *et al*., 2021). In the case of AISI 304, corrosion mechanisms are broadly categorized as crevice corrosion, generalized corrosion, pitting corrosion, and microbiologically influenced corrosion. Corrosion initiates when the electrochemical attachment on the metal surface, acting as a passive layer, undergoes failure over time, initiating reactions with the metal surface in different environmental conditions (Piere, 2008). During the alloying process of metals, energy is introduced to enhance the surface properties of materials. However, when the surface undergoes corrosion, this energy is dissipated, and the affected layer of metals reverts to its original state it had before alloying (Rutala and Weber, 2019). The passivity of stainless-steel materials is influenced by exposure to factors such as pressure, temperature, moisture, acidic solutions, saline solutions and alkaline solutions (Karki and Singh, 2017; Reset *et al*., 2020; Li *et al*., 2021).

Steam autoclave are vital machines within the medical, pharmaceutical, and research sectors, fulfilling the crucial task of sterilization. Their operation relies on core principles; including pre-vacuum, heating, sterilization, cooling, and air break cycles, which are essential for ensuring the effective disinfection of instruments and media or solution (Dion and Parker, 2013). Steam autoclave operates under high-temperature and pressure conditions, typically

reaching up to 134°C and 2 bar, respectively. The autoclave chambers are subjected to continuous exposure to high-temperature steam and sterilization agents. This persistent exposure raises concerns about potential corrosion, a phenomenon that could compromise the performance and safety of the chambers (Boniardi and Casaroli, 2014; Folkhard, 2012).

The predominant material employed in steam autoclave chambers is AISI 304 stainless steel, which is susceptible to corrosion under the harsh conditions of operation. Examining the underlying factors leading to corrosion on AISI 304 within steam autoclave chambers becomes essential to safeguard the chambers' reliability and extend their service life. This investigation holds significant importance not only for sustaining the efficiency of these vital sterilization units but also for advancing the comprehension of material behaviors in rigorous industrial settings

The steam sterilizing autoclave chamber is a crucial machine in numerous pharmaceutical and laboratory setups, often constructed from AISI 304 stainless steel material, rendering it susceptible to corrosion. The ensuing Figure1.1 illustrates the corrosion observed in an autoclave chamber within the pharmaceutical industry at the National Veterinary Institute of Ethiopia, located in Bishoftu

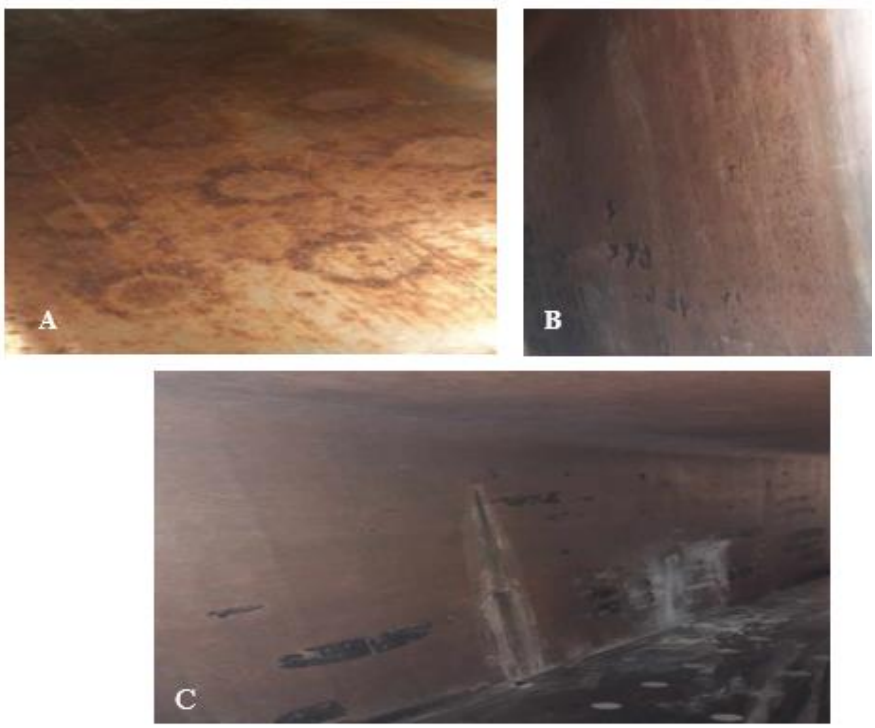

Figure1.1**:** Available working steam autoclave at National Veterinary Institute industry at Bishoftu, Ethiopia;(a) Upper part of chamber, (b) Right side chamber and (c) Left side of chamber (Photo).

Understanding the underlying causes of corrosion on SS304 within steam autoclave chambers is paramount for maintaining the integrity of sterilization processes and ensuring equipment sustainability. Corrosion not only compromises the structural integrity of autoclave components but also poses the risk of contamination, potentially compromising the efficacy of sterilization procedures. Therefore, a comprehensive investigation into the corrosion mechanisms affecting SS304 within steam autoclave environments was done to mitigate these risks and enhance the reliability of sterilization equipment (Gardner, 2019).

This research aim was to investigate the factors contributing to corrosion on SS304 within steam autoclave chambers through a systematic examination of the environmental conditions, material properties, and corrosion processes involved. By identifying the root causes of corrosion, this study proposed effective mitigation strategies and design modifications to enhance the corrosion resistance of SS304 in steam autoclave applications. Furthermore, the insights gained from this research will contribute to the broader understanding of corrosion mechanisms in stainless steel alloys within steam autoclave machine and inform the development of more robust materials and engineering solutions for demanding industrial environments.

1.2 Statement of the Problem

In accordance with world health organization (WHO) manufacturing guidelines, both the pharmaceutical and food industries mandate that production and laboratory equipment should remain free of contaminants and corrosion. Furthermore, in adherence to the protocols outlined in the current Good Manufacturing Practices (cGMPs), all pharmaceutical manufacturing enterprises are required to comply with GMP standards to remain competitive in the global market. Within the scope of cGMP guidelines, it is imperative that all manufacturing equipment remains free from corrosion and contamination. Recently, the National Veterinary Institute has decided to adopt current Good Manufacturing Practices (cGMP) in their production and quality systems to enhance their competitiveness in the global market. Figure 1.1 clearly depicts the current situation of steam autoclave chamber. The figure shows that is high corrosion effect in the chambers. Despite the prevalent utilization of SS304 in autoclave construction, a significant knowledge gap exists concerning the corrosion mechanisms within these steam-rich environments. The intricate interplay of temperature, pressure, and steam composition poses distinctive challenges that necessitate through investigation.

1.3 Motivation of the Research

Recently, the National Veterinary Institute has planned to implement current Good Manufacturing Practice (cGMP) in their production and quality systems to become competitive in the global market. While working at this company for eight years. It was realized that corrosion could hinder the company from achieving its goals. Although the institute provides training on applying cGMP, it has not acknowledged the impact of corrosion on their long-term objectives. Among the machinery used in the factory, the causes of corrosion in the steam autoclave chamber were revealed.

The driving force behind this research is the essential need to fully understand and address the factors contributing to corrosion in SS304 within steam autoclave environments. This issue not only threatens the longevity of the autoclave components but also poses potential risks of product contamination and compromised structural integrity, which can affect both product quality and industrial safety. By examining the intricacies of corrosion within the autoclave chamber, these research aims to gain essential insights into the mechanisms and environmental factors influencing the corrosion of SS304. Overall, this research was motivated by the pressing need to address corrosion challenges in SS304 within steam autoclave chambers.

1.4 Objectives of the Research

1.4.1 Main objective

The main objective of this research is experimentally investigating causes of corrosion on AISI 304 SS alloy in 3.5% $NaCl_2$ solution within steam Autoclave chamber and room temperature. The study aim was to contribute valuable insights into the underlying mechanisms and environmental factors influencing the corrosion of SS304, a material widely employed in the construction of autoclaves for various industrial applications.

1.4.2 Specific objectives

In order to achieve the above objective, the following specific objectives were designed:

1. To investigate the cause of corrosion on SS304 surfaces within the autoclave chamber.
2. To analyze the effect of process parameters of steam autoclave like temperature, pressure and steam impurities on corrosion of SS304.
3. To characterize corrosion morphology using optical microscopy (OM), scanning electron microscopy (SEM) and XRD for phase analysis.
4. To investigate the effect of different corrosive environments (pure water, hard water, 0.5%$NaCl_2$ solutions, 3.5%$NaCl_2$ solutions) both at room condition (25^{o}c and at 1

atmosphere pressure) and at steam autoclave conditions on corrosion rate and surface hardness of SS304

5. To propose effective corrosion mitigation methods, depend on the root causes.

1.5 Significance of the Research

Understanding the causes of corrosion in SS304 within steam autoclave chambers is of paramount importance for industries relying on autoclave technology. This research not only contributes to the fundamental understanding of materials behavior but also offers practical insights for optimizing autoclave performance, ensuring equipment integrity, and minimizing maintenance costs. Research on "experimental investigation of corrosion causes on AISI 304 SS alloy in 3.5% NaCl solution within steam Autoclave chamber and room temperature" holds significant importance for following reasons:

a. Equipment reliability and safety

Autoclave chambers are widely used in various industries for sterilization and material processing. Understanding the causes of corrosion in SS304 within these chambers is crucial for ensuring the reliability and safety of the equipment. Corrosion can compromise the structural integrity of the autoclave, leading to equipment failure and potential safety hazards.

b. Material selection and design improvement

Insights gained from the research can contribute to the selection of appropriate materials for autoclave construction. Understanding the specific corrosion mechanisms acting on SS304 within the autoclave environment can inform the development of improved materials or coatings that better resist corrosion under these conditions. This, in turn, can lead to more durable and corrosion-resistant autoclave systems.

c. Cost savings

Corrosion-related failures can result in significant repair or replacement costs for autoclave equipment. Through the identification of the fundamental causes of corrosion and the implementation of preventive measures, industries have the opportunity to reduce maintenance and replacement costs significantly. This research can provide cost-effective strategies for extending the service life of autoclave systems.

d. Advancements in materials science

The study of corrosion mechanisms in SS304 within autoclave chambers contributes to the broader field of materials science. Findings from this research can advance our understanding of corrosion-resistant materials and mechanisms, potentially leading to innovations in material design for various applications beyond autoclave systems.

Finally, investigating the causes of corrosion in AISI SS304 within autoclave chambers is essential for ensuring the reliability, safety, and efficiency of industrial processes. The findings have practical implications for material selection, design improvement, and operational optimization, ultimately benefiting industries that rely on autoclave technology.

1.6 Scope and Limitation of the Research

1.6.1 Scope of the research

This research aims to investigate the causes of corrosion in SS304 within a steam autoclave chamber, focusing on identifying the key factors that contribute to corrosion initiation and progression. The study encompasses several specific objectives: First, the preparation and experimental setup involve preparing SS304 material specimens as flat coupons with standardized dimensions. A laboratory-scale autoclave chamber constructed from SS316 stainless steel, with controlled temperature and pressure systems, is utilized to simulate industrial steam autoclave conditions.

The exposure conditions include immersing SS304 specimens in various corrosion-inducing solutions, such as 0.5% sodium chloride solution, 3.5% sodium chloride solution, deionized pure water, and groundwater samples, to simulate different environmental conditions at room temperature. The specimens are subjected to steam autoclave conditions at a typical operational temperature of 121°C and a pressure of 1.5 bar for specified durations ranging from 72 hours to 168 hours.

To monitor corrosion behavior, weight loss measurements are applied to assess the severity of corrosion over time. Additionally, surface analysis using scanning electron microscopy (SEM) and X-ray diffraction (XRD) is performed to investigate the surface morphology and chemical composition of the corroded specimens. The metallographic microstructure is also examined using an optical microscope.

Corrosion rates are calculated by analyzing the weight loss data relative to the duration of exposure to the corrosive conditions. The hardness of the samples after exposure to various conditions is also evaluated. The study aims to assess the influence of temperature, pressure, and solution chemistry on the corrosion behavior of SS304, comparing corrosion rates and surface morphologies of specimens exposed to different conditions to identify the key factors contributing to corrosion.

1.6.2 Limitations of the research

- Conducting experiments or simulations to replicate corrosion conditions in autoclave chambers was challenging due to the complexity of environmental factors and the need for specialized equipment.

- The study focuses primarily on corrosion causes within the autoclave chamber itself, overlooking potential external factors that could contribute to corrosion, such as the condition of material being sterilized and surrounding environmental conditions.
- Findings from the investigation of the thesis is specific to the particular autoclave chamber located at the national veterinary institute and cannot directly applied to other contexts.

1.7 Organization of the Thesis

This thesis is documented basically on investigation of causes of corrosion on SS304 material within the steam autoclave chamber located at the national veterinary institute in Ethiopia. The thesis organized by five chapters and the content of each chapter's presents in the following manner.

At first section introduction of research is incorporated in chapter one. This section of the report provides background information, emphasizing the significance of studying corrosion in SS304 within steam autoclave chambers. It highlights the importance of this research in maintaining the integrity and longevity of equipment and ensuring the safety of processes in various industries. Additionally, the section defines the research objectives, emphasizing the need to identify the factors contributing to corrosion. The significance and scope of the study are also outlined, with a focus on contributing to the existing body of knowledge on corrosion in SS304 within steam autoclave chambers. Finally, the structure of the thesis is outlined, providing a roadmap for the reader to navigate through the subsequent chapters and sections of the report.

Next to introduction the literature review of paper is included in chapter two. The literature review section of this thesis provides a comprehensive overview of corrosion mechanisms, factors influencing corrosion in SS304, and previous studies related to corrosion in steam autoclave environments. It examines relevant scholarly works to establish a theoretical framework for the research. The review looked into various corrosion mechanisms, such as pitting, crevice corrosion, and stress corrosion cracking, exploring how these mechanisms manifest in SS304 under steam autoclave conditions. Additionally, it discusses the key factors influencing corrosion, including temperature, pressure and the presence of aggressive ions (Cl^- ions). By synthesizing existing literature, this section aims to establish a solid foundation of knowledge upon which the current study builds, contributing to a deeper understanding of corrosion behavior in SS304 within steam autoclave environments.

In addition, Material and Methodology also included in chapter three. The methodology section of this thesis provides a detailed description of the experimental setup used to

investigate corrosion in SS304 within steam autoclave chambers. It outlines the specifications of the autoclave chamber, including temperature, pressure, and other relevant parameters. Details regarding the preparation and selection of SS304 specimens are provided, along with information on exposure scenarios and corrosion monitoring techniques employed throughout the study. The section offers a step-by-step account of the experimental procedures followed, from specimen preparation to exposure to the autoclave environment and subsequent corrosion monitoring. Additionally, it discusses any validation processes, quality control measures, and ethical considerations undertaken to ensure the reliability and integrity of the experimental data. This comprehensive methodology aims to provide transparency and reproducibility, ensuring the rigor and validity of the research findings.

On next part of the section result discussion is included in chapter four. The findings section of this thesis presents the results of the corrosion investigation conducted on SS304 within steam autoclave chambers. Experimental data, including corrosion rates, electrochemical measurements, weight loss measurements, and surface analysis results, are meticulously documented and analyzed. The data are effectively illustrated using tables, figures, and graphs, facilitating clear interpretation and understanding. The results are interpreted and analyzed in the context of the research objectives, with a focus on identifying patterns, trends, and correlations observed in the data. Furthermore, the implications of the findings are discussed, and comparisons are made with previous studies to provide additional context. Any limitations or discrepancies encountered during the research are also addressed, ensuring a comprehensive and transparent presentation of the research outcomes.

At last conclusion and recommendation parts is incorporated in the thesis. The conclusion of this study summarizes its main findings, emphasizing their significance in the context of mitigating corrosion and enhancing the performance of SS304 materials in steam autoclave environments. It reiterates the research objectives and highlights the key contributions of the research, providing a comprehensive overview of the study's outcomes. Additionally, the conclusion suggests avenues for future research and areas requiring further investigation, contributing to the ongoing development of corrosion mitigation strategies.

CHAPTER TWO:

2. LITERATURE REVIEW

2.1 Introduction

Stainless Steel 304 has developed widespread use in various industrial applications due to its good corrosion resistance properties. Nevertheless, its performance within autoclave chambers introduces a distinctive set of challenges. This literature review aims to offer an encompassing view of prior research endeavors concerning the causes of corrosion in AISI SS304 within autoclave environments. Through an exploration of existing literature, this review aims to elucidate key findings, identify research gaps, and underscore the paramount importance of comprehensively addressing this corrosion-related issue

2.2 Stainless Steel Materials and Its Classifications

In the early 1970s, the invention of new steel refining and casting technologies facilitated the advancement of stainless steel from its existing stage to high-performance austenite stainless steel (HPASS) grades. These advancements in steel-making technology included the implementation of processes such as argon-oxygen decarburization (AOD) and vacuum-oxygen decarburization (VOD). These processes were utilized to achieve economically feasible low carbon content, high alloy recovery, and better composition control in stainless steel production. Stainless steels are often selected for specific applications due to their exceptional corrosion resistance, despite being characterized by relatively limited wear resistance and surface motion properties (Weidmann *et al*.,2005).

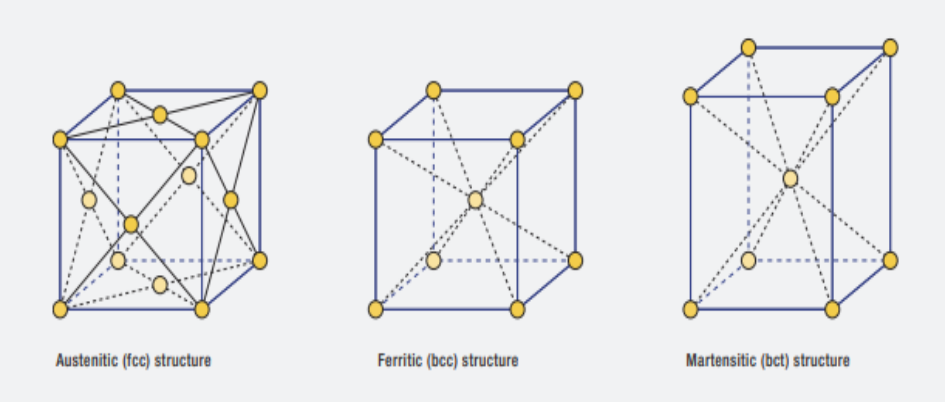

Figure 2.1: Crystal structure of austenite, ferritic and martensitic (Cladera *et al*., 2014).

The classification of stainless steels is based on their crystallographic microstructure, resulting in categories such as austenitic, martensitic, ferritic, duplex, and precipitation hardenable. Figure 2.1 and Figure2.2 indicates different categories of crystal structure of materials. Ranging from austenite to duplex stainless steel, these materials undergo various

alloying and different treatment processes to enhance corrosion resistance, mechanical properties and physical properties (Cladera *et al*., 2014).

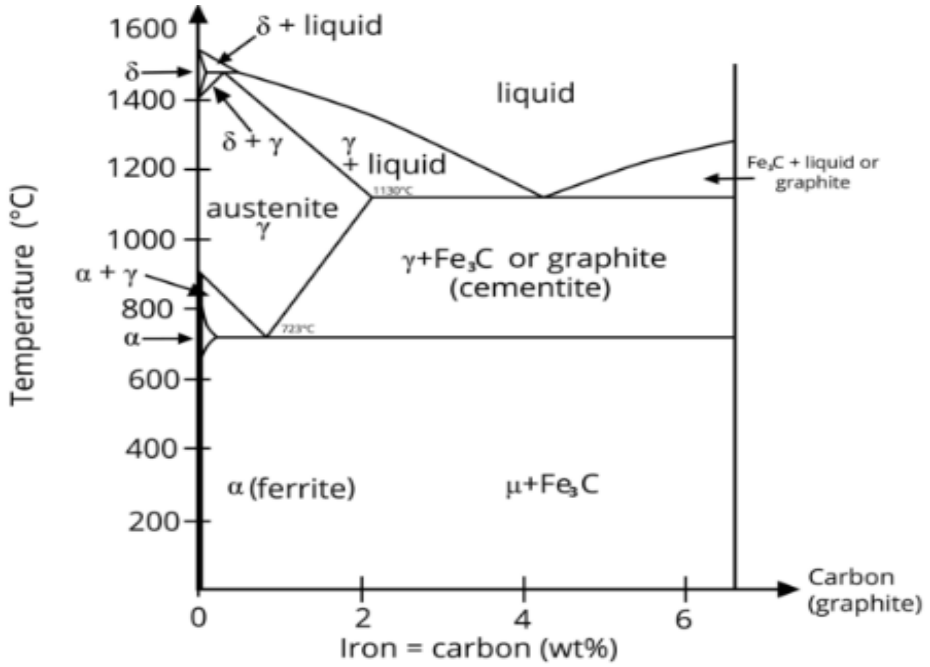

Figure 2.2: Carbon iron-carbon phase diagram (Cladera *et al*., 2014).

The various types of stainless-steel materials are designated according to the AISI system or UNS and are readily available in the market. Notably, AISI 304 or UNS S30400, one of commercially available stainless steels, is specifically chosen for its corrosion resistance in various corrosive environments. The composition of most types of stainless-steel materials, along with their characteristics and the importance of different categories of elements in various types of corrosion mechanisms, is shown in Figure 2.3.

2.2.1 Martensitic stainless steel

Martensitic stainless steels are body centered tetragonal (BCT) and body centered cubic (BCC) structure with least corrosion resistance among the types of stainless steel. Martensitic phase of body centered tetragonal structure is obtained by austenitizing during heat treatment of steel in temperature range of 970^{o}C – 1100^{o}C followed by oil quenching which affects mechanical toughness and ductility properties of materials. Tempering of the material in the temperature range of 200^{o}C-700^{o}C is preventing formation of brittle materials. Application of this material is limited to less aggressive corrosive environments and has extensive usage in wear resistance areas.

Compared to other stainless steel it has higher mechanical strength properties due to high carbon content and addition of nitrogen (Folkhard, 2012). Sometimes sulfur is added to

improve machinability and alloyed with nickel in fewer amounts to improve its weld ability. Grain structure of martensite SS material is clearly shown in Figure 2.3.

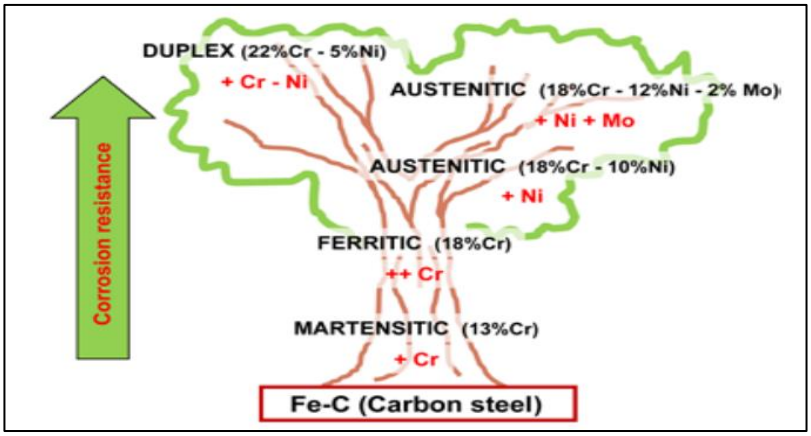

Figure 2.3: Stainless steel classification tree (Boniardi and Casaroli, 2014).

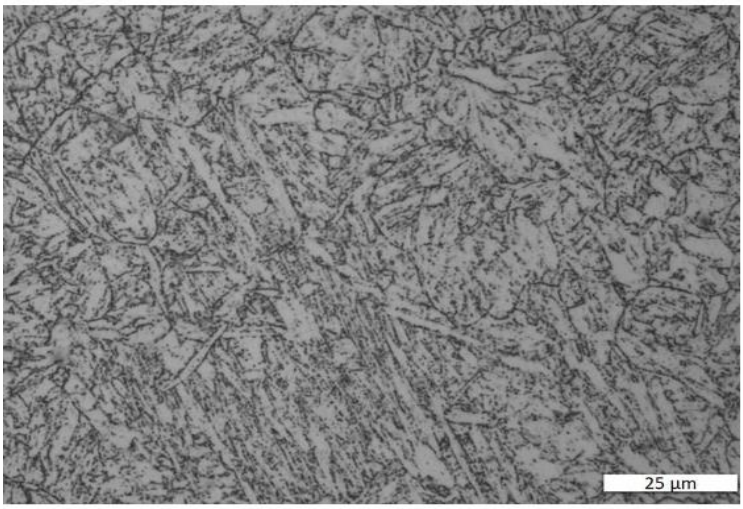

Figure 2.4: Martensitic grain structure of stainless-steel materials (Weidmann *et al.*, 2005).

2.2.2 Ferritic stainless steel

Ferritic stainless steel is body-centered cubic (BCC) crystal structure material which contains chromium as corrosion resistance and some small amount austenite forming element, such as nitrogen, carbon and nickel. Ferritic contains 11% to 30% of chromium (Cr) to improve its corrosion passivity against corrosive environments (Tuthill and Covert, 2000). Additionally, titanium (Ti) and niobium (Nb) are incorporated to improve its resistance to intergranular corrosion, particularly by counteracting the influence of chromium carbide at grain boundaries in chloride-rich environments (Rovere *et al.*, 2012).

2.2.3 Austenite stainless steel

Austenitic stainless steel exhibits a non-magnetic face-centered cubic (FCC) crystal structure, similar to iron at high temperatures, and is widely used in various industrial applications due to its excellent corrosion resistance. Nickel is the primary stabilizing

element in these types of stainless steel, along with nitrogen and carbon, owing to their solubility in the FCC structure. The corrosion resistance of austenitic stainless steel is achieved through the alloying of elements such as molybdenum (Mo) and chromium (Cr) with nickel (Ni), manganese (Mn), and nitrogen (N), in combination with iron as the balancing element. The addition of manganese is crucial in increasing nitrogen solubility and preventing martensitic transformations, thereby forming carbides at grain boundaries (Rovere *et al*., 2012). Additionally, nitrogen addition in the alloy enhances its mechanical strength.

The austenitic stainless steel undergoes heat treatment by annealing at temperatures ranging from 1000°C to 1100°C. This process aims to reduce the effects of cold work by improving recrystallization, thereby controlling grain size and dissolving precipitated carbides at grain boundaries. Initially, austenitic stainless steel forms ferrite after solidification and subsequent cooling to room temperature, which is later dissolved during the normal processing stages and forms austenite. The Schaeffer diagram, shown in the Figure 2.5, clearly illustrates the percentage of ferrite formation, as determined by the following equation:

$$\%\text{Ferrite} = 3(\text{Cr} + 1.5\text{Si} + \text{Mo}) - 2.8(\text{Ni} + 0.5\text{Mn}) - 84(\text{C} + \text{N}) - 19.8\% \quad (2.1)$$

Whereas the Creq (Chromium equivalent) and Nieq (Nickel equivalent) are calculated using the equations:

$$\text{Creq} = \%\text{Cr} + 1.37\%\text{Mo} + 1.5\%\text{Si} + 2\%\text{Nb} + 3\%\text{Ti} \quad (2.2)$$

$$\text{Nieq} = \%\text{Ni} + 0.31\%\text{Mn} + 22\%\text{C} + 14\%\text{N} + \%\text{Cu} \quad (2.3)$$

Carbon, as an impurity in austenitic alloys, forms carbide precipitates at grain boundaries if not properly controlled to remain in solid solution. The formation of carbide precipitates adversely affects corrosion resistance by inducing sensitization. Sensitization increases when the carbon concentration exceeds 0.03%, whereas alloying with nitrogen and manganese helps mitigate sensitization (Duan *et al*.,2022).

Austenite stainless steel surface forms shields against corrosive environment due to its passive property formed by oxidation of chromium elements in the oxidizing environments. The passivity of austenite stainless steel varies when percentage of chromium element composition of material is changed. These stainless-steel alloys are primarily designed to resist localized corrosion, such as pitting and crevice corrosion, and their resistance depends on the chemical composition of alloying elements. For alloy of stainless-steel materials, pitting corrosion resistance capacity is determined by PREN (pitting Corrosion Resistance Equivalent Number) and which is dependent on the composition of chromium, molybdenum

and nitrogen in the alloy. To determine PREN equation 2.4 empirical formula was employed by various corrosion engineers and many industry experts and researchers. As shown in Figure 2.5 the eutectic line, alloys solidify in the preferred austenitic mode, below the eutectic line; alloys solidify in the preferred ferritic mode

$$PREN = \%Cr + 3.3(\%Mo) + 16(\%N) \quad (2.4)$$

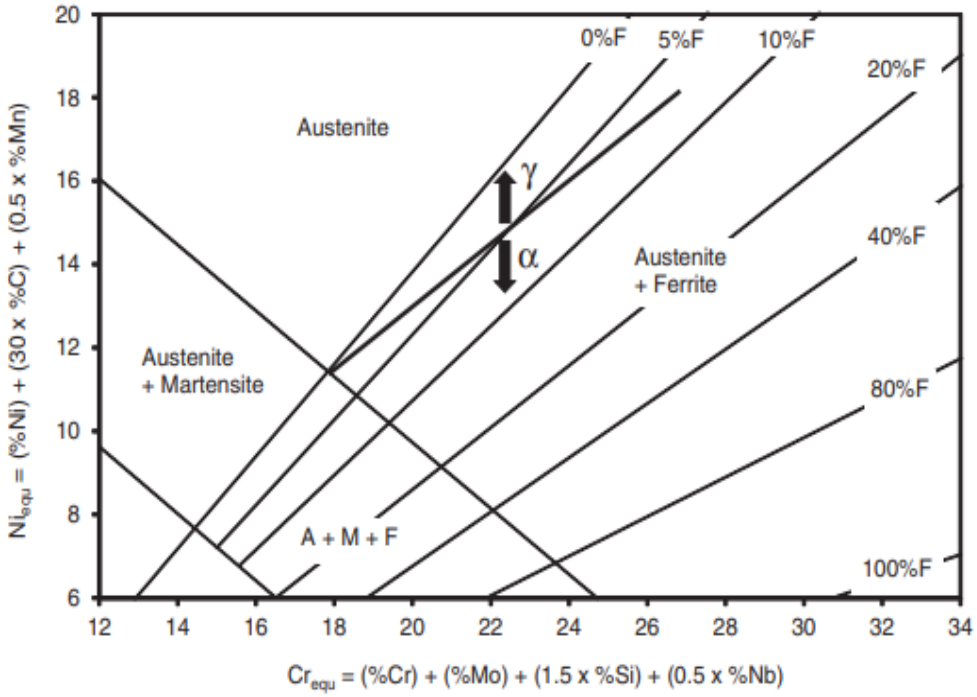

Figure 2.5: Modified Schaeffer diagram with eutectic solidification line (Raghavan and Antia, 1994).

2.2.3.1 Role of alloying element in austenite stainless steel

The chemical composition of alloying elements has a significant impact on stainless steel metallurgy, crystal structure, mechanical properties, aesthetic properties, and resistance to corrosion. Alloying elements such as molybdenum, chromium, and nickel replace iron at the crystal lattice corners and face centers, while nitrogen and carbon occupy the spaces between these elements. Carbon and nitrogen contribute to the hardening of the alloy, but when situated in these interstitial spaces, they create lattice strain. Below, the importance of each element is discussed in detail (Odette and Zinkle, 2019). Activities of different categories of alloying elements in austenite stainless steel are described in following manner:

a) **Chromium (Cr):** Chromium is an alloying element crucial for creating the passive film in stainless steel, thereby imparting its stainless properties. Stainless steel typically contains chromium levels ranging from 11% to 30%, with standard stainless-steel

compositions falling between 11% Cr and 18% Cr, while high-passivity stainless steel (HPASS) contains chromium levels ranging from 20% to 30%, enhancing corrosion resistance.

b) **Nickel (Ni):** Nickel serves the purpose of forming the austenite structure and stabilizing it, thereby enhancing the material's resistance to corrosion, particularly in reducing acids and stress corrosion cracking. Nickel content in HPASS alloys can reach up to 20%.

c) **Molybdenum (Mo):** Molybdenum is added to stainless steel alloys to improve resistance to pitting and crevice corrosion in chloride environments, working synergistically with chromium and nitrogen. It also provides corrosion resistance against reducing environments such as hydrochloric acid and dilute sulfuric acid. Molybdenum is typically added in concentrations ranging from 2% to 7.5%.

d) **Carbon (C):** Carbon contributes to stabilizing and strengthening the austenite phase formed, making it suitable for high-temperature applications. Austenitic stainless steel typically contains carbon levels below 0.03%, with effectiveness increasing at lower levels.

e) **Nitrogen (N):** Nitrogen is alloyed in stainless steel up to 0.5% to strengthen and stabilize the austenite phase and retard the formation of secondary phases, reducing carbide sensitization at grain boundaries. Nitrogen is particularly effective in preventing pitting and crevice corrosion in chloride environments.

f) **Manganese (Mn):** Similar to nitrogen and carbon, manganese acts as a stabilizer in austenitic stainless steel, increasing nitrogen solubility to improve strength and corrosion resistance. Additionally, manganese aids in deoxidizing molten steel to reduce residual elements in stainless steel.

g) **Copper (Cu):** Copper is added as an alloying element to enhance corrosion resistance in reducing acids in stainless steel.

h) **Silicon (Si):** Silicon is included as an alloying element in austenitic stainless steel to improve resistance in concentrated acids and highly oxidizing environments. Like manganese, silicon serves as a deoxidizer in molten steel to reduce residual elements.

i) **Niobium (Nb) and Titanium (Ti):** Niobium and titanium are added to stainless steel to lower carbon content by forming strong carbides, thereby preventing sensitization effects and improving strength at high temperatures. They also serve as deoxidizers and are found in small amounts as residual elements.

j) **Sulfur (S) and Phosphorus (P):** Sulfur aids in resisting pitting by forming manganese sulfide and improving machinability but can detrimentally affect hot workability.

Phosphorus must be limited due to its detrimental effects on hot workability during forging and rolling and its promotion of hot cracking during cooling after welding.

2.2.3.2 Mechanical and physical property of austenite stainless steel

One big point that needs to be raised here is that austenite stainless steel cannot be hardened by heat treatment, but when there is an area where strength is required, it can be hardened by using various methods. According to research conducted at Outokumpu research center for unstable austenite cold working which is rolling-annealing-pickling method have found good applications and by the method of solid solution strengthening from substitution element and interstitial addition of nitrogen and carbon (Schweitzer, 1996). When the physical property of austenite is considered all have the same property, but when compared to the carbon steel it has lower young's modulus, lower thermal conductivity and higher coefficient of thermal expansions.

2.2.4 Duplex stainless steel

Duplex stainless steel is the material processed by combining both austenite and ferrite structure and contains (18%-28%) chromium and (4.5%-8%) nickel with ≤4%molybdenum content to improve its passivity level against stress corrosion cracking. Additionally, its mechanical strength property, welding and formable properties of metals are improved relatively (Francis and Byrne, 2021).

Furthermore, table 2.1 shows the summary of effect of alloying element in stainless steel process.

2.2.5 Precipitation hardenable stainless steel

Precipitation-Hardenable (PH) stainless steel comprises chromium-nickel alloy along with aluminum, copper, titanium, and niobium. These elements facilitate the hardening process through a solution and aging heat treatment conducted at approximately 725°C, following annealing at temperatures surpassing 1000°C (Mariani *et al*., 2016). This stainless steel has high mechanical strength, relatively good ductility, and good corrosion resistance at moderate temperatures; making it applicable in modern aircraft structural components, pump covers, bolts, and knives are the most area of application for this material (Villegas-Tovar *et al*.2023). Depending on the solution-annealed microstructure, PH stainless steel is classified as austenitic, semi-austenitic, or martensitic, forming intermetallic compounds.

Precipitation-hardenable stainless steels maintain their mechanical strength and corrosion resistance due to increments of chromium, nickel, and molybdenum at low carbon content. The mechanical properties of PH martensitic steel can be improved by heat treatments.

According to research findings on 15-5PH stainless steel, the precipitation of copper and the resulting strain around the copper particles during the aging process improve the mechanical

Table2.1: Effect of alloying element in duplex stainless steel (Liou et al., 2001).

Element in Alloy	Effect in the Alloy	Changes in Duplex Stainless-Steel Metallurgy
Nickel (Ni)	Austenite stabilizer	- The composition of Ni in DSS/SDSS is intermediate, typically around 4-7%. - Addition of Ni prevents the formation of detrimental intermetallic phases in austenitic stainless steel.
Nitrogen (N)	Austenite stabilizer	- Added to prevent the formation of sigma phase by Cr and Mn. - Increases resistance to pitting and crevice corrosion.
Manganese (Mn)	Austenite stabilizer	- Increases N solubility in austenitic stainless steel and stabilizes austenite.
Copper (Cu)	Austenite stabilizer	- Maximum content is up to 2%. - Reduces cavitation erosion.
Chromium (Cr)	Ferrite stabilizer	- Enhances corrosion resistance. - Duplex stainless steel is more corrosion resistant than ferritic and 304/316 stainless steels.
Molybdenum (Mo)	Ferrite stabilizer	- Improves chloride corrosion resistance in conjunction with chromium.
Silicon (Si)	Ferrite stabilizer	- Enhances resistance to oxidation at high temperatures in stainless steel.
Tungsten (W)		- Increases Pitting Resistance Equivalent (PRE*w*).
Titanium and Niobium (Ti & Nb)	Ferrite stabilizer	- Binds carbon and forms carbides, preventing chromium from forming harmful chromium carbides at grain boundaries.
Sulfur (S)	Impurity	- Improves machining properties. - Among detrimental elements, sulfur has the worst effect.

DSS = Duplex Stainless Steel, SDSS = Super Duplex Stainless Steel

$(PREN = Pitting\ Resistance\ Equivalent\ (\%Cr + 3.3x\%Mo + 16x\%N)$ (2.5)

$(PREW = C\ r\% + 3{,}3x(Mo\% + 0{,}5W) + 16\%N)$ (2.6)

strength and hardness of PH stainless steel, thereby affecting machining parameters, such as increased cutting force for heat-treated PH (Palanisamy *et al*., 2016; Wang *et al*., 2018; Zhou *et al*., 2018; Ravitej, *et al*., 2018). Copper particles incorporated into the precipitation hardening process of martensitic stainless steel enhance strain coherency and crystalline size, consequently improving its mechanical strength (Bahmani Oskooee *et al*., 2018; Ye *et al*., 2012; Hauser *et al*., 2023; Huang *et al*., 2023).

2.3 Properties of SS304

AISI 304 (UNS30400) is an austenite type of stainless-steel material which is commercially applicable in various environments due to its good mechanical strength and prominent corrosion resistance properties. The SS material undergoes an alloying process, a highly effective method utilized to enhance its properties. Recently SS material undergoes continuous refinement of its material properties through alloying processes and one of prominent variants is SS304, classified as an austenitic type of stainless steel. SS304 is produced by incorporating elements such as chromium, nickel, manganese, phosphorus, silicon, sulfur, with iron serving as the base material in the alloying material. The alloyed chemical composition of SS304 includes Cr (18% - 20%)Wt, Ni (8% - 10%), C ≤0.08%, Mn≤2%, P≤0.045%, S ≤0.03%, Si≤1%, and with iron as the balancing element (Boniardi and Casaroli, 2014).

Alloying chromium material is required to create a barrier layer of stainless steel against different forms of corrosions. Chromium exhibits instability upon exposure to oxygen, leading to the formation of a thin film oxide layer on the metal surface. This chromium oxide layer is highly stable, acting as a barrier against further oxidation and rendering the steel layer against corrosion (Shoemaker and Crum 2000). Augmentation of chromium content in the stainless-steel alloy results in the formation of a stable oxide film layer thereby enhancing corrosion resistance against aggressive environments.

Furthermore, addition of molybdenum and nickel to the alloys enhances the stability and adherence of the oxide film to the underlying steel materials respectively. Recently various researchers incorporate nitrogen (N) and molybdenum as one of the effective elements for stabilizing the oxide layer. This contributes to the stability of stainless steel against various forms of corrosion such as crevice corrosion, stress corrosion cracking, pitting corrosion, and intergranular corrosion, especially at elevated temperatures.

2.3.1 Austenite structure of SS304 and its effect on corrosion resistance

In the solidification process, both metals and nonmetals typically adopt a crystalline structure. This structure entails the orderly and repetitive arrangement of atoms or ions across the entire surface, forming a lattice. Metals commonly exhibit three types of crystal structures: face-centered cubic (FCC), body-centered cubic (BCC), and hexagonal-close packed (HCP) structures. Austenitic stainless steel, for instance, is characterized by its FCC lattice structure during the recrystallization process to room temperature. As shown in Figure 2.6 for a visualization of the FCC lattice arrangement in the metallic structure of austenitic stainless steel.

Crystallographic property of material is affected by the property of grain size, composition of microstructure content, types of formed phase and carbide distribution along grain boundaries. According to various experiments done on corrosion resistance of material with respect to grain size shows microstructure grain size is inversely proportional to corrosion resistance potential (Liu *et al*., 2023; Alharbi et al., 2024). During grain size increases the chemical activity of the grain boundary is activated and increases chemical reaction of materials (Soleimani *et al*., 2020). According to literature done on carbide precipitation, chromium or iron forms chromium carbide or iron carbide when carbon is not in the form of

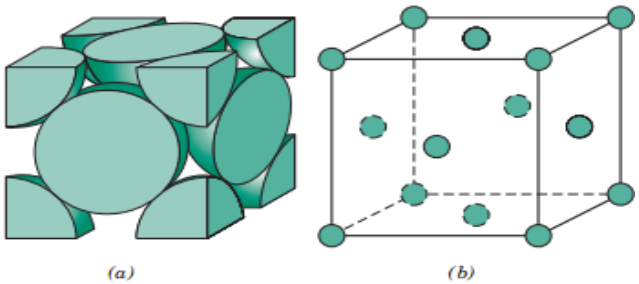

Figure 2.6: FCC structure, (a) Hard sphere unit cell representation, (b) Reduced-sphere unit cell (Xiong *et al*., 2018).

solid solution. This precipitates carbon on grain boundaries of SS304 materials and makes the surrounding depletion of chromium due to chromium diffusion to form carbides at grain boundary. Depletion of chromium creates electrolyte difference in the layer and forms intergranular corrosion during high temperature exposure and oxidation (Elmquist and Hartland 2016).

Addition of elements such as nitrogen, titanium, boron and niobium to the alloy of austenite FCC structure stainless steel improves both mechanical property and corrosion resistance by enhancing its microstructure (Ali *et al*., 2022). Not only addition of element, but distortion of grain arrangement, which is dislocation and twinning method affects microstructure

property of material to improve intergranular corrosion resistance (Guide, 2013). According to various research done recently, twinning is becoming the favorable process to improve mechanical strength of material in which its grain structure develops large size grain twinning (Yuan *et al*., 2023; Zhang *et al*., 2019).

2.3.2 Passivity of SS304

The passive layer of SS304 plays a crucial role in stainless steel corrosion resistance. The protective surface layer of stainless steel, often referred to as the passive layer, is composed of a thin film of chromium oxide or chromium hydroxide which is formed When exposed to oxygen in the atmosphere or in an oxidizing environment and the chromium present in the alloy reacts with the oxygen to form a thin layer of chromium oxide or chromium hydroxide on the surface of the steel. This layer serves as a barrier, offering protection against corrosion. It effectively shields the underlying steel bulk layer from external reactive environments and prevents the penetration of corrosive agents such as corrosive water, chloride ions, and other chemicals due to its stability against oxidizing environments. This upper surface of AISI 304 remains stable against corrosive agents and can quickly regenerate its protective oxide film in the presence of oxygen or other oxidizing agents. The addition of molybdenum in small amounts prevents the breakdown of passive films by chloride ions (Malik *et al.*, 1992; Simionescu and Benea, 2017; Rahman *et al.*, 2018).

The passive layer developed on stainless steel alloys, including SS304, and other stainless-steel metals enhances corrosion resistance. The strength of corrosion resistance provided by the stainless-steel passive film depends on the passive film compositions, formed layer thickness, and microstructure forms. Various studies conducted by researchers, during the formation of passive films, some halogens delay the dissolution of the layer, which increases its thickness. Improving the thickness of the corrosion barrier layer enhances the corrosion erosion resistance of SS materials and provides consistent protection against corrosion in a wide range of environments, including marine areas, chemical solutions, and industrial processing areas. Two types of ideas regarding passive layer structure have been raised, one suggesting a three-layer structure and the other describing a two-layer structure. According to the former, there is an outer, middle, and interior layer composed of chromium oxide and hydroxide at the outer layer, nickel oxide and iron sulfide at the middle layer, and iron oxide structured during the addition of chromate. According to the latter, there is a double layer, with the outer layer composed of chromium oxide and the inner layer containing nickel hydroxide, molybdenum hydroxide, chromium hydroxide, and iron hydroxide as compositions. Without this passive layer, stainless steel would be much more susceptible to

corrosion and degradation (*Marcus and Oudar, 2002*; Meguid *et al.*, 1998). While SS304 exhibits resistance to corrosion, its passivity can be compromised in harsh environments, leading to gradual dissolution of the protective layer. Research indicates a progression of passive layer breakdown characterized by three stages: pit initiation, metastable pit growth, and stable pit growth. High concentrations of chloride ions (Cl-) are known to locally attack the passive layer, eventually causing complete dissolution. Moreover, as the concentration of chloride ions increases, their aggressive action on the passive layer intensifies, although at lower concentrations, the passive layer thickens and becomes more stable. Simultaneous exposure to multiple halogens further accelerates the breakdown of the passive layer. Combined ion exposure, including Cl-, NO3-, H2S, HCO3-, SO4-, NH4+, and other halogens, promotes the dissolution of the passive film, exacerbating corrosion of the stainless-steel substrate. Additionally, hydrogen diffusion, as reported in various studies, elevates the passive current density and reduces the pitting potential of stainless steel, rendering it more susceptible to various forms of corrosion (Parangusan *et al.*, 2021).

The passivity of stainless steel can be improved by affecting the chemical composition of alloys, which is used to enhance corrosion resistance in various environments.

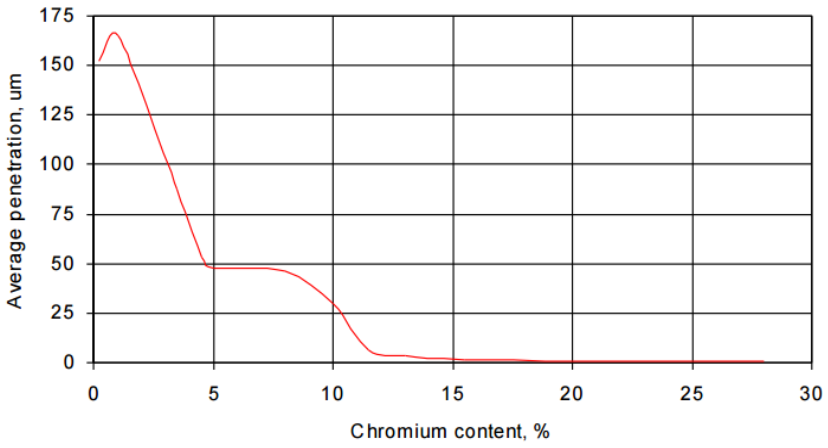

Figure 2.7: Effect of chromium content on passivity (*Firmanto and Budhyantoro, 2023*).

Additionally, improving the surface finish can improve passivity. According to multiple researchers, surface finish of stainless steel is improved with vibratory polishing surface finishing, high-temperature annealing, and electrochemical machining (ECM). On the other hand, the passive film of austenitic stainless steel is improved by increasing the nitrogen content in the alloying element. Figure 2.7 illustrates the significant effect of chromium increments in the stainless-steel alloy on improving corrosion resistance.

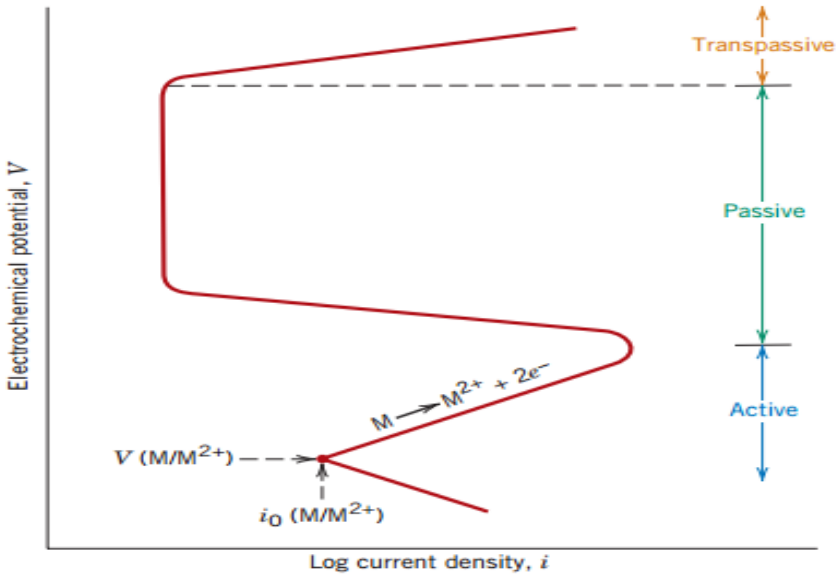

Figure 2.8: Polarization curve for active-passive transition (Lindell and Pettersson, 2015).

On the other hand, the effectiveness of passivation for metal can be expressed with the help of polarization-log curve, which uses current density and electrochemical potential to show the active and passive states of metals (Lindell and Pettersson, 2015; Neupane *et al.*,2022). Fig.2.8 illustrates the Active-Passive-Trans passive process of stainless-steel materials.

2.4 Theory of Autoclave and Its Working Environments

Steam, which is water vapor, is utilized for the sterilization of items that can withstand high temperature and moisture. Autoclaves employ steam at elevated temperature and pressure for various applications such as laboratory equipment sterilization, water treatment, pharmaceutical product sterilization, controlled waste product decontamination, and sterilization of non-porous goods with direct steam contact. However, recent studies have shown limitations in the application of steam autoclaves for solid waste decontamination due to bacterial regrowth after a certain period (Hossain *et al.*, 2015). Conversely, other studies suggest the importance of incorporating steam sterilization with supercritical carbon dioxide (SC-CO2) to prevent bacterial regrowth after the decontamination process (Salimon *et al.*,2022; Nele, 2016). Additionally, steam autoclaves find applications in curing various products that require controlled temperatures, particularly in the manufacturing of high-performance composite parts used predominantly in aeronautical science (Hamlin, 2012). Steam sterilization typically involves different phases of a cycle to complete the sterilization process. The first phase is the heating phase, where the temperature increases from room temperature to the sterilization temperature. The second phase is the exposure phase, during which the temperature is maintained at the sterilization temperature until all bacteria are killed. Finally, the cooling and drying phase helps to reduce the chamber temperature from

the sterilization temperature to around 100°C to enable the opening of the chamber (Lewis, 2002). Two methods, volumetric and interfacial, are employed to accomplish this process. The volumetric method utilizes an electrical power source to heat the entire bulk, which takes time to complete both during heating and cooling. In contrast, the interfacial method, which is more time-saving, uses solar energy as a power source and heats only the top layer of water to generate steam.

Autoclave process is mainly processed either by the vacuum or non-vacuum method of air removal and drying. The vacuum autoclave sterilization method is used to remove trapped air prior steam exposure and remove steam during drying to prevent the wetting of goods by condensed steam in the chamber (the dryness quality of removed goods need to be at least >95% (Li *et al*., 2018). The steam autoclave is constructed using stainless steel materials, with the inner chamber being made of SS304, SS316 to withstand high pressure and resist corrosion. Most autoclave machines consist of essential components such as the lid/door, pressure chamber, power switch, control panel, water level indicator, pressure gauge, whistle, safety valve, electrical heater, thermometer, and stand structure.

The principles of autoclaving depend on five critical parameters: exposure time, temperature, moisture content, direct steam contact, air removal, and the drying process. Exposure time is the minimum period required to kill all organisms, with higher steam temperatures (121°C) reducing the time needed for sterilization, while lower temperatures (40°C to 80°C) require more time. Geobacillus stearothermophilus spores, resistant to high-temperature moist steam vapor, are used to validate steam autoclaves, with the D-value representing (shown in Figure 2.9) the time to reduce the microbial population by 90%. Temperature is directly proportional to steam pressure and affects sterilization duration. Saturated steam is preferred for its protein-coagulation ability, and steam pressure in the autoclave chamber jacket must be lower than in the chamber to prevent the formation of superheated steam. Direct steam contact with all surface's require sterilization is crucial, as the energy from steam must be condensed on the surface to effectively transfer heat. Air removal through repeated vacuuming is essential to ensure saturated steam contacts the necessary surfaces, preventing sterility issues and chamber leaks. Finally, during the drying process, trapped moisture from condensed steam must be vaporized and removed under deep vacuum to prevent recontamination (Bearss *et al*., 2017; Sandle, 2013; Oyawale and Olaoye, 2007; Salas and Wiener, 2009).

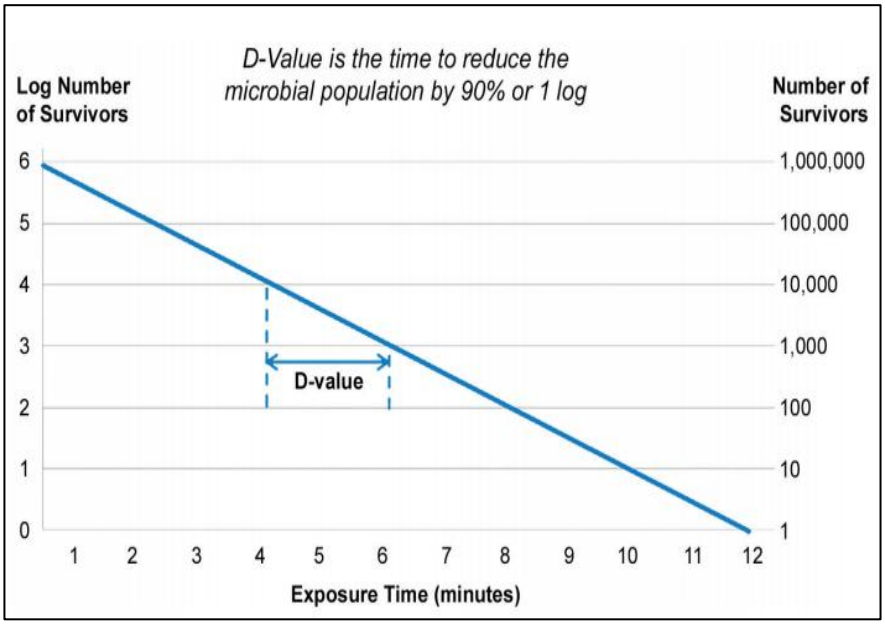

Figure 2.9: Typical survivor curve (Salas and Wiener, 2009).

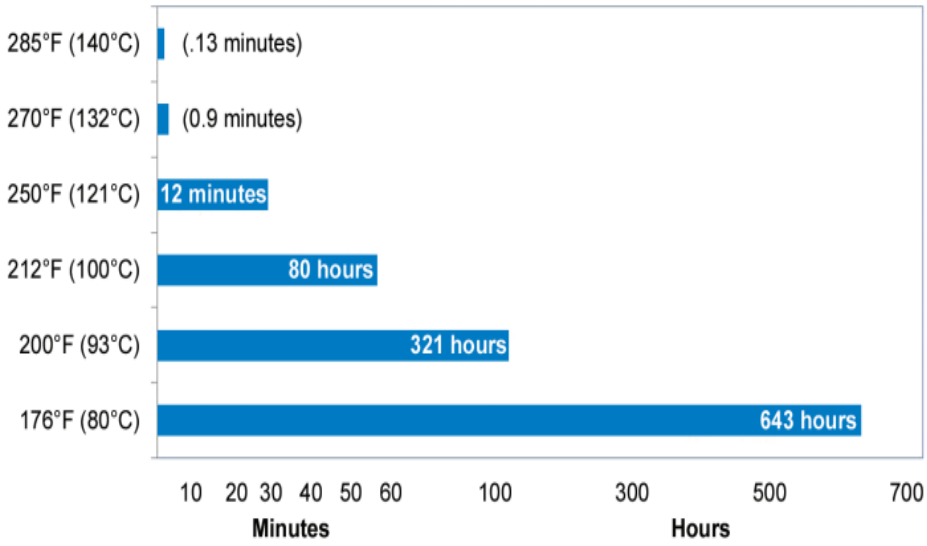

Figure 2.10: Sterilization time versus temperature (Salas and Wiener, 2009).

2.5 Corrosion Mechanism of SS304

The questions why materials corrode have been asked since ancient times and continue to be a topic of interest for various researchers, scientists, engineers, and individuals from diverse backgrounds. Many scientists and researchers have described that material corrosion is a natural consequence of materials returning to their thermodynamically stable states. Energy is imparted to minerals and ores during the processing of materials for various products and alloys. When these materials are exposed to environmental conditions, they release this energy, leading to oxidation or reduction reactions. Therefore, most researchers attribute corrosion to natural conditions resulting from electrochemical reactions (wet corrosion) and

chemical corrosion (high temperature or dry corrosion) (Revie, 2008; Ahmad, 2006; Saefuloh *et al*., 2020). General metal oxidation can be described with the following 2.7 general equation:

$$M(s) = M^{ne} + ne^{-} \quad 2.7$$

Where M is metal and the above equation shows corrosion of metal forms oxidation of metal into metal ions with valence charge of n+ and release of n electron.

Corrosion on the other hand can happen on reduction reaction of metal, which is electron deposition of metal surface. Equation 2.8 shows general form of metal reduction reaction.

$$M^{n+} + ne- \rightarrow M \quad 2.8$$

Where M^{n+} is a positively charged metal element and gained n+ electron developed during the reduction process.

The general chemical reaction for the corrosion of SS304 involves the dissolution of iron (Fe) and chromium (Cr) from the stainless-steel matrix in the presence of an electrolyte, usually water, and the subsequent formation of corrosion products such as iron oxide (rust) and chromium hydroxide. The reactions can be summarized as follows:

Formation of iron oxide (rust):

$$Fe+2H_2O \rightarrow Fe(OH)_2+H_2 \quad 2.9$$

$$4Fe(OH)_2+O_2 \rightarrow 2Fe_2O_3+2H_2O \quad 2.10$$

Dissolution of chromium:

$$Cr+3H_2O \rightarrow Cr(OH)_3+3H^{+}+3e^{-} \quad 2.11$$

$$Cr(OH)_3+3H^{+} \rightarrow Cr_3^{+}+3H_2O \quad 2.12$$

Formation of chromium hydroxide:

$$Cr(OH)_3+OH^{-} \rightarrow Cr(OH)_4^{-} \quad 2.13$$

Formation of iron chlorides (in the presence of chlorides):

$$Fe+2Cl^{-} \rightarrow FeCl_2+2e^{-} \quad 2.14$$

$$Fe3^{+}+Cl^{-} \rightarrow FeCl_2^{+}+e^{-} \quad 2.15$$

Despite its good corrosion resistance, SS304 can still corrode under certain conditions. Exposure of SS304 to electrolyte solution environments, such as moisture, salt, acidic conditions, the presence of impurities, and the availability of gasses, can cause the refined metal alloys changes to thermodynamically stable compounds such as metal sulfides, metal oxides, or metal hydroxides.

2.6 Forms of Corrosion in SS304

Stainless steel AISI 304 is renowned for its good corrosion resistance, making it a preferred material in various industries, including marine, chemical processing, pharmaceuticals, and

food processing. However, despite its resistance to corrosion, it is still susceptible to various forms of corrosion under certain conditions. Understanding these forms of corrosion is crucial for implementing effective preventive measures and maintaining the integrity of SS304 components. In this literature review, we explore the different forms of corrosion commonly observed within SS304.

2.6.1 Uniform corrosion

Uniform corrosion is a prevalent form of corrosion characterized by the consistent dissolution of the metal surface, leading to an overall loss of material across the entire surface area. In the case of SS304, this alloy is generally known for its robust resistance to uniform corrosion in a wide range of environments. However, it's crucial to recognize that certain conditions can still render SS304 susceptible to this form of corrosion, particularly when exposed to aggressive chemicals or elevated temperatures for prolonged periods. According to research done by Saefuloh *et al*. (2020), during immersion of 304 SS in Concentration of Chloride Acid Solution and Temperature Variations dissolution of passive layer and oxide layer formed is covered the entire surface and corrosion rate increase with concentration and temperature increments (Parangusan *et al.*, 2021).

Uniform corrosion of SS304 typically occurs in environments where the protective oxide layer is compromised or in aggressive chemical environments. The primary chemical reactions involved in the uniform corrosion of SS304 are as follows:

Formation of iron oxide:

$$Fe+2H2O \rightarrow Fe\ (OH)2+H2 \qquad 2.16$$

This reaction shows the formation of ferrous hydroxide ($Fe\ (OH)_2$) from the reaction of iron (Fe) with water (H_2O). Ferrous hydroxide further reacts with oxygen to form iron oxide (Fe_2O_3), commonly known as rust.

$$4Fe\ (OH)2+O2 \rightarrow 2Fe2O3+2H2O \qquad 2.17$$

Dissolution of chromium:

$$Cr+3H_2O \rightarrow Cr\ (OH)_3+3H^+ +3e^- \qquad 2.18$$

This reaction shows the dissolution of chromium (Cr) from the stainless-steel matrix, forming chromium hydroxide ($Cr\ (OH)_3$) and releasing protons (H^+) and electrons (e^-).

$$Cr\ (OH)_3+3H^+ \rightarrow Cr_3{}^+ +3H_2O \qquad 2.19$$

Formation of chromium hydroxide:

$$Cr\ (OH)_3+OH^- \rightarrow Cr\ (OH)_4{}^- \qquad 2.20$$

This reaction shows the formation of chromate ions ($Cr\ (OH)_4{}^-$) in alkaline conditions.

The resistance of SS304 to uniform corrosion is heavily influenced by various factors, including pH levels, temperature fluctuations, and the specific chemical composition of the environment. In environments with extreme pH levels or highly acidic or alkaline solutions, the passive oxide layer that typically protects SS304 may become compromised, increasing the likelihood of uniform corrosion. Similarly, exposure to high temperatures can accelerate corrosion processes and diminish the protective properties of the oxide layer, making it more vulnerable to uniform corrosion (Karafyllis, 2017).

Moreover, the chemical composition of the environment plays a crucial role in determining the susceptibility of SS304 to uniform corrosion. Environments containing chloride ions, sulfides, or other aggressive chemicals can significantly increase the corrosion rate of SS304, even in the absence of extreme pH levels or high temperatures (Ul-Hamid *et al*., 2017; Li *et al*., 2021). Therefore, careful consideration of the operating environment and appropriate corrosion mitigation strategies are essential to ensure the long-term integrity and reliability of SS components.

In addition, while SS304 boasts high resistance to uniform corrosion under typical conditions, it's essential to remain alert and proactive in monitoring and controlling environmental factors that could compromise its corrosion resistance. By understanding the complex interplay between Ph, temperature, chemical composition, and material properties, engineers and researchers can effectively mitigate the risk of uniform corrosion and prolong the service life of SS304 components in various applications.

2.6.2 Pitting corrosion

Pitting corrosion represents a localized and often highly damaging form of corrosion, manifesting as small pits or craters on the surface of metal materials. While SS304moderately resistant to pitting corrosion under standard atmospheric and aqueous conditions, it is not totally resistant to this corrosive phenomenon. Pitting corrosion can occur when SS304 is exposed to environments containing chloride ions, particularly in marine or industrial settings where such ions are prevalent (Nuthalapati *et al*.,2023; Montoya *et al*., 2023).

Chloride ions have a particularly detrimental effect on the passive oxide layer that typically protects stainless steel surfaces. When chloride ions are present, they can destabilize the protective oxide layer, leading to localized breakdowns and the initiation of pitting corrosion. Once initiated, pitting corrosion can propagate rapidly, causing extensive damage to the metal surface and compromising the structural integrity of SS304 components (Freire *et al*., 2011; Mohammed Ali, 2016; Maher *et al*., 2022). Pitting corrosion of SS304 involves

the localized attack on the material, resulting in the formation of small pits or craters on the surface. The primary chemical reactions involved in pitting corrosion of SS304 are as follows:

Initiation of pitting:

$$Fe+2H_2O \rightarrow Fe(OH)_2+H_2 \quad 2.21$$

This reaction shows the formation of ferrous hydroxide ($Fe(OH)_2$) from the reaction of iron (Fe) with water (H_2O).

Formation of ferric hydroxide:

$$Fe(OH)_2+O_2 \rightarrow Fe(OH)_3 \quad 2.22$$

Ferrous hydroxide further reacts with oxygen to form ferric hydroxide ($Fe(OH)_3$).

Acidification of pits:

$$Fe(OH)_3+3H^+ \rightarrow Fe^{3+}+3H2O \quad 2.23$$

Ferric hydroxide reacts with protons (H^+) to form ferric ions (Fe^{3+}) and water (H_2O).

Chloride attack:

$$Fe^{3+}+Cl^- \rightarrow FeCl_2^+ + e^- \quad 2.24$$

Ferric ions react with chloride ions (Cl^-) to form ferrous chloride ($FeCl_2$) and release electrons.

$$FeCl^{2+}+Cl^- \rightarrow FeCl_2 \quad 2.25$$

Ferrous chloride further reacts with chloride ions to form ferric chloride ($FeCl_3$).

The consequences of pitting corrosion can be severe, especially in critical applications where the reliability and longevity of SS304 components are very important. Pits and craters formed by pitting corrosion can serve as initiation points for further corrosion processes, leading to material loss, leaks, and ultimately, component failure (Al-Taheret al., 2014; Lakkam *et al*., 2019; Ha *et al*., 2021; Li *et al*., 2022). Hence, it is imperative to recognize and resolve the root causes of pitting corrosion to effectively minimize its adverse consequences.

Preventive measures against pitting corrosion include the implementation of corrosion-resistant coatings, the use of alternative materials in chloride-rich environments, or the adoption of cathodic protection techniques. Additionally, regular inspection and maintenance practices can help detect early signs of pitting corrosion and allow for timely intervention to prevent further damage (Momeni *et al*.,2012; Han *et al*, 2023; He et al., 2020; Aslam *et al*., 2022; Wang et al., 2012; Lin *et al*., 2017; Zeng *et al*.,2021; Kamaraj and Erning, 2020).

2.6.3 Crevice corrosion

Crevice corrosion, a common form of corrosion, arises in confined spaces or crevices where stagnant or low-oxygen conditions prevail. These spaces often occur between SS304components or beneath deposits of corrosion products, providing ideal environments for accelerated corrosion. The localized chemical imbalances within crevices promote the initiation and propagation of corrosion, posing a significant threat to the integrity of SS304 structures (Ech Charqy *et al*.,2023; Al Ansari, 2023; Mohanty, 2022; Puspalata *et al*., 2022).

The crevice corrosion of stainless-steel grade SS304 can be represented by the following chemical reaction:

Anodic reaction (metal dissolution)

$$Fe \rightarrow Fe^{2+} + 2e^{-} \qquad 2.26$$

Cathodic reaction (oxygen reduction)

$$O2 + 2H_2O + 4e^{-} \rightarrow 4OH^{-} \qquad 2.27$$

Overall reaction

$$Fe + O_2 + 2H_2O \rightarrow Fe^{2+} + 4OH^{-} \qquad 2.28$$

This reaction demonstrates the oxidation of iron (Fe) to ferrous ions (Fe^{2+}) at the anode and the reduction of oxygen to hydroxide ions (OH^{-}) at the cathode.

SS304 is susceptible to crevice corrosion, particularly in environments where oxygen levels are limited, such as seawater or areas with high chloride concentrations. In these settings, the presence of chloride ions amplifies the corrosive process, further compromising the protective oxide layer on SS304 surfaces. As a result, crevice corrosion can lead to the formation of localized pits and cracks, ultimately weakening SS304 components and increasing the risk of structural failure.

Effective prevention of crevice corrosion in SS304 components requires careful design considerations and proactive maintenance practices. Design modifications may include minimizing crevice geometries, using corrosion-resistant materials for gaskets and seals, and ensuring adequate drainage to prevent the accumulation of corrosive agents. Additionally, regular inspection and cleaning procedures are essential to identify and remove potential crevice corrosion sites before significant damage occurs (Herath *et al,* 2022; Kim and Kim, 2018).

Furthermore, the application of corrosion inhibitors or protective coatings can help mitigate the risk of crevice corrosion and prolong the service life of SS304 components in challenging environments. By implementing these preventive measures and adopting a

proactive approach to corrosion management, engineers can minimize the impact of crevice corrosion on SS304 structures and ensure their long-term reliability and performance.

2.6.4 Intergranular corrosion

Intergranular corrosion represents a significant concern in the corrosion behavior of metals, including SS304. This form of corrosion occurs along the grain boundaries of a metal, where the material is inherently weaker due to the atomic structure at these interfaces. SS304, like many stainless steels, contains chromium, which forms a passive oxide layer on the surface. This oxide layer acts as a barrier, protecting the underlying material from corrosion.

However, sensitization of SS304 can occur under certain conditions, particularly prolonged exposure to high temperatures. During sensitization, chromium carbides can precipitate along the grain boundaries, depleting the chromium content in these regions. As a result, the passive oxide layer becomes compromised, leaving the grain boundaries susceptible to corrosion attack. This phenomenon is known as intergranular corrosion (Bansod *et al*., 2016).

The chemical reaction involved in intergranular corrosion of SS304 can be represented as follows:

$$Fe+2Cr \rightarrow Fe^{2+}+2Cr^{3+}+4e^{-} \qquad 2.29$$

This reaction shows the dissolution of iron (Fe) and chromium (Cr) from the grain boundaries of SS304. Chromium is preferentially dissolved from the grain boundaries, leaving behind a chromium-depleted zone susceptible to further corrosion.

Additionally, the formation of chromium carbides along the grain boundaries, as a result of sensitization, accelerates the corrosion process. The reaction for the formation of chromium carbides is:

$$Cr+C \rightarrow Cr_3C_2 \qquad 2.30$$

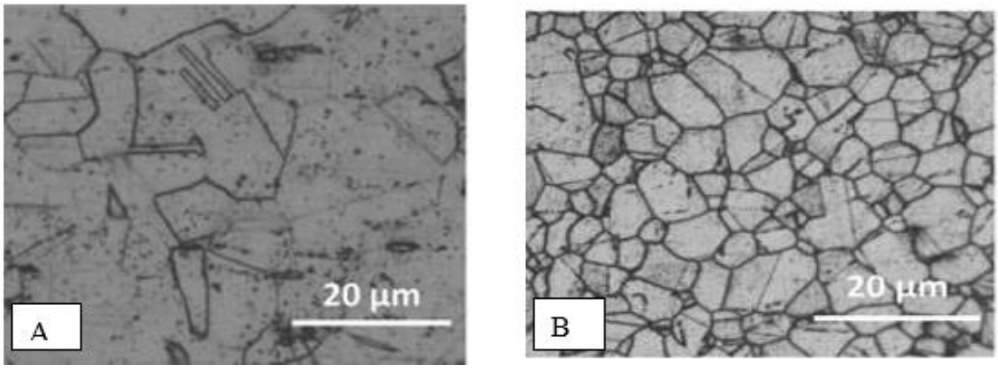

Figure 2.11: Optical micrographs of SS304; (a) Before exposure, (b) After exposure to 700°C for 1440 minutes (Shit *et al*., 2023)

Intergranular corrosion has the potential to greatly affect the mechanical characteristics and structural soundness of SS304 components, especially in scenarios where the material is subjected to harsh environments. To minimize the threat of intergranular corrosion, diverse strategies can be implemented. One approach is to implement heat treatments, such as solution annealing or sensitization heat treatments, to restore the chromium-depleted grain boundaries and promote the formation of a more uniform passive oxide layer (Singh *et al*., 2003).

Additionally, intergranular corrosion of AISI304 improved by increased cold deformation process. Cold deformation processes such as cold rolling or cold drawing induce plastic deformation in SS304, generating dislocations within its crystal structure and creating internal stresses. This increases the density of dislocations within the material, effectively strengthening the grain boundaries. As a result, it becomes more challenging for chromium carbides to form, reducing the material's susceptibility to sensitization. By inhibiting the formation of chromium carbides and preventing the subsequent depletion of chromium along the grain boundaries, cold deformation significantly improves SS304's resistance to intergranular corrosion. Furthermore, the increased dislocation density and strain hardening help retain chromium in solid solution, preventing its precipitation as chromium carbides along the grain boundaries (Shit *et al*.,2023; Spisák and Szávai, 2019).

Furthermore, proper fabrication and welding practices are essential to minimize the risk of sensitization and intergranular corrosion in SS304 components. Techniques such as post-weld heat treatment and the use of filler materials with low carbon content can help maintain the corrosion resistance of SS 304 weldment.

In summary, while SS304 offers excellent resistance to corrosion in many environments, it is crucial to address the risk of intergranular corrosion, particularly in applications involving high temperatures or aggressive chemical exposures. Through careful material selection, heat treatments, and fabrication practices, the risk of intergranular corrosion in SS316 can be effectively mitigated, ensuring the long-term performance and reliability of components made from this material.

2.6.5 Stress corrosion cracking (SCC)

Stress corrosion cracking (SCC) is a particularly gradual form of corrosion that can lead to catastrophic failure of materials, including SS304, in service. This type of corrosion-induced fracture occurs under tensile stress in the presence of a corrosive environment, where the combination of stress and corrosion significantly reduces the material's resistance to cracking. Stress corrosion cracking (SCC) of SS304 typically occurs in environments

containing chlorides, such as seawater or brine, under tensile stress. The chemical reaction involved in stress corrosion cracking of SS304 in chloride-containing environments can be represented as follows:

$$Fe+2Cl^{-}\rightarrow FeCl_2+2e^{-} \quad 2.31$$

This reaction shows the dissolution of iron (Fe) in the presence of chloride ions (Cl^{-}) to form ferrous chloride ($FeCl_2$) and release electrons.

Additionally, the formation of chromium chloride ($CrCl_3$) can occur, which further depletes chromium from the stainless-steel matrix:

$$Cr+3Cl^{-}\rightarrow CrCl_3+3e^{-} \quad 2.32$$

The depletion of chromium and dissolution of iron weakens the passive oxide layer on the surface of SS304, making it more susceptible to stress corrosion cracking.

SS304 is generally known for its excellent resistance to SCC in a wide range of environments. However, certain conditions can render SS304 susceptible to SCC, particularly when exposed to aggressive chemical environments combined with tensile stress. For example, exposure to chlorides, such as those found in seawater or industrial environments, can initiate SCC in SS304 components. Similarly, caustic solutions containing alkaline or acidic compounds can also contribute to the initiation and propagation of SCC in SS304 (Khalifeh, 2020; PE, 2009; Ul-Hamid *et al*., 2017). Preventing stress corrosion cracking (SCC) in SS304 structures involves addressing mechanical and environmental factors that contribute to crack initiation and propagation. Stress management techniques like stress relief annealing and optimizing component design to minimize stress concentrations are crucial to reduce SCC risk. Environmental control measures, such as removing chloride contaminants and applying corrosion-resistant coatings, help mitigate corrosive effects on SS316 surfaces. Regular inspection and monitoring of SS316 components for SCC signs are vital for identifying vulnerabilities and taking timely corrective actions. Non-destructive testing methods like ultrasonic and eddy current testing can detect early-stage cracking. Proper material selection and alloy modifications, such as increasing molybdenum content or adding nitrogen, can enhance SCC resistance in chloride-rich environments.

2.7 Reviewed Materials and Research Gap

2.7.1 Reviewed materials

Ul-Hamid *et al*. (2017) determined that the corrosion of SS304 and SS316 is influenced by pollutant concentration, temperature, humidity, exposure time, and increased exposure to wet-dry cycles. According to Saefuloh *et al*. (2020), corrosion in soil is higher due to the

unavailability of oxides used for passivation. Other researchers found that SS304 is affected by both concentration and temperature in HCl, $FeCl_3$, and NaCl, with $FeCl_3$ having the highest impact and NaCl the least at various concentrations and temperatures (Adeniyi *et al*., 2019). Additionally, Yang *et al*. (2020) noted that the corrosion rate of SS304 increases under crevice conditions with higher chloride concentrations in marine environments compared to freshwater.

Yang *et al*. (2020) indicated that stress corrosion cracking (SCC) of SS304 is influenced by H2SO4 and HCl, with temperature increments causing pitting corrosion to progress to SCC through intergranular and transgranular corrosion (Liao *et al*., 2019). Liao et al. further elaborated that SCC in notched materials reduces fatigue life, increasing susceptibility to stress fatigue, with fatigue life diminishing as temperature rises and material strain increases. However, Tan *et al*. (2020) found that the fatigue life of notched material is superior at 325°C compared to 280°C. Tan also explored the corrosion fatigue of SS304, noting that cyclic loading and factors such as temperature, dissolved oxygen (DO), and pH eventually lead to material strain aging (Galan *et al*., 2020)

Corrosion rate of SS304L is higher than SS310S when exposed to a supercritical water reactor (SCWR) and oxidation of both materials is affected with exposure time (Rosidah *et al.*,2021). SS310S is more stable comparatively due to higher concentration of Cr and Ni. Rosidah also determines that with exposure time of SS304 in 0.5M H2SO4 corrosion rate is increased. When time is less the oxide on surface Cr_2O_3 acts as a passive element and with time the passivity of this oxide becomes reduced and acidic solution forms spot corrosion which later forms intergranular corrosion (Jian *et al*.,2015). The study result of SS304 corrosion analysis using XRD shows concentration of FeC is higher. On the other hand Jian et, al. determines corrosion rate increase from passivation to pitting corrosion type with temperature increase from 20^oc to 80^oc for SS304 in NaCl solution by using electrochemical noise method (Sanchez et al.,2018). Sanchez also explained that oxidation of 304 SS surface makes the surface gain weight during corrosion and the gain is higher during high pressure water than the steam (Nair *et al.*,2020).

Through Zn coating passivity of surface against corrosion becomes increased. Through potential dynamic polarization, comparatively Zn coated SS304 is more resistant against corrosion (Fouda *et al*., 2017). On the other hand, Foudal explained resistance of organic compounds (O, N and S) on SS304 in acidic solutions. The organic compound makes the SS surface active and prevents rusting (Ajay *et al*.,2021,). Ajay also determines coating ZrO_2 has become familiar in recent years to improve passivity of SS304 surface. Zn doped with

ZrO_2 shows some significant corrosion rate decrease with more than 83% than uncoated substrate. ZrO_2 is more corrosive resistant with more than 87% corrosion rate reduction compared to uncoated SS304 (Fayomi *et al*.,2019). According to Fayomi corrosion of SS304 is an irreversible process which has direct and indirect impacts on a country's economy. According to the researchers' idea, millions of moneys is splashed either to prevent corrosion from happening or to correct after happening before catastrophic failure happens (Saefuloh *et al*., 2020).

2.7.*2* Research gap

Extensive research has been conducted on corrosion in various materials and methods, but there is a lack of understanding about how steam affects the corrosion of SS304 in sterilizing autoclaves. This study aims to fill this gap by exploring the root causes of SS304 corrosion in vacuum sterilizing autoclave chambers. Recognizing the different types of corrosion in SS304 is crucial for maintaining the durability and dependability of components made from this material. By identifying the specific corrosion mechanisms and their root causes, engineers and researchers can develop effective strategies to protect SS304 components from corrosion-related issues. This study focuses on investigating the reasons behind SS304 material corrosion in vacuum sterilizing autoclave chambers, an area that has not been extensively studied in current literature.

CHAPTER THREE:

3. MATERIALS AND METHODOLOGY

3.1 Introduction

This section provides a comprehensive description of the experimental approach used to investigate the causes of corrosion in SS304 material within a steam autoclave chamber. It details the experimental setup, materials used, and methodologies employed to simulate and monitor corrosion under these conditions. The procedures used in this research involved several key steps: preparation of SS304 flat coupons with standardized dimensions of 4 cm x 4 cm x 0.1 cm, and the preparation of solutions for steam generation and immersion at room temperature, including 0.5% sodium chloride, 3.5% sodium chloride solutions, purified water, and ground hard water. After sample preparation, the specimens were exposed to the steam autoclave and immersed in solutions at room temperature and pressure, subjected to various scenarios within the autoclave chamber to assess corrosion behavior over time. After removal from the corrosive environments, the samples were investigated and monitored for corrosion using the weight loss method, and the corroded surfaces were characterized by Scanning Electron Microscopy (SEM), X-ray Diffraction (XRD), Optical Microscopy (OM), and hardness tester. Data obtained during the experiments were extensively analyzed using statistical methods (SAS software) and interpretation techniques to identify corrosion mechanisms and understand the behavior of SS304 material in steam autoclave environments. The investigation utilized a laboratory-scale autoclave available at the National Veterinary Institute, which controls temperature and pressure to replicate steam autoclave environments. The flow diagram in Figure 3.1 illustrates the experimental procedures conducted in this research. By following these detailed methodologies, the study aimed to elucidate the corrosion mechanisms affecting SS304 material under steam autoclave conditions.

3.2 Experimental Site

The study was conducted at several locations, including the National Veterinary Institute at Mechanical Workshop, and the Quality Control Laboratory. Additional research was performed at Adama Science and Technology University and the Defense Engineering College, specifically within their Material Science Laboratories. Various analytical techniques were employed to comprehensively investigate the corrosion of SS304 stainless steel.

Phase identification and crystal structure analysis of the corroded surfaces were performed using X-ray diffraction (XRD). Surface characterization and microstructure analysis of the

corroded specimens were carried out using scanning electron microscopy (SEM). The metallographic grain structure of the corroded material was identified using an optical microscope (OM).

In addition to these analyses, surface hardness testing and measurements of sample weight loss were conducted to assess the severity and extent of corrosion. These methods provided a thorough understanding of the corrosion mechanisms affecting SS304 stainless steel under different conditions.

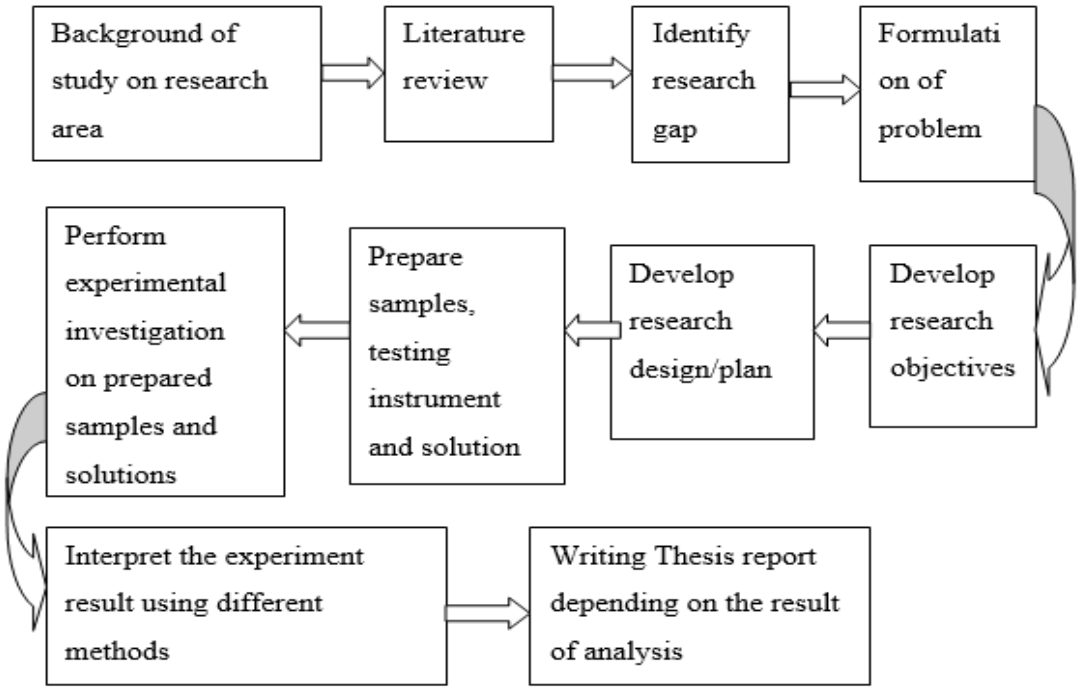

Figure 3.1: Over all research layout

3.3 Materials and Solution Employed in the Research

3.3.1 Immersion cup

In the study of corrosion behavior of SS304 stainless steel, the immersion test is a critical method to simulate real-world corrosive environments and assess the material's durability. An essential component of this test is the immersion cup, which holds the test specimens and the corrosive solutions. This report details the materials and design considerations for the immersion cup used in the corrosion study of SS304. Known for its excellent chemical resistance, especially against acids and bases, polypropylene (PP) was chosen for its ability to withstand the corrosive solutions used in the study, such as sodium chloride solutions and groundwater samples. PP also has good thermal stability, making it suitable for the elevated temperatures in the autoclave. Figure 3.2 shows prepared cups for immersion test.

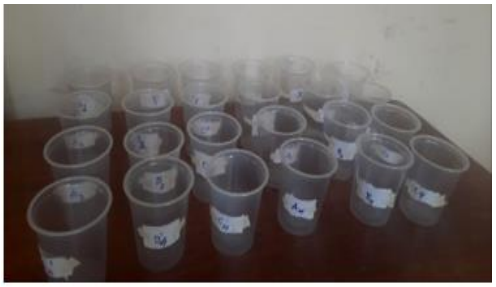

Figure 3.2: Polypropylene cups prepared for immersion taste at room temperature (Photo).

3.3.2 SS 304 specimens (samples)

304 SS is a stainless-steel alloy renowned for its high levels of chromium (Cr) and nickel (Ni). It was selected from sheet stock at the National Veterinary Institute due to its compatibility with the autoclave chamber, which is known for its susceptibility to corrosion. The chosen samples, measuring 4 cm x 4 cm x 0.1 mm, were ideally suited for immersion in the test cup. In the research, the samples were classified into three separate groups.

Table 3.1: Category and name of samples employed in different solution at various condition and exposure time.

Categories	Sample Name	Immersion solution	Temperature condition	Exposure time (hours)
Category one	A1	Pure water	Room temperature	72
	B1	Pure water	Room temperature	120
	C1	Pure water	Room temperature	168
	A2	Hard water	Room temperature	72
	B2	Hard water	Room temperature	120
	C2	Hard water	Room temperature	168
	A3	0.5%$NaCl_2$ solution	Room temperature	72
	B3	0.5%$NaCl_2$ solution	Room temperature	120
	C3	0.5%$NaCl_2$ solution	Room temperature	1698
	A4	3.5%$NaCl_2$ solution	Room temperature	72
	B4	3.5%$NaCl_2$ solution	Room temperature	120
	C4	3.5%$NaCl_2$ solution	Room temperature	168
	A5	Pure water	Steam Autoclave	72
	B5	Pure water	Steam Autoclave	120
	C5	Pure water	Steam Autoclave	168
	A6	Hard water	Steam Autoclave	72

Category two	B6	Hard water	Steam Autoclave	120
	C6	Hard water	Steam Autoclave	168
	A7	0.5%$NaCl_2$ solution	Steam Autoclave	72
	B7	0.5%$NaCl_2$ solution	Steam Autoclave	120
	C7	0.5%$NaCl_2$ solution	Steam Autoclave	168
	A8	3.5%$NaCl_2$ solution	Steam Autoclave	72
	B8	3.5%$NaCl_2$ solution	Steam Autoclave	120
	C8	3.5%$NaCl_2$ solution	Steam Autoclave	168

I) Category One: - Samples were prepared for immersion in different types of solutions and environments at room temperature in sealed environment. Experimental setup involves exposing metal samples to various aqueous environments. Samples immersed in pure water at room temperature and pressure are labeled A1, B1, and C1, indicating exposure durations of 72, 120, and 168 hours, respectively. Samples in hard water under similar conditions are denoted as A2, B2, and C2, with exposure times of 72, 120, and 168 hours. Additionally, samples in 0.5% NaCl solution at room temperature are marked A3, B3, and C3, immersed for 72, 120, and 168 hours. Lastly, metal samples in a 3.5% NaCl solution under the same conditions are named A4, B4, and C4, immersed for 72, 120, and 168 hours. This systematic categorization enables a comprehensive investigation into how different aqueous environments and exposure durations impact the properties and performance of the metal samples, enhancing understanding of their corrosion behavior.

II) Category Two: - Represents samples were employed for taste in a steam autoclave chamber. In this study, metal samples were tested under varying conditions in a steam autoclave with different aqueous solutions. Samples in pure water were labeled A5, B5, and C5, corresponding to exposure times of 72, 120, and 168 hours. Likewise, samples in hard water steam were marked as A6, B6, and C6 with exposure times of 72, 120, and 168 hours. Metal samples in a 0.5% NaCl solution were named A7, B7, and C7 with exposure times of 72, 120, and 168 hours. Lastly, samples in a 3.5% NaCl solution were denoted as A8, B8, and C8 with exposure times of 72, 120, and 168 hours. This categorization allowed for a thorough investigation into how the different steam autoclave environments and exposure times affected the corrosion behavior and properties of the metal samples, offering valuable insights for practical applications and material selection considerations.

Figure 3.3: Prepared samples for immersion and exposure to steam autoclave (photo)

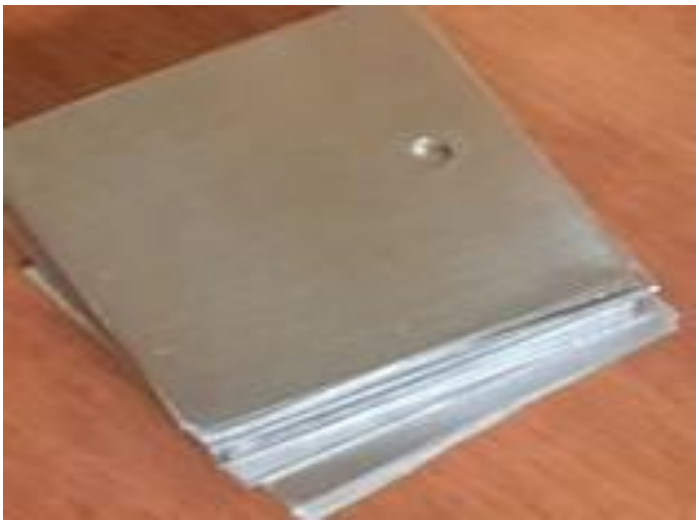

Figure 3.4: Samples prepared for exposure to steam autoclave conditions (Photo).

II) Category Three: The samples utilized in this study were employed to investigate the corrosion conditions under normal operating conditions of the steam autoclave. These samples were carefully selected from components of the autoclaves that were in use for various applications in production.

3.3.3 Hand power hacksaw cutting machine and hand hacksaw

The cutting tool was employed to size sheet metal to required standard dimension of 4 cm x 4cm x 0.1cm samples for corrosion study. Bosch hand power hacksaw was used to size the sheet metal into standard dimensions of coupons. Additionally, a manual hand hacksaw was also incorporated for the same purpose.

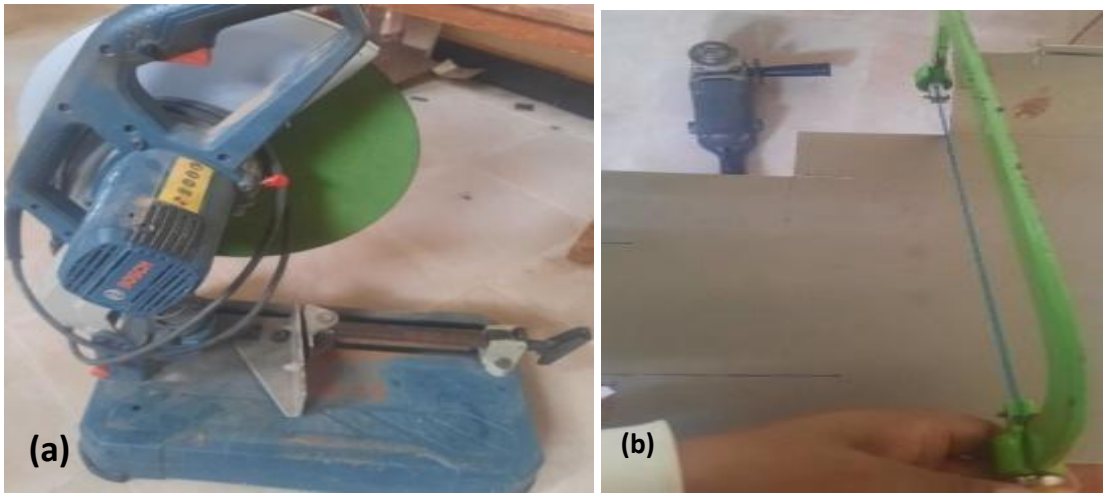

Figure 3.5: Sample cutter (a) Hand hacksaw and (b) Hand powered hacksaw cutting machine (Photo).

3.3.4 Polishing material

In the corrosion investigation of SS304 specimens, achieving a mirror finish was considered crucial for subsequent analyses to reduce the effect of surface finish on corrosion. To fulfill this activity, sandpaper abrasive materials with grit sizes of #120, #360 and #400 along with polishing cloth were utilized for mechanical polishing. Sandpaper, recognized for its effective abrasion and surface smoothing capabilities, was selected due to its composition of a flexible substrate coated with abrasive particles such as aluminum oxide or silicon carbide, bonded together with adhesive. Various grit sizes of sandpaper were employed, ranging from coarse to fine, to progressively enhance the surface texture of the SS304 specimens. Coarser grits (#120) were initially used to eliminate surface imperfections and scratches, while finer grits (#360 and #400) were subsequently applied to achieve a smoother surface finish. Following the sandpaper polishing process, polishing cloths composed of soft and flexible materials (cotton) were employed. They facilitate the application and distribution of polishing compounds, thereby enhancing the polishing efficiency and surface luster. The choice of polishing cloth material was made to minimize scratching and ensure uniform polishing across the specimen surface.

3.3.5 Solvent chemical

In the investigation of SS304 specimens, ensuring cleanliness and the removal of contaminants were essential steps to maintain the integrity of subsequent analyses. To accomplish this task, cleaning agents such as acetone and ethanol were employed.

Acetone was selected for its high volatility and efficacy as a solvent. It was chosen due to its capability to dissolve various contaminants such as oils, grease, and residual polishing

compounds. Its rapid evaporation rate minimizes the risk of leaving behind residue, ensuring thorough cleaning of the SS304 specimens. Acetone is also non-reactive with stainless steel, making it suitable for use without compromising the material's surface integrity.

Figure 3.6: Acetone solution used to clean samples before and after exposure to the corrosive environment (photo).

On the other hand, ethanol was employed as an alternative solvent for cleaning SS304 specimens. With its excellent solvent properties and low toxicity, ethanol effectively removes organic residues and contaminants from the specimen surfaces. Additionally, ethanol evaporates quickly, leaving behind minimal residue and facilitating the rapid drying of the cleaned specimens.

3.3.6 Solutions for sample immersion and steam of autoclave environment

A solution containing 0.5% weight of $NaCl_2$, 3.5% weight of sodium chloride ($NaCl_2$) was carefully prepared by dissolving analytical-grade sodium chloride in deionized water. This solution was needed to compute the saline environment encountered within a steam autoclave. Saline solution, a product frequently subjected to sterilization in steam autoclaves, is formulated by dissolving NaCl2 in deionized purified water.

In these corrosion investigations, the incorporation of purified water played a vital role in clarifying the potential confounding factors affecting the corrosion behavior of the materials under examination. Purified water used for immersion at room condition and at autoclave conditions contains 0.3µs/cm conductivity and pH value of 7. It is well-established that impurities such as dissolved ions, organic compounds, and particulate matter prevalent in untreated water can introduce extraneous variables that uncertain the genuine mechanisms underlying corrosion processes.

Within the area of steam autoclave corrosion investigations, purified water assumes a pivotal role as the primary medium for exposing materials to elevated temperatures and pressures, thereby replicating real-world operational scenarios. By employing purified water, the taste was aimed to carefully isolate the influence of steam exposure on material corrosion, free from any interference attributable to impurities inherent in conventional water sources. On the other hand, to determine the effect of tap water utilized for steam generation, hard tap water was employed and its effect on SS304 corrosion was examined. according to study done on underground water of around NVI institute area the water had the following parameters

Table 3.2: Quality Parameters of Hard Water at 22°C (Daniel and Tsehaye, 2022)

Description	pH	E. conductivity (µs/cm)	total alkalinity/L	Cl-ion (mg/l)	acidity (mg/l)	total hardness (mg/l)	K- (mg/l)	No_3- (mg/l)	TDS (mg/l)
Concentrations	7.60	830	291.	27.99	20	376	9.50	22	825

3.4 Equipment and Instruments Employed in the Study

3.4.1 Laboratory scale steam autoclave

Autoclaves play a pivotal role in sterilizing materials containing water, a task unachievable through dry heat sterilization methods alone. The laboratory-scale autoclave chamber employed in this study was available at the national veterinary institute laboratory and consists of controlled temperature and pressure conditions encountered in steam autoclave environments. The autoclave machine served as the primary experimental apparatus for investigating the corrosion behavior of SS304 material within steam autoclave conditions. The autoclave employed in this research is a vertical cylindrical type with a chamber dimension of 60cm (diameter) x 80 cm (height), which is suitable for placement of sample specimens during investigation. The selected autoclave chamber was constructed entirely from SS316 stainless steel chamber, chosen for its excellent corrosion resistance and compatibility with high-temperature and high-pressure environments.

SS304 stainless steel is widely used in industrial applications, including steam autoclaves, due to its good mechanical properties and resistance to corrosion in aggressive

environments. As shown in Figure 3.7 and Figure 3.8 the small-scale laboratory autoclave used for research consists of a pressure chamber, lid/door, pressure gauge, pressure releasing unit, safety valve, steam generator heater, waste water drainage system and integrated temperature and pressure controller.

The autoclave chamber was equipped with advanced temperature and pressure control systems to maintain precise operating conditions throughout the experiments. Temperature control was achieved using integrated heating elements and a digital temperature controller, allowing for precise adjustment of the chamber temperature within the desired range. Pressure within the autoclave chamber was regulated using a pressure control system, ensuring that the chamber operated at the specified pressure conditions consistent with steam autoclave environments. The pressure control system maintained a constant pressure of 1.5bar-2bar, typical of standard steam sterilization processes. Overall, in order to enhance safety and functionality, the autoclave chamber was incorporated with safety mechanisms, including pressure relief valves and overheats protection systems, to prevent overpressure and overheating. Overall, the laboratory-scale autoclave chamber provided a controlled and reliable environment for conducting corrosion studies on SS304 material within steam autoclave conditions.

Figure 3.7: Construction of small-scale steam autoclave chamber (photo).

Figure 3.8: Interior surface of steam autoclave exposed to taste solution (photo).

3.4.2 Analytical balance

This thesis investigated corrosion tendencies of SS304 material within a steam autoclave chamber, utilized a particular analytical balance (Model AUX220 from Shimadzu manufacturer). An analytical balance with high precision (accuracy: ±0.001 g) was employed for measuring the weight of SS304 specimens before and after exposure to corrosive conditions. Prior to the experimentation, attention was given to verifying the analytical balance specifications, including its sensitivity, readability, and capacity, to meet the requirements of the corrosion test protocol.

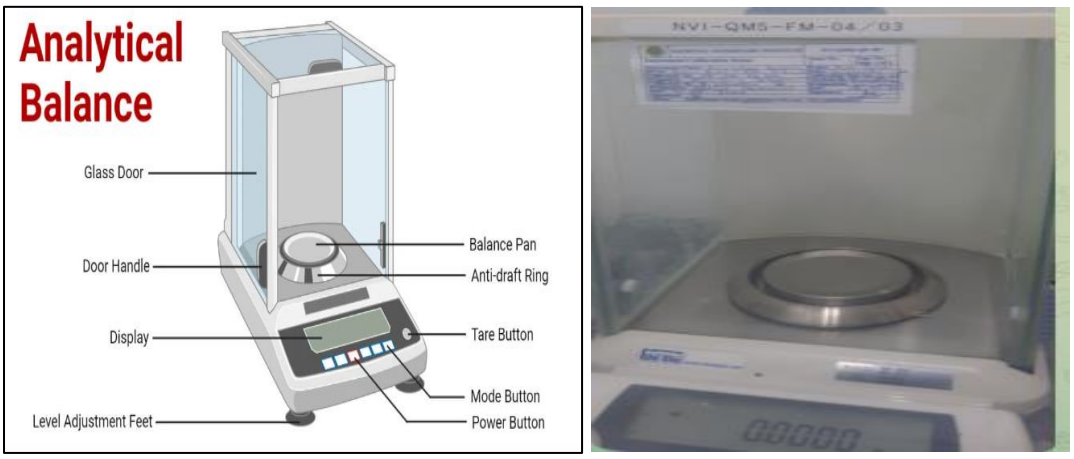

Figure 3.9: Analytical balance schematic description of parts (photo).

Throughout the experimental process, the analytical balance facilitated precise measurement of sample masses before and after exposure to corrosive environments. The integration of the analytical balance model alongside standardized corrosion testing protocols facilitated a

thorough assessment of the corrosion resistance exhibited by SS304 material within the steam autoclave chamber setting.

3.4.3 Scanning electron microscope (SEM)

The scanning electron microscope (SEM) (Model GSM 6000) was employed to investigate the micro structural morphology and chemical composition of the corroded surfaces of 304 stainless steel (SS) specimens exposed to the steam autoclave environment. Prior to SEM analysis, the corroded specimens were carefully prepared by mounting them on SEM stubs and sputter-coated with a thin layer of conductive material to enhance conductivity and minimize surface charging effects. SEM imaging was conducted at various magnifications to examine the surface features. Figure 3.10 shows the SEM instrument employed to analysis surface characteristics of corroded samples.

3.4.4 Vickers hardness tester

The Vickers hardness test is a widely used method for measuring the hardness of materials. It is based on the principle of indentation hardness testing, where a known force (10kgf) is applied to a material using a diamond indenter, and the size of the resulting indentation is measured to determine the material's hardness. Figure 3.11, shows the Vickers hardness tester instrument employed for the hardness taste.

One of the key advantages of the Vickers hardness test is its versatility and applicability to a wide range of materials. Unlike some other hardness testing methods that are limited to specific material types, such as metals or ceramics, the Vickers test can be used for various materials, including metals, ceramics, polymers, and composites. This versatility makes it a valuable tool for material characterization in diverse industries, including automotive, aerospace, manufacturing, and research laboratories.

Figure 3.10: SEM for corrosion surface analysis (Photo).

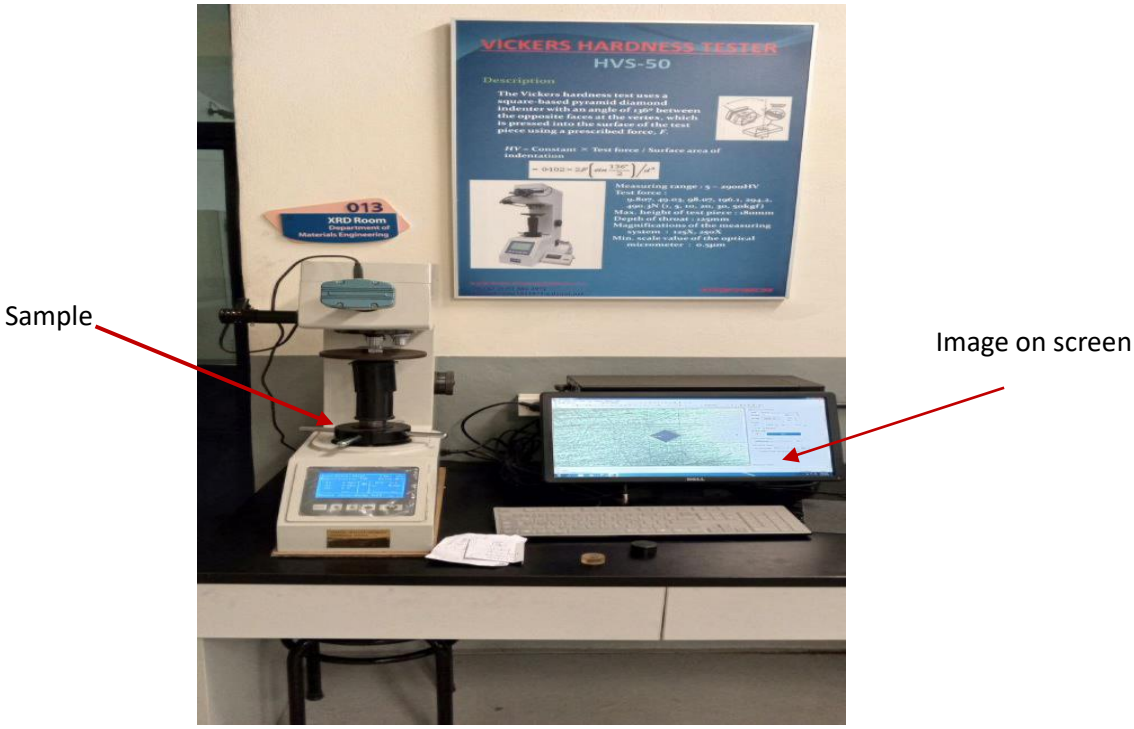

Figure 3.11: Vickers hardness tester machine (Photo).

3.4.5 Optical microscopy

In this study, optical microscopy played a pivotal role in elucidating the underlying causes of corrosion observed on SS304 within a steam autoclave chamber environment. By employing optical microscopy techniques, dark-field microscopy, detailed examination of the corroded surface morphology and microstructural features of the SS304 specimens was conducted. Figure 3.12 shows optical microscope instrument used during examination of corroded samples microstructures. Through high-resolution imaging, the presence of localized pitting corrosion, surface roughening, and formation of corrosion products such as iron oxides and chromium compounds were identified. Furthermore, optical microscopy facilitated the characterization of corrosion attack patterns and the extent of damage across the SS304 surfaces. These findings were instrumental in elucidating the mechanisms driving corrosion initiation and propagation within the steam autoclave chamber, including exposure to elevated temperatures, steam, and corrosive agents. By leveraging the capabilities of optical microscopy, this study provided valuable insights into the specific factors contributing to corrosion susceptibility in SS304 under steam autoclave conditions, informing strategies for corrosion mitigation and material selection in similar industrial environments.

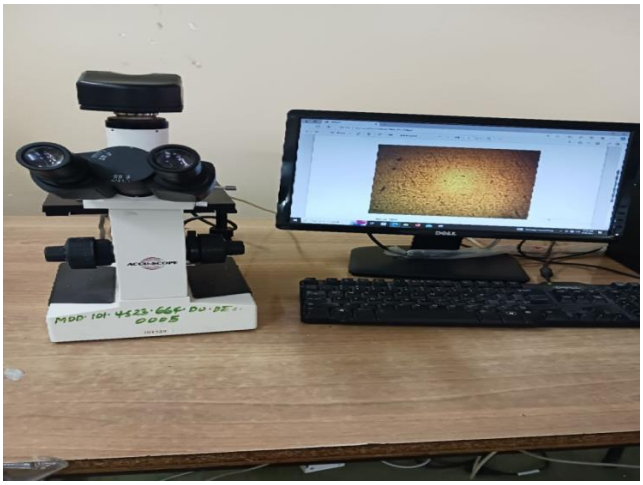

Figure 3.12: Optical microscopy shows analysis of metallographic microstructure (Photo).

3.4.6 X-ray fluorescence (XRF) spectroscopy

X-ray Fluorescence (XRF) spectroscopy is a non-destructive analytical technique utilized to determine the elemental composition of various materials. XRF is based on the principle that when a material is irradiated with high-energy X-rays, it emits secondary (fluorescent) X-rays. The energy of these fluorescent X-rays is characteristic of the elements present in the sample, making XRF a powerful tool for qualitative and quantitative analysis of elemental composition.

When a sample is exposed to primary X-rays, the energy from the X-rays ejects inner-shell electrons from the atoms within the sample. This ejection creates vacancies that are filled by electrons from higher energy levels, resulting in the emission of X-rays with energies specific to the difference between the energy levels. These emitted X-rays are characteristic of the elements in the sample and are detected and analyzed to determine the elemental composition.

Figure 3.13: X-ray fluorescence (XRF) spectroscopy

3.4.7 X-ray diffractor (XRD)

X-ray Diffraction (XRD) is a powerful analytical technique used to identify and characterize the crystalline structure of materials. It provides detailed information about the atomic arrangement within a crystal lattice, allowing researchers to determine phase identification, crystallite size, and lattice parameters. XRD is widely used in materials science, chemistry, geology, and various engineering fields.

XRD operates on the principle of Bragg's Law, which relates the wavelength of incident X-rays to the diffraction angles and the lattice spacings in a crystalline sample. When a crystalline material is irradiated with X-rays, the X-rays are scattered by the electrons in the crystal lattice. Constructive interference occurs when the path difference between the scattered X-rays is an integer multiple of the wavelength, resulting in diffraction peaks that are characteristic of the crystal structure.

3.5 Methodology Used to Perform Experiment Investigation and Analyses

3.5.1 Design of experiments

The experiment was conducted using a full factorial design involving three factors with 4*2*3 levels each: solution type (S), conditions (C), and exposure times (E). Each factor had four, two, and three levels, respectively. The solution types included pure water, hard water, 0.5% NaCl, and 3.5% NaCl. Conditions comprised room temperature, steam autoclave, while exposure times were 72, 120, and 168 hours. In total, there were 4×2×3=24 experiments, and each experimental treatment was conducted in triplicates.

Table 3.3: Experiment design factor

Factor 1 (Solution Type)	**Factor 2 (Condition)**		**Factor 3 (Exposure Time)**					
			E_1		E_2		E_3	
S_1	C_1	C_2	$S_1C_1E_1$	$S_1C_2E_1$	$S_1C_1E_2$	$S_1C_2E_2$	$S_1C_1E_3$	$S_1C_2E_3$
S_2			$S_2C_1E_1$	$S_1C_2E_1$	$S_2C_1E_2$	$S_1C_2E_2$	$S_2C_1E_3$	$S_1C_2E_3$
S_3			$S_3C_1E_1$	$S_3C_2E_1$	$S_3C_1E_2$	$S_3C_2E_2$	$S_3C_1E_3$	$S_3C_2E_3$
S_4			$S_4C_1E_1$	$S_4C_2E_1$	$S_4C_1E_2$	$S_4C_2E_2$	$S_4C_1E_3$	$S_4C_2E_3$

where: S_1 is Pure Water Solution level one, S_2 is Hard Water Solution level two, S_3 is 0.5% NaCl Solution level three, S_4 is 3.5% NaCl solution level four, C_1 is room temperature

condition, C_2 is Steam Autoclave, E_1 is Exposure Time for 72hr., E_2 is Exposure Time for 120hr., E_3 is Exposure Time for 168 hr.

3.5.2 Experiment setup

a. **Immersion testing**

For the corrosion study, 304 SS material specimens were prepared as flat coupons with standardized dimensions of 4cm x 4cm x 0.1cm. The sample's immersion taste was applied according to ASTM-G31-72 standard procedure. These specimens were subjected to various corrosive environments to assess their corrosion resistance. The test solutions included 0.5% NaCl2 solution, 3.5% NaCl2 solution (simulating saline environments in a steam autoclave), deionized pure water (used as a control), and groundwater samples collected from the environment near the National Veterinary Institute (NVI) located at Bishoftu (simulating the conditions of steam used in the autoclave machine). Throughout the corrosion testing period, the behavior of the specimens was monitored using weight loss measurements, visual inspection, and surface analysis techniques such as scanning electron microscopy (SEM). Additionally, x-ray diffraction (XRD) analysis was employed to analyze the composition of corrosion products formed on the surface of the specimens, providing valuable insights into their corrosion behavior and mechanisms.

b. **Inline autoclave system**

To simulate the conditions experienced by 304 SS material in steam autoclaves, a laboratory-scale autoclave chamber constructed from SS316 stainless steel was utilized. This chamber was equipped with temperature and pressure control systems, allowing for precise replication of steam autoclave conditions. 304 SS material specimens were subjected to these controlled conditions for specified durations, providing valuable insights into their corrosion resistance and behavior in steam autoclave environments. Through this experimental setup, the effects of temperature, pressure, and steam exposure on the corrosion properties of 304SS could be thoroughly investigated and analyzed for the thesis report.

c. **Experimental parameters**

To accurately simulate industrial conditions, the steam autoclave temperatures were carefully maintained within the range typically encountered in industrial settings, specifically 121±3°C. Additionally, pressure levels consistent with steam autoclave operation, ranging from 1.5 to 2 bar ±1, were maintained throughout the experiments. To assess both short-term and long-term corrosion effects, immersion testing and inline autoclave exposure were conducted for predetermined durations of 72 hours, 120 hours, and

168 hours. These experimental setups allowed for a comprehensive investigation of the corrosion behavior of the 304 SS material under conditions that closely mimic those encountered in real-world steam autoclave environments. The results obtained from these experiments provided valuable insights into the short-term and long-term corrosion resistance of 304SS, contributing significantly to the thesis report.

d.**Analysis methods**

To assess the severity of corrosion, precise quantification of weight loss experienced by the specimens before and after exposure to corrosive environments was conducted using a sensitive laboratory analytical balance. This allowed for accurate measurement of the corrosion-induced mass loss of the specimens. Additionally, scanning electron microscopy (SEM) characterizes the surface morphology of the corroded specimens. This analysis provided detailed insights into the corrosion mechanisms and the nature of corrosion products formed on the specimen surfaces. Furthermore, corrosion rates were calculated by analyzing the weight loss data in relation to the duration of exposure to the corrosive conditions. These comprehensive analytical approaches facilitated a thorough understanding of the corrosion behavior of the specimens and provided valuable data for the thesis report.

e.**Data analysis**

To comprehensively analyze the corrosion behavior of 304 SS within steam autoclave environments, a comparative study was conducted. The corrosion rates and surface morphologies of specimens exposed to different corrosion-inducing solutions and steam autoclave conditions were carefully compared. By analyzing the data obtained from weight loss measurements and scanning electron microscopy (SEM) analysis, the effects of various environmental parameters such as temperature, pressure, and solution chemistry on corrosion behavior were thoroughly examined. Through this analysis, key factors contributing to corrosion initiation and progression in 304 SS within steam autoclave environments were identified. This comparative study provided valuable insights into the corrosion mechanisms of 304 SS and its performance under different environmental conditions, contributing significantly to the understanding of material behavior in steam autoclave environments for the thesis report.

3.5.3 Sample preparation method for immersion coupon.

Before conducting examinations on the specimens, suitable materials were carefully selected and prepared to meet the required standard dimensions. The samples employed were prepared according to ASTM G48 protocol and preparation of the specimens involved various methods, as outlined below.

Step1: Selection of raw materials

Raw materials for specimen preparation were carefully chosen based on the desired chemical compositions and properties required for the study. SS304 sheets were carefully selected from material available at the National Veterinary Industry. These sheets were sourced from machinery known for their diverse functions and were guaranteed to possess the necessary composition and quality. Throughout the selection process, careful consideration was given to factors such as alloy composition, surface finish, and the absence of surface defects to ensure the integrity of the specimens for subsequent corrosion taste. Figure 3.13 shows a prepared sheet of SS material for sample preparation. The other samples were prepared from this sheet metal by cut to required standard dimensions.

Step2: Cutting and machining of SS304 sheets into standard dimension and surface finish

SS304 sheets were precisely cut or machined into standardized dimensions suitable for corrosion testing. This involved the use of hand powered hacksaw of model Bosch and Bosch hand hacksaw machining equipment to achieve accuracy and uniformity in specimen dimensions. Standardized dimensions, typically measuring 4 cm x 4 cm x 0.1 cm, were chosen based on experimental requirements and industry standards for corrosion testing in steam autoclave chambers.

Step3: Surface cleaning and preparation techniques

Surface cleaning and preparation of SS304 specimens were essential steps to ensure the removal of contaminants and surface irregularities that could affect corrosion behavior. this process was employed following the ASTM G1-03 for sample preparation, cleaning and analysis. The cleaning process involved immersing the SS304 specimens in acetone, followed by gentle agitation to facilitate the dissolution and removal of contaminants. Alternatively, the solvents could be applied to the specimen surfaces using lint-free wipes or brushes to target specific areas requiring cleaning. After cleaning, the specimens were air-dried and dried using compressed air to remove any residual solvent.

The following techniques were employed to clean the specimens before applied to corrosive environments:

a) **Degreasing:** -SS304 specimens were degreased using solvents such as acetone and ethanol to remove any oily residues or contaminants from the surface.
b) **Surface scrubbing:** Mechanical scrubbing with lint-free wipes or brushes was performed to remove loose debris and particles adhering to the surface.

Figure 3.14: Shows the SS304 sheet metal selected for study (Photo).

c) **Acid cleaning:** pickling in dilute acid solutions (nitric acid), were employed to remove surface oxides and scales and to passivate the surface.

d) **Surface drying:** After cleaning, the specimens were thoroughly rinsed with deionized water to remove residual cleaning agents and then dried using compressed air and a drying oven to prevent water spotting and ensure a clean, dry surface.

3.5.4 Solution preparation method for 0.5%$NaCl_2$ and 3.5%$NaCl_2$ solution

The preparation of sodium chloride (NaCl) solutions with precise concentrations is crucial for conducting a corrosion study by the immersion method. This section details the methodology employed during preparation 0.5% $NaCl_2$ and 3.5% $NaCl_2$ solutions, which are used to simulate corrosive environments in the study of SS304 stainless steel. Preparation of this solution was according to ASTM G31-72 standard.

Materials employed for preparing the solution

a) Sodium Chloride (NaCl): Analytical grade, high purity.
b) Deionized Water: Free from impurities to ensure accurate solution concentration.
c) Analytical Balance: For precise measurement of NaCl.
d) Volumetric Flasks: 1-liter capacity, calibrated.
e) Stirring Rod or Magnetic Stirrer: For thorough mixing.
f) Beakers and Measuring Cylinders: For preliminary measurements and transfers.

Preparation of 0.5% NaCl solution

1. Calculate the Required Amount of NaCl:

To prepare 1 liter of 0.5% NaCl solution, calculate the amount of NaCl needed:

Mass of NaCl=Desired concentration x Volume of solution

Mass of NaCl=0.5 g/100 mL×1000 mL=5 g

2. Weigh the NaCl: Using an analytical balance, accurately weighed 5 grams of NaCl (as shown in figure 3.14)

3. Dissolve the NaCl in Water:

The weighed NaCl was added to a beaker containing approximately 800 mL of deionized water. And after added the solution stirred with stirring rod.

4. Make up to Volume: Deionized water was added to the volumetric flask until the bottom of the meniscus reaches the 1-liter mark and mixed through many times to keep its homogeneity

Preparation of 3.5% NaCl solution

1. Calculate the Required Amount of NaCl:

To prepare 1 liter of 3.5% NaCl solution, calculate the amount of NaCl needed:

Mass of NaCl=Desired concentration × Volume of solution

Mass of NaCl=3.5 g/100 mL×1000 mL=35 g

2. Using an analytical balance, accurately weigh 35 grams of NaCl was weigh.
3. Dissolve the NaCl in Water: after the weighed add NaCl to a beaker contains approximately 800 mL of deionized water and stirred the solution using a stirring rod until all the NaCl has completely dissolved.
4. Transfer to Volumetric Flask:

Transfer the dissolved solution into a 1-liter volumetric flask and rinse the beaker with deionized water and add the rinsing to the volumetric flask to ensure all NaCl is transferred.

5. Make up to Volume: Add deionized water to the volumetric flask until the bottom of the meniscus reaches the 1-liter mark. And mixed through many times to keep its homogeneity.

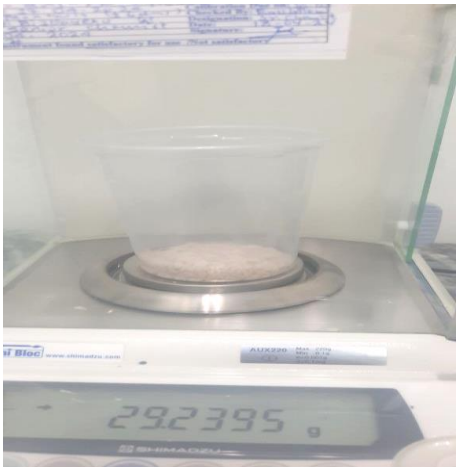

Figure 3.15: Weighing of $NaCl_2$ salts for solution preparation (Photo).

3.5.5 Methodology for weighing using an analytical balance

Step1: Selection of a suitable location

Before performing weighing procedures, an appropriate location was identified to minimize external influences on measurements, ensuring a stable and level surface devoid of external disturbances. Measures were taken to avoid exposure to direct sunlight and drastic temperature variations. Additionally, precautions were implemented to steer clear of magnetic objects or equipment that may generate magnetic fields. Furthermore, efforts were made to ensure a dust-free environment and minimize air currents originating from sources such as ventilators, air conditioners, doors, or windows.

Step2: Leveling the analytical balance

To ensure precise measurements, the analytical balance was horizontally aligned, and its level was adjusted meticulously. Proper leveling of the balance accounted for any minor deviations or tilts. The leveling feet were adjusted until the air bubble in the indicator aligned at the center, ensuring optimal balance alignment for accurate measurements.

Step 3: Calibration of the analytical balance

Calibration is important to guarantee the accurate weighing of samples. To ensure precision, calibration was conducted under varying usage locations or environmental conditions. The analytical balance underwent calibration to maintain accuracy and reliability in measurement.

Step 4: Weighing procedure:

To ensure accurate and reliable measurements, the following procedures were followed when using the analytical balance. The balance was preheated for one hour before usage to stabilize its temperature. Prior to weighing, the balance was zeroed in the unloaded condition by pressing the "tare" button. The SS304 specimens were put at the center of the weighing pan, and the glass door was closed. After waiting for the displayed value to stabilize, indicated by a stability mark, the 'TARE' button was pressed to reset the scale to zero if the mass of the container needed to be subtracted from the measurement. The substance to be weighed was then added after removing the container from the balance to prevent contamination. Finally, the balance was reset with the container, and the mass reading was allowed to stabilize for 5-10 seconds, or longer, if necessary, before recording the measurement. Figure 3.15 shows the procedure during weighing.

Step 5: Recording data

The following data recording data sheet was used to record the weight of samples before and after exposure to the various corrosive environments.

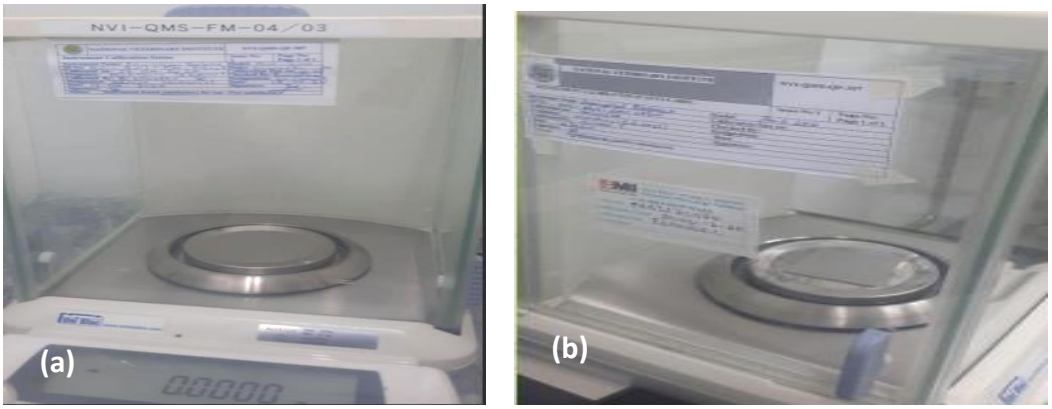

Figure 3.16: Weighing operation process; (a) Tare, (b) Put sample on weighing pad (Photo).

3.5.5.1 Weight loss and corrosion rate calculation

For determine the corrosion rate and weight loss of various samples exposed to different conditions of corrosive solutions the following methods was used:

Step1: Sample preparation: SS304 specimens were prepared by cutting into uniform dimensions, ensuring consistency across samples. The surfaces were mechanically polished to remove any surface imperfections and contaminants, followed by thorough cleaning using a suitable solvent to ensure a pristine surface for testing.

Step2: Exposure to corrosive environment: The prepared SS304 specimens were exposed to the corrosive environment mimicking conditions within the steam autoclave chamber. This involved placing the specimens within the autoclave chamber and subjecting them to steam at elevated temperatures, typical of the operating conditions.

Steap3: Exposure duration: The exposure duration was carefully controlled to simulate real-world operating conditions while ensuring that sufficient data points were obtained for accurate corrosion rate determination. Multiple exposure periods were considered to capture the progression of corrosion over time.

Step4: Weight loss measurement: After the predetermined exposure duration, the SS304 specimens were removed from the autoclave chamber and allowed to cool to room temperature in a to prevent moisture absorption. The specimens were then carefully cleaned to remove any corrosion products and dried thoroughly. The weight loss of each specimen was measured using a precision balance before and after exposure to calculate the mass loss due to corrosion.

$$Wloss = Winitial - Wfinal$$

Step5: Corrosion rate calculation: The corrosion rate of SS304 was determined using the weight loss data obtained from the experiments. The corrosion rate (CR) was calculated using the following formula:

$$CR = \frac{k * Weight\ loss}{Density * Exposed\ Area * Exposure\ Time} \quad (3.1)$$

Where:

K-constant of depend on unit of corrosion rate (87.6 for mm/year and 537 for mpy)

CR is Corrosion rate in mm/year,

Weight Loss: Mass loss of the SS304 specimen due to corrosion (milligrams)

Density: Density of SS304 (grams per cubic centimeter)

Exposed Area: Surface area of the SS304 specimen exposed to the corrosive environment (square centimeters)

Exposure Time: Duration of exposure to the corrosive environment (hours).

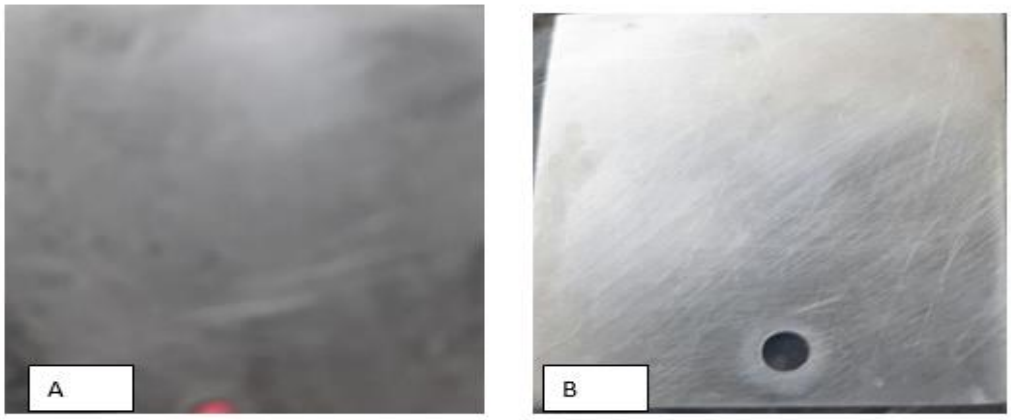

Figure 3.17: Samples; (a) Exposed to corrosive steam autoclave environment, (b) Cleaned samples for weight loss measurement (Photo).

Step6: Statistical analysis: Statistical analysis was performed on the corrosion rate data to determine the variability and significance of the results. Descriptive statistics such as mean corrosion rate, standard deviation, and confidence intervals were calculated to assess the reliability of the experimental measurements.

3.5.6 Corroded sample hardness number tester

The Vickers hardness test was utilized to assess the hardness properties of the SS304 specimens before and after exposure to the corrosive environment. Subsequent to the removal of the samples from the corrosive media and their cleaning, they were taken to the Vickers hardness tester machine to determine the hardness number of the samples after exposure to various solutions and conditions for different durations. Figure 3.17 shows samples hardness measuring process on Vickers harness instrument.

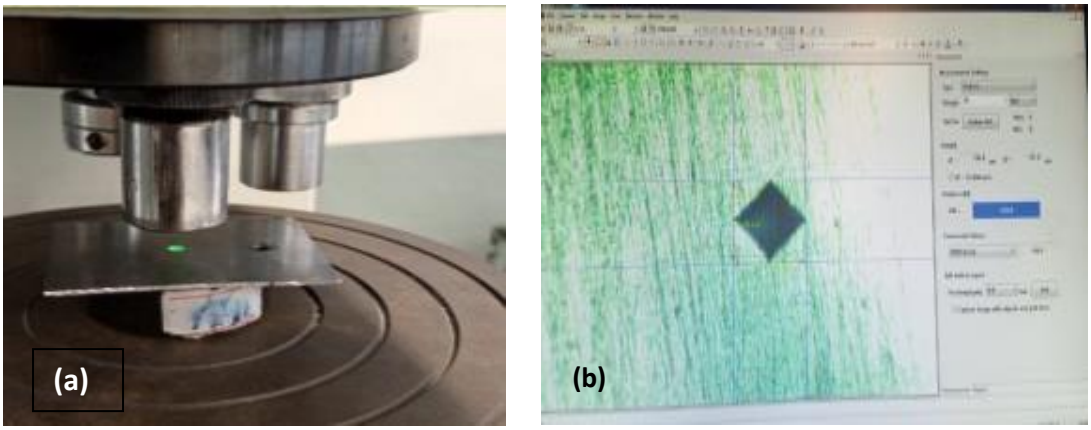

Figure 3.18: Hardness tester; (a) Hardness testing process, (b) Test result (Photo).

3.5.7 Sample material composition testing using x-ray fluorescence (XRF) spectrometer

General procedure used for measuring the material composition of stainless steel 304 (SS304) using X-ray fluorescence (XRF) spectroscopy of Spectro Maxx model of SpectromaxxVer 7.0 using Fe-01-M method. Figure 3.18 show XRF spectroscope instrument employed in samples materials identifications. The following step is employed during analysis of SS304 specimen's elemental compositions.

Step 1: Instrument setup

To ensure accurate measurements, the X-ray fluorescence (XRF) spectrometer was turned on, and it was allowed to warm up according to the manufacturer's instructions. Following this, the instrument was calibrated using certified reference materials to ensure precision and accuracy in the measurements.

Step 2: Sample preparation

To ensure accurate analysis, the SS304 samples were meticulously prepared according to the following protocol. Each sample was thoroughly cleaned to remove any contaminants, ensuring its pristine condition. In the case of bulk materials, efforts were made to ensure homogeneity and flatness to guarantee uniformity in subsequent analyses. For irregularly shaped or coated samples, additional steps such as grinding or polishing were undertaken to achieve a flat surface, eliminating any surface coatings and facilitating precise measurements.

Step 3: Instrument calibration

To ensure the accuracy and reliability of the analysis, the instrument was calibrated using a set of reference standards with known compositions covering the elements of interest in SS304, such as iron, chromium, nickel, and manganese. This calibration process allowed for precise quantification of these elements in the SS304 samples. Additionally, a background

correction was performed to account for any signals originating from the sample holder or air, ensuring the accuracy of the measurements

Step 4: Measurement setup

To begin the analysis, the SS304 sample was carefully placed in the X-ray fluorescence (XRF) instrument's sample chamber. Subsequently, the appropriate measurement mode and parameters were selected to optimize the analysis. This involved choosing the most suitable excitation conditions, including voltage and current, based on the elements of interest and their expected concentration ranges. These steps ensured that the XRF analysis was conducted under optimal conditions, allowing for accurate and reliable determination of the elemental composition of the SS304 sample.

Step 5: Measurement procedure

To begin the X-ray fluorescence (XRF) analysis, the measurement was initiated, and the instrument emitted X-rays onto the SS304 sample, causing it to fluoresce. The characteristic X-rays emitted by the sample for each element of interest were then measured. To ensure accuracy and precision, multiple measurements were acquired. These steps allowed for a thorough analysis of the elemental composition of the SS304 sample, providing reliable results for further interpretation and analysis.

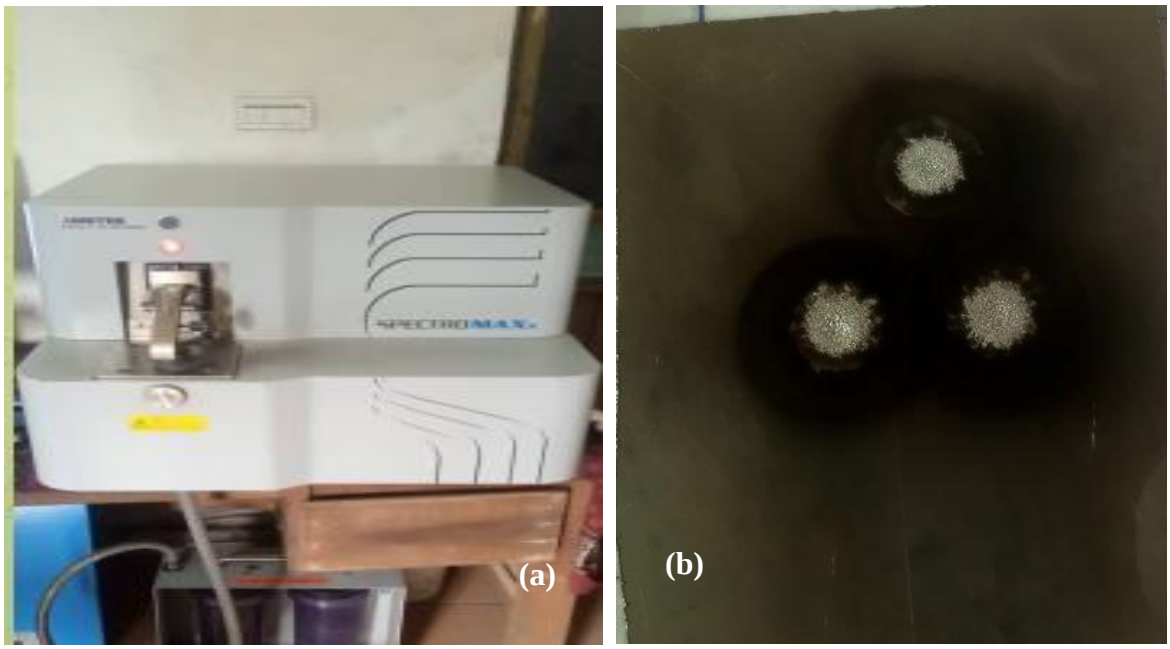

Figure 3.19 (a) X-ray fluorescence (XRF) spectrometer, (b) Samples bombarded by electron and shows after taste (Photo).

Step 6: Data analysis

Following the X-ray fluorescence (XRF) analysis, the obtained spectra from the SS304 sample were carefully analyzed. Using the calibration curve generated during the calibration

process, the elemental concentrations were quantified accurately. This allowed for the calculation of the composition of the SS304 sample based on the measured elemental concentrations. By meticulously analyzing the XRF spectra and quantifying the elemental concentrations, a comprehensive understanding of the composition of the SS304 sample was achieved, providing valuable insights for the thesis report.

Step 7: Reporting

After completing the X-ray fluorescence (XRF) analysis and quantifying the elemental concentrations of the SS304 sample, the results were compiled into a comprehensive report. This report included detailed information about the measured elemental concentrations, as well as any relevant information about the sample and measurement conditions. By summarizing the findings in this manner, the report provided a clear and concise overview of the analysis, ensuring that the results could be effectively communicated and interpreted within the context of the thesis.

Step 8: Instrument shutdown

Upon completion of the X-ray fluorescence (XRF) analysis, the spectrometer was turned off, adhering to all manufacturer-recommended shutdown procedures. Following this, the instrument and sample chamber were thoroughly cleaned as necessary. These steps were taken to maintain the instrument in optimal condition and to ensure that subsequent analyses would not be affected by any residual material or contamination. By following proper shutdown and cleaning procedures, the integrity of the instrument was preserved, and reliable results could be obtained for future analyses.

3.5.7 Scanning electron microscope (SEM) methodology

The procedure for using a scanning electron microscope (SEM) to investigate the corrosion of stainless steel (SS) 304 typically involves the following steps:

a. Sample preparation: samples were reduced to 10 mm x10 mmx1mm suitable sizes for SEM putter, ensuring that representative areas of interest are included.
b. Clean the specimen thoroughly to remove any surface contaminants or oxides that could interfere with the analysis.
c. Mounting procedure: The SS304 specimens were carefully mounted onto the sample mounts using conductive adhesive. Prior to mounting, the specimen surfaces were cleaned to remove any contaminants or residues that could interfere with SEM analysis. Once mounted, the specimens were securely affixed to the mounts, ensuring stability during SEM imaging and analysis.

d. Loading the Specimen into the SEM: Carefully load the mounted SS 304 specimen into the SEM chamber using a manipulator or sample holder, taking care to avoid damaging the specimen during loading.
e. SEM instrument calibration: Calibrate the SEM instrument, including adjusting electron beam settings such as accelerating voltage, beam current, and spot size, to optimize imaging conditions for the SS 304 specimen.
f. Surface imaging: Capture high-resolution SEM images of the SS 304 specimen's surface to scrutinize its micro structural morphology and corrosion characteristics...Employ imaging methods such as secondary electron imaging (SEI) or backscattered electron imaging (BEI) to observe surface features and characteristics.
g. X-ray diffraction spectroscopy (XRD) analysis was conducted to ascertain the elemental composition of corrosion products and identification of surface element crystal phase.
h. Data analysis and interpretation: SEM images were analyzed and XRD analysis data characterized the corrosion features observed on the surface of the SS 304 specimen.
i. Interpret the results to gain insights into the corrosion mechanisms and behavior of SS 304 under the specific environmental conditions.

3.5.8 Experimental conditions for exposure to steam autoclave

1. Temperature range: SS304 specimens were exposed to a controlled temperature range within the autoclave chamber, replicating typical steam autoclave conditions. The temperature range varied between 121°C to 134°C, reflecting the range commonly encountered in steam sterilization processes. Temperature control within the autoclave chamber was achieved using precision heating elements and a digital temperature controller to maintain stability and accuracy throughout the experiments.
2. Pressure maintained within the autoclave chamber: Pressure within the autoclave chamber was carefully regulated to simulate steam autoclave environments accurately. The pressure maintained within the autoclave chamber was set to 15 psi (pounds per square inch), consistent with standard operating conditions for steam sterilization processes. Pressure control systems were implemented to ensure uniform pressure distribution and stability within the autoclave chamber during the experiments.
3. Duration of exposure: SS304 specimens were subjected to prolonged exposure durations within the steam autoclave chamber to assess corrosion behavior over time. Exposure durations varied from short-term experiments lasting 72 hours to

long-term studies lasting up to 168 hours and each day the samples were exposed to 3cycle of autoclave process. By varying the duration of exposure, the study aimed to evaluate the corrosion resistance of SS304 material under different time frames and conditions representative of real-world applications.

Operating procedure of an autoclave

1. An autoclave functions at 121℃ temperature for at least 30 minutes, utilizing saturated steam under a pressure of 1.5bar – 2bar. The operational steps for running an autoclave are outlined below:
2. Pre-check: Before starting operations, the autoclave undergoes an inspection to ensure no residual items from previous cycles are present.
3. Water loading: Sufficient water is added to the chamber.
4. Material placement: The items intended for sterilization are positioned within the chamber.
5. Sealing and heating: The chamber lid is securely closed, and the screws are tightened to create an airtight seal. Then, the electric heater is activated.
6. Pressure regulation: Safety valves are adjusted to maintain the required pressure inside the chamber.
7. Air purging: Once water in the chamber reaches boiling point, the air-water mixture is allowed to discharge through the vent tube until all remaining air is expelled, indicated by the absence of water bubbles from the pipe.
8. Pressure stabilization: The drainage pipe is sealed, allowing steam to reach the desired pressure, typically up to 2bar.
9. Pressure release: Excess pressure is released through the whistle mechanism once the desired pressure is reached.
10. Holding period: Following the whistle, the autoclave enters a holding phase, typically lasting 15 minutes.
11. Cooling phase: The electric heater is turned off, and the autoclave is left to cool until the pressure gauge indicates atmospheric pressure.
12. Air reintroduction: The discharge pipe is opened to allow external air back into the autoclave.
13. Material retrieval: Finally, the lid is opened, allowing access to the sterilized items within the chamber. Overall, the experimental conditions for exposure to steam autoclave were carefully controlled and monitored to replicate the temperature,

pressure, and duration parameters encountered in industrial steam sterilization processes.

3.5.9 Corrosion monitoring method

To investigate corroded surface and effect of corrosion on samples different method was employed. The method used to monitor corrosion and its effect discussed as follows:

1. **Weight loss measurements and corrosion rate calculation:**

Weight loss measurements were conducted to quantitatively assess the corrosion rates of SS304 specimens exposed to steam autoclave conditions. Before exposure, the initial weight of each SS304 coupon was recorded using a high-precision analytical balance with an accuracy of ±0.001 g. After exposure, the coupons were carefully removed from the autoclave chamber, cleaned to remove any surface contaminants, and re-weighed to determine the weight loss. The corrosion rate of SS304 was calculated based on the difference in weight before and after exposure and expressed in millimeters per year (mm/year) and grams per square meter per hour ($g/m^2/h$).

2. **Hardness number identification:**

Methodology and procedure for identifying surface hardness number using vickers hardness test to study corrosion of SS304.

1. Sample preparation

SS304 samples were prepared for the Vickers hardness test. The samples, measuring 4 cm x 4 cm x 0.1 mm, were cut from sheet stock. The surfaces of the samples were polished using progressively finer grades of silicon carbide (SiC) paper, followed by polishing with alumina slurry to achieve a mirror finish. This ensured the removal of any surface irregularities and contaminants that could affect the hardness measurement.

2. Mounting

The polished samples were mounted on a suitable holder to ensure stability during the hardness test. The mounting process involved securing the samples in a way that prevented any movement or displacement during indentation.

3. Vickers Hardness Testing

The Vickers hardness test was conducted using a Vickers hardness tester. The following steps were undertaken:

1. Loading: A diamond indenter, shaped as a right pyramid with a square base and an angle of 136° between opposite faces, was pressed into the surface of the sample under a specific load. For this study, a load of 10kgf (grams-force) was applied.

2. Indentation: The load was applied smoothly and without shock for a dwell time of 10 seconds to ensure proper indentation.
3. Measurement: After the load was removed, the two diagonals of the resulting indentation were measured using a microscope attached to the hardness tester. The measurements were taken to the nearest micrometer.

4. Calculation of Vickers hardness number (VHN)

The Vickers Hardness Number (VHN) was calculated using the following formula:

$$\mathrm{VHN} = \frac{1.8544 \times F}{d^2} \qquad (3.2)$$

where F is the applied load in kilograms-force (kgf), and d is the average length of the two diagonals of the indentation in millimeters (mm).

3. **Surface analysis techniques (SEM):** Scanning electron microscopy (SEM) was employed for surface analysis of SS304 specimens to characterize corrosion products and surface morphology. After exposure, SS304 specimens were carefully prepared for SEM analysis by mounting them on conductive SEM sample mounts and sputter-coating with a thin layer of gold or carbon to enhance conductivity. SEM imaging was conducted at various magnifications to visualize surface features, corrosion pits, and cracks.

Overall, the combination of hardness effect, weight loss measurements, and surface analysis techniques provided comprehensive insights into the corrosion behavior of SS304 material within a steam autoclave chamber and immersed conditions.

3.5.10 Data collection during experiments

1. Data from Weight Loss of SS316 Specimens: Weight loss of SS304 specimens before and after exposure to steam autoclave conditions was measured using a high-precision analytical balance. Before exposure, the initial weight of each SS304 coupon was recorded. After exposure, the coupons were carefully cleaned to remove any surface contaminants, dried, and re-weighed to determine the weight loss. The difference in weight before and after exposure was calculated to determine the corrosion rate of SS304.
2. Data from the hardness tests were also utilized to analyze the effects of corrosion on the material after exposure to various solutions and conditions under different circumstances. The hardness numbers of samples exposed to these conditions were analyzed and determined using a digital electronics method Vickers hardness tester. Specifically, the model HVS-50 instrument was employed for this purpose.

3. Captured image of corroded surface by SEM method and surface morphology was analyzed. Scanning electron microscopy (SEM) was used to capture high-resolution images of the surface morphology of SS304 specimens before and after exposure to steam autoclave conditions. SEM images were captured at various magnifications to visualize surface features such as corrosion pits, cracks, and surface roughness.

3.5.11 Methods used to analyze collected data

Statistical analysis techniques were employed to analyze the collected data, including weight loss measurements, and XRD. In addition, data interpretation involves comparing results obtained from different experimental conditions and analyzing trends and patterns.

Qualitative analysis of SEM images and XRD spectra was conducted to identify corrosion products, surface defects, and elemental composition changes.OM also was examined the metal microstructure.

CHAPTER FOUR:

4. RESULTS AND DISCUSSION

4.1 Introduction

This chapter presents the results and discussion on the causes of corrosion of SS304. The corrosion behavior was investigated by immersing samples in various environments, both at room temperature and within a steam autoclave chamber. The immersion tests included exposure to 0.5% $NaCl_2$, 3.5% $NaCl_2$, hard water from tap water sources, and pure water. Additionally, in-line tests were conducted within the steam autoclave chamber, with solutions containing 3.5% $NaCl_2$, 0.5% $NaCl_2$, deionized purified water, and hard water, under controlled temperature and pressure conditions.

The data collected from the samples was examined and analyzed using several methods. These included the weight loss method to determine corrosion rates, surface analysis using scanning electron microscopy (SEM) to visualize corroded products and examine surface morphology, and X-ray diffraction (XRD) to identify phases of crystal structure on corroded surface and used determine corrosive element found in the oxide and OM is used to image the metallographic microstructure of corroded surface. Additionally, using XRD the corrosion oxide of samples cutout and taken from the autoclave chamber is determined.

Table 4.1: Elemental compositions of 304 SS specimens for samples employed for experiment

List of elements	**Alloy element name and its symbol**	**Weight Percentage composition (%)**
1	Chromium (Cr)	18.75
2	Nickel (Ni)	8.17
3	Molybdenum (Mo)	0.13
4	Iron (Fe)	Balancing element
5	Carbon (C)	0.073
6	Manganese (Mn)	1.58
7	Silicon (Si)	0.42
8	Phosphorus	0.036
9	Sulfur (S)	0.009

The presence of these alloying elements imparts superior corrosion resistance properties to 304 SS, making it suitable for applications in aggressive environments.

4.2 Corrosion Behavior of SS304 in Steam Autoclave and Room Temperature

For the test of samples immersed in deionized pure and hard water there was no significant change visualized with eyes for the first three-days immersion time. But the surface of samples immersed in hard water is getting darker as the immersion time is increased from 3 days to 5 days and 7days. While, the surface of the sample within pure water at room temperature remains the same. On the other samples immersed in 0.5%$NaCl_2$ and .3.5%$NaCl_2$ solutions become slightly darker on exposure of 3 days. These two samples develop soft passive layers when visualized after seven days of exposure. Samples with 3.5%$NaCl_2$ solutions are totally covered by deposited solid contaminants which segregate at the bottom of the container and form a dark layer. The surface of the sample is gradually changed with the exposed samples into sodium chloride solution. Small, localized pits were observed on the surface of the SS304 samples. These pits appeared to be shallow, with diameters ranging from a few micrometers to several hundred micrometers. The pits exhibited irregular shapes and were distributed unevenly across the surface.

Figure 4.1 shows exposed surface of samples to 0.5%$NaCl_2$ exposed for 168 hours and the picture revealed that there was some deposit of solid contaminant and formation of softer layer of passive film to protect against reaction with cl^- ions in water. Additionally, there was also some visible pit initiation on the surface of samples.

Figure 4.1: Sample of SS304 after exposed to 3.5%$NaCl_2$ solution for 120 hours before cleaning at room temperature (Photo).

Figure 4.2: Samples of SS304 after exposure to pure water for 7 days before cleaning at room temperature (Photo).

Figure 4.2 shows there was no significance visual variation on the surface. The surface clearly shows the sample was protecting against minor contaminants that would probably available in the solution. On the other hand, samples shown in Figure 4.3 shows pitting corrosion of samples exposed to 3.5%$NaCl_2$ solutions for 168 hours. Corrosion of samples imitates by dissolve the passive surface used to protect against corrosive media. Presence of Cl^- ion activates the instability of passive layer and develops shallow pit on surface.

Figure 4.3: Samples exposed to 3.5%$NaCl_2$ solution for 168 hours at room temperature. (Photo).

Figure 4.4: Samples exposed to hard water for 168 hours at room temperature (Photo).

Figure 4.5: Samples exposed to 3.5%$NaCl_2$ solution steam autoclave at 121^{o}c for 168 hours (Photo).

Figure 4.6: Samples taken from corroded autoclave part (Photo).

The images shown in Figures 4.4 and 4.5 depict the conditions of samples exposed to various solutions under different conditions. Figure 4.4 shows samples exposed to hard water for 168 hours at room temperature. Samples shows starting of passive layer formation. The passive layer formed is due to reaction of some contaminants in hard water react with chromium and start formation oxide. Figure 4.5 shows samples exposed to a 3.5% $NaCl_2$ solution in steam autoclave chamber for 168 hours. The samples at these conditions depicts $NaCl_2$ developed a hard layer after 168 hours of exposure formed. This is due to the chromium and nickel content in the material, which forms a corrosion-resistant layer when exposed to high chlorine levels and elevated temperatures. Over time, stainless steel forms highly stable oxides, such as iron oxide and chromium oxide, which prevent the metal from corrosion. Even though the oxide layer formed on the SS surface is strong the pitting was initiated on some part of samples. These were recognized because of high pressure and temperature with chlorine breaks the passive layers protections (Wang *et al.,* 2012).

In the investigation conducted within the autoclave chamber, discernible distinctions were observed in the formation of oxide layers among the samples compared to those exposed at

ambient room temperature. Specifically, when examining the surfaces of samples exposed to pure water and hard water, no significant differences were apparent upon visual inspection. However, upon prolonged exposure (5 days and 7 days) to hard water, a robust layer formed on the surface, displaying resistance to removal during cleaning procedures. Conversely, samples exposed to pure water exhibited the development of a faint dark layer, albeit with minimal alteration in comparison to those exposed to hard water. Contrastingly, samples subjected to 0.5% NaCl and 3.5% NaCl solutions demonstrated the deposition of a distinct layer on the sample surface. This layer began to manifest from day 3 and exhibited increasing strength through day 7 of exposure.

4.3 Weight Loss and Corrosion Rate Measurement

All specimens immersed at the same time in the experimental media of 0.5%$NaCl_2$ solution, 3.5% $NaCl_2$ solution, purified water and hard ground water at room temperature and at steam autoclave condition. The weight-loss values of 304 SS were measured after 3, 5 and 7days intervals from each of these solutions. After samples are removed from exposed area, they chemically cleaned to remove the corrosion products using acetone and distilled water for rinsing the samples for samples with soft layer corrosion and for hard layer corrosion they immersed in to acid solution prepared by 10% nitric acid and 5%HCL with deionized purified water, rinsed with purified water and dried in oven for at 45^{o}c for 15minutes. After dried the samples where weighed and data was recorded. The data was taken to be nearest to 0.0001g. Rec

The corrosion rate of SS304 was determined using the weight loss method. Table 4.2 summarizes the weight loss measurements for each specimen, and the corrosion rates were calculated using the formula (*Schweitzer, 2009*).

Corrosion rate (mpy) = 534W/DAT

Where

mpy – mills per year

W = Weight loss of the specimen (grams)

A = Surface area of the specimen (in^2)

T = Exposure time (hours)

D- Density of materials (g/cm^3) and for SS304 D=7.89 g/cm^3

Table 4.2 shows the average result of weight loss (mg) and corrosion rate (mm/year) for the specimens exposed to pure water, hard water, 0.5%$NaCl_2$, and 3.5%$NaCl_2$ solutions at room temperature and steam autoclave chamber conditions of all solutions. The results of this data were employed to plot the graph of corrosion rate and weight loss of specimens exposed to

Table 4.2: Weight loss and corrosion rate result of exposure at room temperature and autoclave conditions

Samples	Solution Type	Condition	Exposure Time(hrs)	Weight Loss (mg)	Corrosion Rate(mm/year)
A1	Pure Water	25	72	0.01	9.45E-05
B1	Pure Water	25	120	0.01	5.67E-05
C1	Pure Water	25	168	0.02	8.25E-05
A2	Hard Water	25	72	0.05	0.000478
B2	Hard Water	25	120	0.07	0.000396
C2	Hard Water	25	168	0.1	0.000588
A3	0.5% NaCl	25	72	0.2	0.001949
B3	0.5% NaCl	25	120	0.35	0.001886
C3	0.5% NaCl	25	168	0.45	0.001826
A4	3.5%NaCl	25	72	1.1	0.010284
B4	3.5%NaCl	25	120	1.5	0.010399
C4	3.5%NaCl	25	168	1.9	0.007709
A5	Pure Water	121	72	0.05	0.000481
B5	Pure Water	121	120	0.085	0.00049
C5	Pure Water	121	168	0.14	0.000572
A6	Hard Water	121	72	0.15	0.001435
B6	Hard Water	121	120	0.24	0.001358
C6	Hard Water	121	168	0.32	0.001316
A7	0.5% NaCl	121	72	1.3	0.012474
B7	0.5% NaCl	121	120	1.7	0.009664
C7	0.5% NaCl	121	168	2.2	0.009048
A8	3.5%NaCl	121	72	6	0.055521
B8	3.5% NaCl	121	120	7.5	0.041559
C8	3.5% NaCl	121	168	9	0.036305

various solutions and conditions with respect various exposure times.

From the table A1, B1, and C1 were represented the samples immersed in pure water at room temperatures. A2, B2, and C2 were represented samples immersed in hard water at room temperatures for 72hours, 120hours and 168 hours respectively. On the other hand A3, B3, and C3 were represented samples of specimens immersed in to 0.5%$NaCl_2$ solutions for

72 hours, 120 hours and 168hours respectively. A4, B4, and C4 were samples represent exposure of specimens immersed in to 3.5% $NaCl_2$ solution for 72 hours, 120hours and 168 hours respectively. Same way A5 up to C8 represents samples which are exposed to autoclave environments for 72 hours, 120 hours and 168 hours in respective ways to pure water steam, hard water steam, 0.5%$NaCl_2$, and 3.5%$NaCl_2$ solutions of steam autoclave. The weight loss of samples immersed 3.5%$NaCl_2$ is higher compared to other solutions. The loss of specimens is higher in higher concentration of $NaCl_2$ solution due to attack of chloride ions on the passive layer of SS304 surface. Cl^- ions attach passive layers and start dissolution of metal into solution in the form of pitting. Pitting was localized attack on metal surface due to its aggressiveness. Even though, weight loss at this concentration was below the allowable expected loss of materials, but as concentration of NaCl solution increase it will greatly affect the metal surface severely.

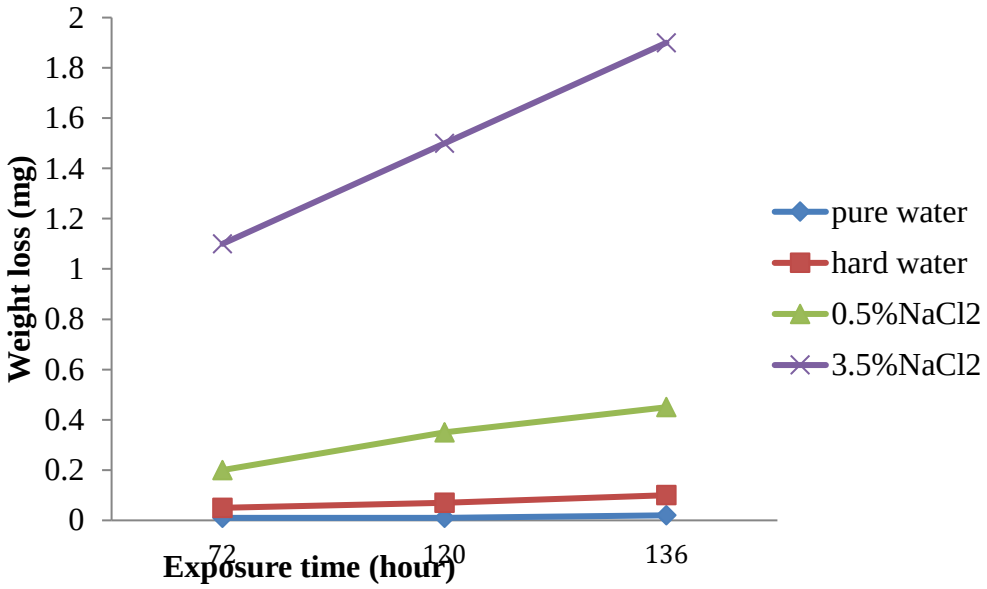

Figure 4.7: Weight loss of specimens at room temperature and solutions like pure water, hard water, 0.5%NaCl, 3.5%NaCl

Figure 4.8 shows weight loss of specimens exposed to pure water, hard water, 0.5%$Nacl_2$ solution and 3.5%$NaCl_2$ solutions for 72 hours, 120hours and 168hours at room temperature and atmospheric pressure. The result shows weight loss of SS304 increase for all types of solutions at different significance with respect to exposure time. For samples immersed in purified water there is minor loss of weight, which is almost insignificant. Samples immersed in hard water for different exposure hours showed some slight difference in weight loss compared to purified water, but still it was small compared to the other samples immersed in NaCl2 solution for different hours. The samples immersed in to 0.5% $NaCl_2$ shows moderate corrosion loss compared to purified and hard water. On the other hand, the

samples immersed in to 3.5%$NaCl_2$ solutions were higher than other samples exposed to different solutions for the same time of exposure at room temperature. According to various researchers, as the concentration of $NaCl_2$ increased more the corrosion of SS304 becomes increase (Jian *et al.*, 2015; Sanchez *et al*.,2018).

Figure 4.9 shows weight loss of samples exposed to autoclave condition (121^{o}c temperature and 1.5 bar pressure) for pure water, hard water, 0.5%$NaCl_2$, 3.5%$NaCl_2$ solutions for time exposure of 72hours, 120hours and 168hours. The graph illustrates the weight loss where slightly small for samples exposed to pure water and hard water. On the other hand, samples exposed to $NaCl_2$ solution shows higher and increases with time and concentrations. The weight loss of samples exposed to steam autoclave at 3.5%$NaCl_2$ solution where higher due to chloride ion aggressive reaction on SS304 samples. The chromium and iron forms oxide while the samples exposed to Cl^- ions resistivity of passive layer was dissolved. Pitting corrosion formed because of chloride concentration were visualized on the samples surface. The maximum weight loss 9mg where registered for sample exposed to 3.5%$NaCl_2$ solution for 168 hours.

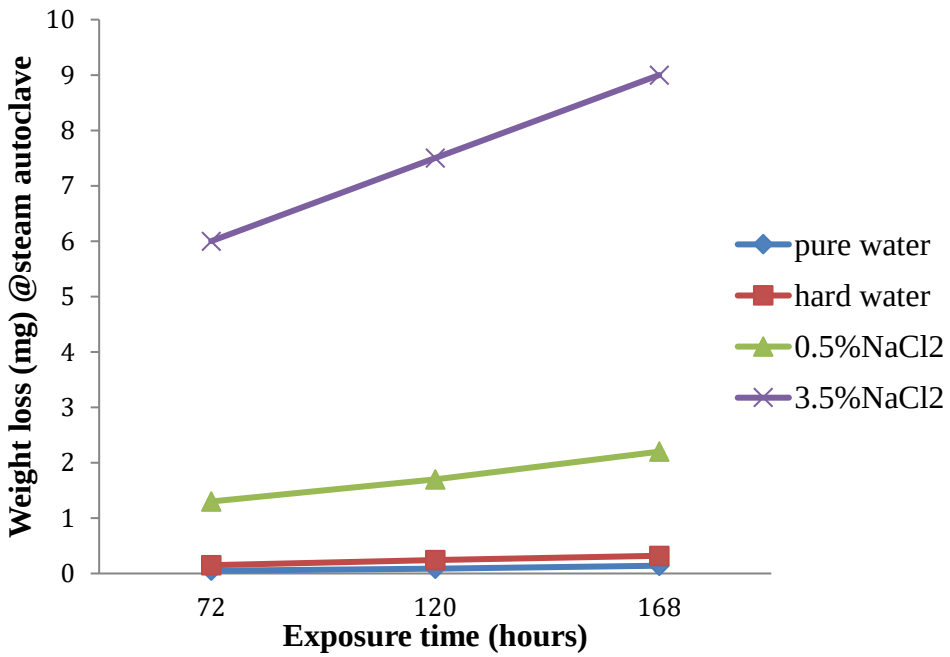

Figure 4.8 Weight of specimens exposed to steam autoclave condition for pure water, hard water, 0.5%NaCl solution and 3.5%NaCl solution at steam autoclave chamber.

Figure 4.10 shows the weight loss comparison between samples exposed to room temperature and samples exposed to steam autoclave at the similar solutions like pure water, hard water, 0.5%$NaCl_2$ solution and 3.5%$NaCl_2$ solution. The graph shows the samples exposed to steam autoclave conditions where loss more weight compared to samples

immersed in same solution and at room temperature. The samples exposed to steam autoclave chamber encounter higher corrosion effect and weight loss due to chloride ion reaction with material is activated at higher temperature. Pitting formation of samples increased for higher temperature and higher concentration (3.5$NaCl_2$ solution) (Nair *et al.*, 2020).

Figure 4.10 shows corrosion rate of samples exposed to both room temperature and atmospheric pressure and steam autoclave conditions (121^{o}c temperature and 1.5bar pressure) at various solutions like pure water, hard water, 0.5%$NaCl_{.2}$ solution and 3.5%$NaCl_2$ solution. The result indicates there was higher corrosion rate with samples exposed to steam autoclave at similar solutions. The result indicates dissolution material where activated at higher temperature. The corrosion rate of samples exposed to 3.5%NaCl2 solution where higher (0.0363mm/year) compared to other samples. These were happened due to chemical reactivity of sodium chloride solution increase at higher temperature and create chemical instability of samples passive layer. Chemical reaction of material increased with temperature and forms corrosion on surface exposed to $NaCl_2$ solutions (Sanchez *et al.*,2018).

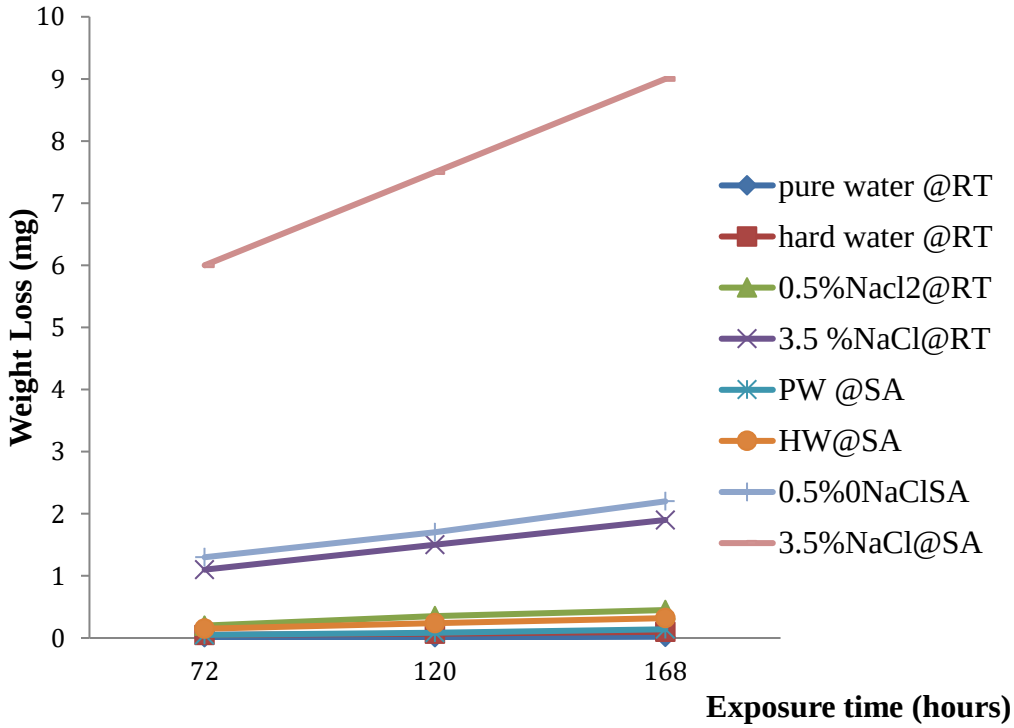

Figure 4.9 Comparison of weight loss for samples exposed to room temperature and autoclave conditions

The graph is shows almost for all types of samples corrosion rate is decrease with time. The corrosion rate of samples where decreased the first few days exposure of samples start

formation of metastable pitting as passive which prevents the surface from corrosion. The stability of this layer start dissolves after certain exposure period of material at higher temperature and higher concentrations. The passive layer of SS304 where start form corrosion initially and after certain time it start forms passive layer which decrease corrosion rate of material (Ajay et al., 2021).

Figs. 4.10 shows the relation between corrosion rate of 304 SS against exposure condition in different concentrations for different exposure time, respectively. The result from the graph shows specimens exposed to steam autoclave conditions experience more weight loss in their respective types of solutions. Samples exposed to 3.5%%$NaCl_2$ experience more weight loss than the other specimens.

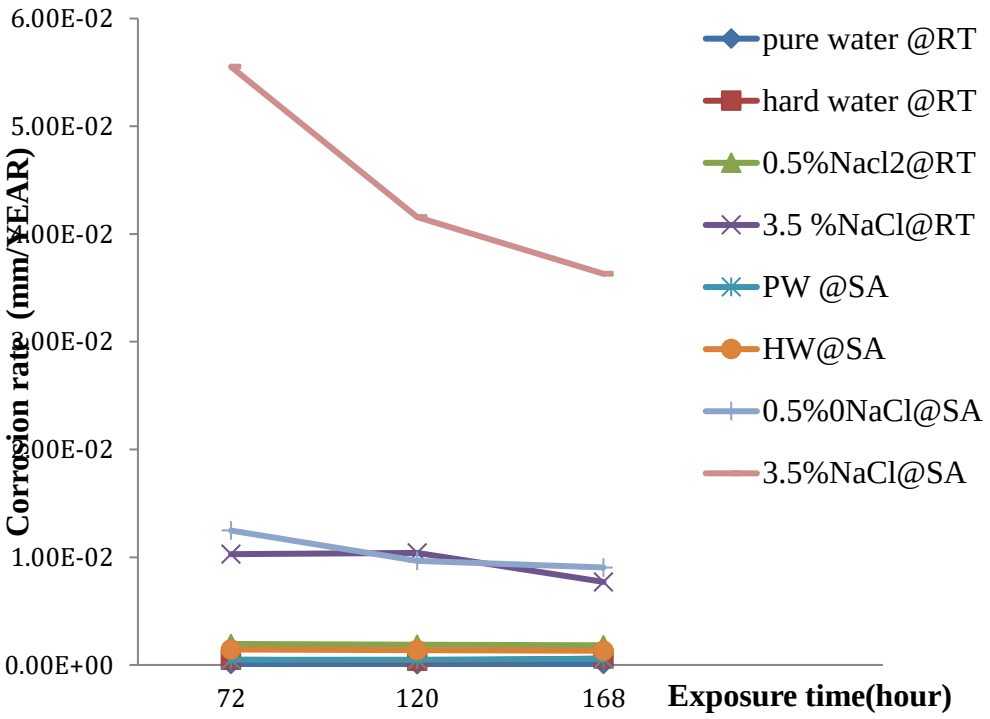

Note : @RT – at room temperature, @PW- at purified water, @HW- at hard water, and @SA-at steam autoclave

Figure 4.10 Comparison of corrosion rate of specimens exposed to various solution at room temperature and autoclave conditions

4.3.1 Main effect of solution type, condition, and exposure time on SS304 corrosion rate and weight loss

The solution type, condition, and exposure time has a significant effect on the corrosion rate and weight loss of SS304, as shown in Table 4.3. The highest corrosion rate and weight loss occur in the 3.5% NaCl solution, with mean values of 0.0256872 mm/year and 4.32333 mg,

respectively. This highlights the high susceptibility of SS304 to corrosion in a saline environment, especially at higher salt concentrations. The 0.5% NaCl solution also exhibits notable corrosion, with a corrosion rate of 0.0064516 mm/year and a weight loss of 1.06358 mg, although these values are notably lower than those in the 3.5% NaCl solution.

In contrast, hard water and pure water demonstrate much lower corrosion rates and weight losses. Hard water displays a corrosion rate of 0.0010434 mm/year and a weight loss of 0.19333 mg, while pure water indicates the lowest corrosion rate and weight loss at 0.0002534 mm/year and 0.04683 mg, respectively. The reduced corrosion rates in hard water and pure water imply that SS304 is considerably more corrosion-resistant in these settings.

Exposure conditions significantly influence the corrosion behavior of SS304. In a steam autoclave, corrosion rates and weight losses are notably higher compared to room temperature exposure. Corrosion rate in the steam autoclave is 0.0137 mm/year with a weight loss of 2.311 mg, whereas at room temperature, the corrosion rate and weight loss are much lower at 0.0030 mm/year and 0.503 mg, respectively. This highlights that high-temperature, high-pressure steam environments speed up the corrosion of SS304.

Exposure time significantly influences the corrosion rate and weight loss of SS304. The data indicates that as exposure time rises, both the corrosion rate and weight loss initially climb and then level off. Following 3 days of exposure, the corrosion rate peaks at 0.010323 mm/year with a weight loss of 1.09563 mg. After 5 days, the corrosion rate slightly drops to 0.007531 mm/year, accompanied by a weight loss of 1.33925 mg. By day 7, the corrosion rate further decreases to 0.00722 mm/year, while the weight loss rises to 1.78543 mg. In summary, the corrosion behavior of SS304 is greatly affected by the solution type, exposure conditions, and duration of exposure. The most significant corrosion rates and weight losses occur in high salinity settings (3.5% NaCl) and in steam autoclave environments. Corrosion rates decline with time, indicating an initial rapid phase followed by a more gradual, stable phase.

Table 4.3: Main effect of solution type, condition and exposure time on the corrosion rate and weight loss of SS304

Factor	Parameters	
Solution Type	Weight Loss (mg)	Corrosion Rate(mm/year)
0.5% NaCl	1.06358± 0.8157941[b]	0.0064516± 0.0046232[b]
3.5% NaCl	4.32333± 2.9641753[a]	0.0256872± 0.0178691[a]
Hard Water	0.19333± 0.2394540[c]	0.0010434 ±0.0009431[c]
Pure Water	0.04683± 0.0488286[c]	0.0002534± 0.0002124[d]
CV (%)	13.82732	12.99383
LSD (0.05)	0.1304	0.0007
Condition		
Room Temperature	0.503± 0.6825218[b]	0.0030± 0.0039684[b]
Steam Autoclave	2.311± 2.9354948[a]	0.0137± 0.0175820[a]
CV (%)	13.82732	12.99383
LSD (0.05)	0.0922	0.0005
Exposure Time		
3 days	1.09563 ± 1.85[c]	0.010323 ± 0.017[a]
5 days	1.33925± 2.23[b]	0.007531 ± 0.012[b]
7 days	1.78543± 2.779[a]	0.00722± 0.0111[b]
CV (%)	13.82732	12.99383
LSD (0.05)	0.1129	0.0006

All values are mean ± standard deviation. Means within a column with the different superscript letters are significantly different at $P<0.05$. Where: CV= coefficient of variance, LSD = least significant difference

4.3.2 Interaction effects of the factors on corrosion rate and weight loss of SS304

Table 4.4 presents the interaction effects of solution type, condition, and exposure time on the corrosion rate and weight loss of SS304 stainless steel, revealing significant variability under different conditions. The highest weight loss occurred under ABC16 (8.6250 mg) and ABC 17 (6.8250 mg), indicating severe material degradation due to aggressive environmental factors. Conversely, ABC7 and ABC18 exhibited the lowest weight loss (0.0100 mg), indicating minimal corrosion. Similarly, the highest corrosion rates were recorded for ABC3 (0.053406 mm/year) and ABC 17 (0.0380330 mm/year), while ABC7

Table 4.4: Interaction effect of solution type, condition and exposure time on the corrosion rate and corrosion loss of SS304

Factor	Parameters	
Code	Weight Loss (mg)	Corrosion Rate (mm/year)
ABC1	0.0185 ± 0.0015^{k}	$0.000078033 \pm 4.4500936E\text{-}6^{j}$
ABC2	0.0650 ± 0.0050^{kj}	$0.000375496 \pm 0.000020752^{j}$
ABC3	5.7000 ± 0.3000^{c}	$0.053406 \pm 0.0021144^{a}$
ABC4	1.1650 ± 0.0650^{g}	$0.0110562 \pm 0.000772510^{ef}$
ABC5	0.6350 ± 0.3150^{h}	$0.0026124 \pm 0.0012959^{ih}$
ABC6	0.0450 ± 0.0050^{kj}	$0.000433544 \pm 0.000044198^{j}$
ABC7	0.0100 ± 0.0000^{k}	$0.000057000 \pm 3E\text{-}7^{j}$
ABC8	0.1150 ± 0.0350^{ikj}	$0.0010876 \pm 0.000346925^{ij}$
ABC9	0.1400 ± 0.0000^{ikj}	$0.000575416 \pm 3.3105E\text{-}6^{ij}$
ABC10	0.0300 ± 0.0200^{k}	$0.000289033 \pm 0.000191934^{j}$
ABC11	1.3000 ± 0.0000^{g}	$0.0124890 \pm 0.000014706^{ed}$
ABC12	1.7000 ± 0.0000^{f}	$0.0099838 \pm 0.000319543^{gf}$
ABC13	2.4500 ± 0.5500^{d}	$0.0136285 \pm 0.0032294^{d}$
ABC14	0.1815 ± 0.1685^{ikj}	$0.000980868 \pm 0.000905370^{ij}$
ABC15	2.3500 ± 0.1500^{ed}	$0.0096952 \pm 0.000647344^{gf}$
ABC16	8.6250 ± 0.3750^{a}	$0.0344127 \pm 0.0018919^{c}$
ABC17	6.8250 ± 0.6750^{b}	$0.0380330 \pm 0.0035255^{b}$
ABC18	0.0100 ± 0.0000^{k}	$0.000096367 \pm 1.8502252E\text{-}6^{j}$
ABC19	0.0725 ± 0.01250^{kj}	$0.000424454 \pm 0.000065152^{j}$
ABC20	0.4000 ± 0.2000^{ihj}	$0.0037261 \pm 0.0017771^{h}$
ABC21	2.0000 ± 0.1000^{ef}	$0.0081930 \pm 0.000483790^{g}$
ABC22	0.4500 ± 0.0000^{ih}	$0.0018346 \pm 8.941E\text{-}6^{ihj}$
ABC23	0.0650 ± 0.0050^{kj}	$0.000375496 \pm 0.000020752^{j}$
ABC24	0.2350 ± 0.0050^{ikj}	$0.0013761 \pm 0.000017616^{ij}$
CV (%)	13.827	12.993
LSD (0.05)	0.3193	0.0018

All values are presented as mean ± standard deviation. Means within a column that have different superscript letters are significantly different at $P<0.05$. Here, CV stands for the

coefficient of variance and LSD stands for least significant difference. The sample identifiers are as follows: ABC2, ABC5, ABC8, ABC6, ABC23, and ABC24 represent hard water; ABC3, ABC4, ABC13, ABC16, ABC17, and ABC21 represent a 3.5% NaCl solution; ABC14, ABC11, ABC15, ABC12, ABC22, and ABC20 represent a 0.5% NaCl solution; and ABC1, ABC7, ABC9, ABC10, ABC18, and ABC19 represent pure water at room temperature and steam autoclaved for 72, 120, and 168 hours, respectively.

(0.000057000 mm/year) and ABC18 (0.000096367 mm/year) showed the lowest rates. Intermediate values were noted for ABC3 and ABC4 in both weight loss and corrosion rate, highlighting varying degrees of corrosion intensity. These findings underscore the significant impact of solution type, condition, and exposure time on SS304's corrosion behavior, with severe conditions likely involving high acidity or alkalinity and extended exposure, while mild conditions suggest neutral pH environments or shorter exposure durations. This study highlights the critical importance of understanding environmental interactions in predicting and mitigating corrosion in SS304. Future research should focus on isolating specific contributing factors within each condition to develop more targeted corrosion prevention strategies.

4.4 Hardness Number Analyses for Samples Exposed to Various Solution and Conditions

The Vickers hardness testing was conducted to evaluate the hardness properties of the SS304 specimens after exposure to the corrosive environment. The following section presents the results of the Vickers hardness tests, including the hardness values obtained for each specimen under different conditions

According to taste result from Table 4.5 and Figure 4.11 the hardness of samples exposed to 3.5%$NaCl_2$ solution is decrease with exposure time. At the first 72hours the hardness of samples was high which is 591.367 HV and for exposure for 168hours the hardness value was dropped to 537.27 HV. As the exposure time of samples to corrosive solution increase the hardness of material becomes dropped. The corrosion react with material makes the bond between the surface element broken due to the electrochemical reaction. Dissolution of material at the surface makes the surface hardness of corroded material becomes soft and decreased. Exposure time affects the hardness value of specimens.

Table 4.5: The effect of exposure time on hardness number of samples exposed to 3.5%$NaCl_2$ solution at room temperature

Samples @various exposure hours at 3.5%$NaCl_2$	Sample 1 (Exposed for 72 hours	Sample 2 (exposed for 120 hours)	Sample 3 (exposed for 168 hours)	Sample 4 (exposed for 336 hours)
Average of Hardness number (HV) from three sample taste	591.367	587.07	557.76	537.27

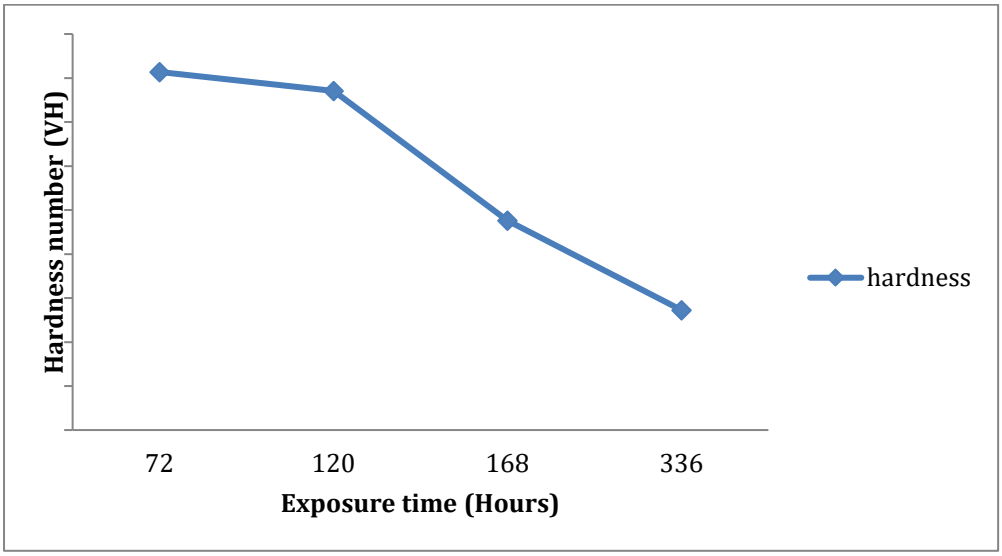

Figure 4.11: Graph shows the effect of corrosion on hardness at exposure time variation

Table 4.6 and Figure 4.12 show the effect of temperature on hardness of materials. The taste was done for samples exposed to 3.5%$NaCl_2$ solution at room temperature and within steam autoclave chamber. The result depicts the hardness is low in high temperature and pressure 3.5%$NaCl_2$ solution. This is happened due to dissolution of passive layer at surface. The temperature increases chemical reaction of element with oxidation chlorine ion.

Table 4.6: Effect of temperature on hardness of samples exposed to 3.5%$NaCl_2$ solutions.

Exposure conditions	Room temperature	Steam autoclave
Average Hardness number (HV)	531.6	458.27

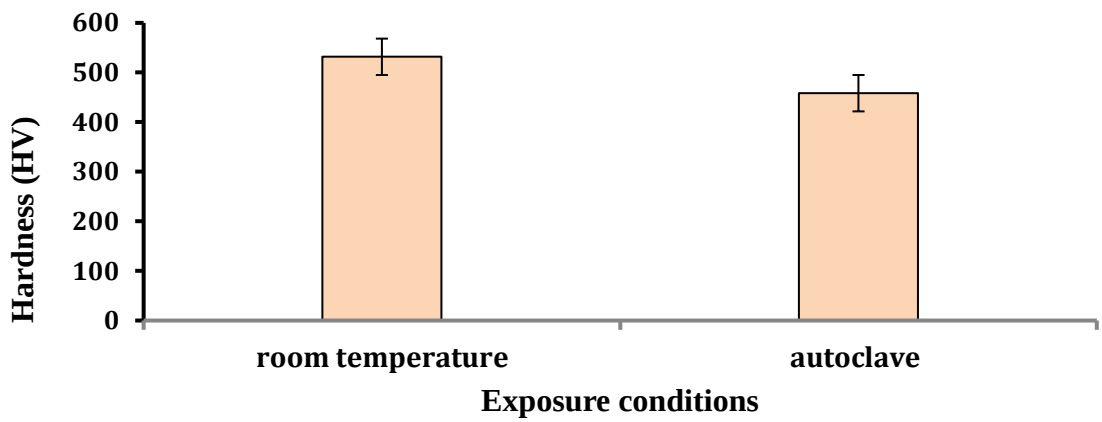

Figure 4.12: Bar chart shows the variation of hardness number with respect to samples exposed to room temperature and steam autoclave.

Table 4.7: Variation of hardness number at different solutions of samples in steam autoclave chamber at exposure of 168 hours.

Solution	Pure water	Hard water	0.5%$NaCl_2$	3.5%$NaCl_2$
Hardness (HV)	576.53	554.93	481.5	460.47

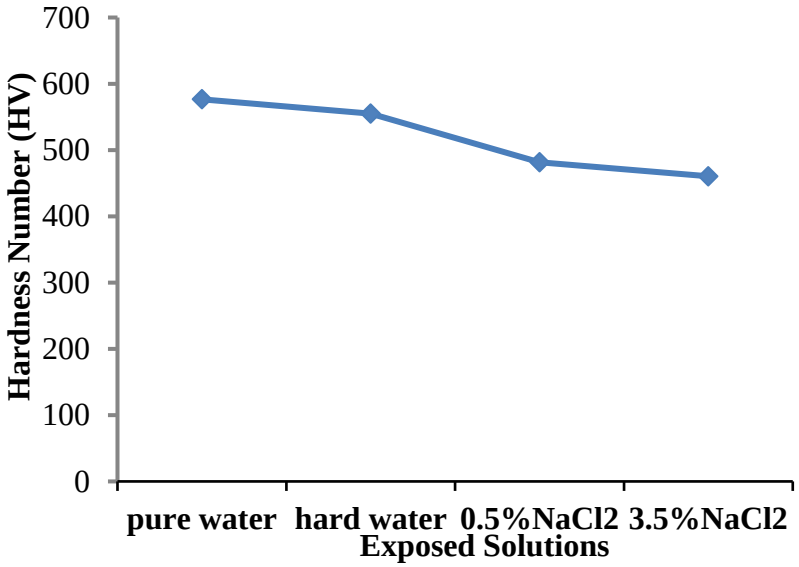

Figure 4.13: Effect of different solution corrosion on material hardness number.

The experiment investigated the corrosion behavior of SS304 in various aqueous environments, including pure water, hard water, 0.5% NaCl solution, and 3.5% NaCl solution, using a steam autoclave chamber. Table 4.7 and Figure 4.13 shows the hardness of each solution was determined using the hardness test, with results indicating 576.53 HV for pure water, 554.93 HV for hard water, 481.5 HV for 0.5% NaCl solution, and 460.47 HV for 3.5% NaCl solution.

4.4.1 Corrosion susceptibility in different environments and its effects on hardness

The obtained results reveal interesting insights into the corrosion susceptibility of SS304 in different environments. The relatively high hardness value recorded for pure water, exceeding expectations for its benign nature, underscores the presence of dissolved ions or impurities that contribute to corrosion processes. Despite being considered less aggressive than saline solutions, pure water's capacity to promote corrosion highlights the importance of thorough environmental analysis in corrosion studies.

In comparison, hard water demonstrated marginally reduced hardness, indicating a slightly lower corrosion potential. However, the persistence of dissolved minerals and ions in hard water underscores the continued risk of corrosion, albeit mitigated to some extent compared to pure water.

4.4.2 Influence of sodium chloride concentration

The observed decrease in hardness with the addition of sodium chloride is notable. In the case of the 0.5% NaCl solution, a decrease in hardness to 481.5 HV suggests a moderating effect on corrosion. This phenomenon could be attributed to the formation of a protective oxide layer on the SS304 surface in the presence of chloride ions, thereby hindering further corrosion progression.

Conversely, the 3.5% NaCl solution exhibited the lowest hardness value of 460.47 HV, indicative of heightened corrosion potential. The higher salt concentration significantly amplifies the aggressiveness of the solution, accelerating the corrosion rate of SS304. This finding underscores the critical role of salt concentration in determining the corrosive behavior of stainless-steel materials.

4.5 Surface Analysis of Corroded Surface Samples (SS304)

4.5.1 SEM analysis of corroded surface of SS304

SEM analysis revealed significant corrosion damage on the surface of the SS304 samples. The general corrosion morphology varied across the samples, with some areas showing extensive corrosion while others remained relatively unaffected. Figure 4.14 shows a SEM image of the corroded SS304 surface during immersion to 3.5%$NaCl_2$ solution at room

temperature. As the image depicts the encircled area shows the initiation of pitting corrosion due to exposure of SS304 to cl^- environment. The white spot shows initiation of pitting corrosion during exposure time.

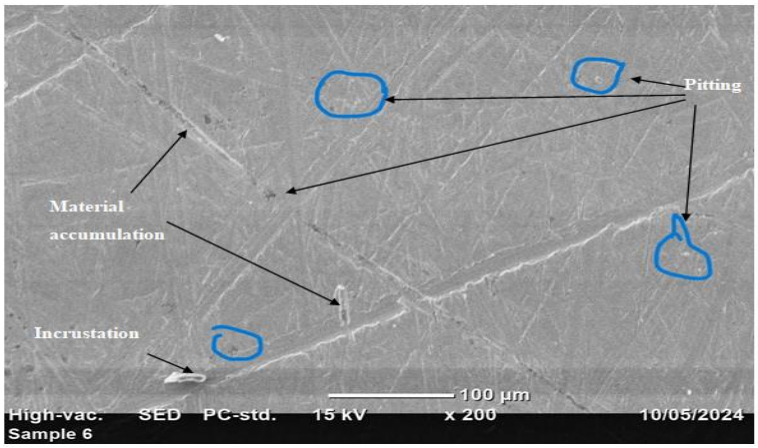

Figure 4.14: SEM images from immersion of SS304 to 3.5%$NaCl_2$ solution for 7 days

The SEM images in Figure 4.15 depict the complete deposition of a passive layer, used at protecting the underlying surface from chloride attack. The surface exhibits the accumulation of iron hydroxides or oxides, resulting from the presence of water, as well as chlorides due to chloride ion attack. As clearly observed in the SEM images, a deposition consisting of oxides and other materials, is evident. According to the image shown during image of SEM from samples b all the surface of samples covered with material deposition and some pitting corrosions are available.

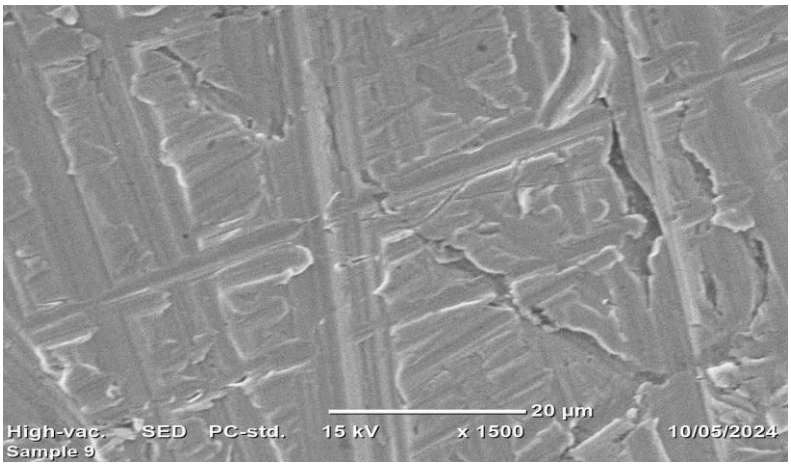

Figure 4.15: SEM Image of corroded SS304 surface for samples in steam autoclave chamber at 3.5%$NaCl_2$ solution, exposed for 136 hours

The samples displayed in the figure 4.16 were extracted from the autoclave component. The affected areas exhibit localized pitting corrosion, resulting in a notable alteration of the microstructure from a coarse grain structure of austenite to a fragmented fine grain structure. As a consequence of the localized corrosion, the grain boundaries on the surface are no

longer clearly defined in this region.

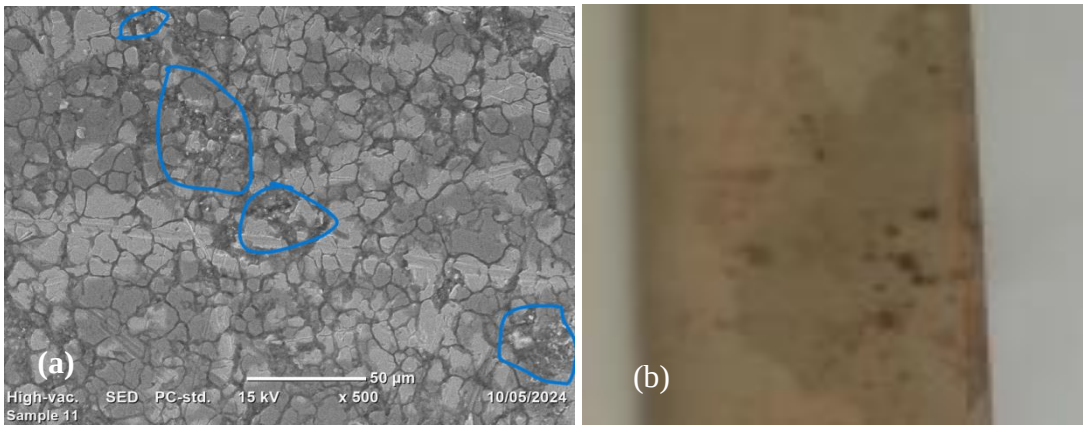

Figure 4.16: Samples taken from the autoclave machine part which was employed in the chamber: (A) SEM images, (B) Corroded surface of autoclave

4.5.2 Metallographic microstructure of corroded surface of SS304

From Figure 4.17 observation of optical microscope result shows pitting. The metallographic analysis of the SS304 samples provided several critical insights into the corrosion behavior and microstructure changes induced by exposure to different environments. The following observations were made:

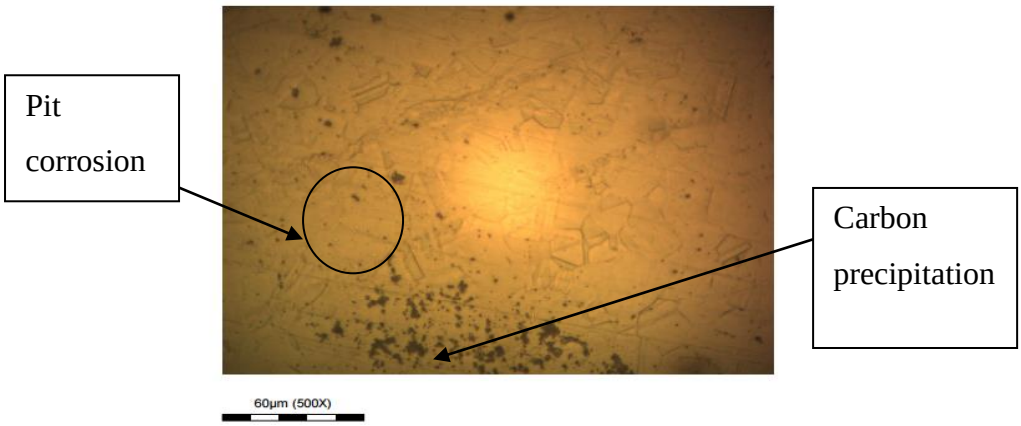

Figure 4.17: Image of metallographic of specimens after exposure to 3.5% $NaCl_2$ solution.

Small Bright Spots shown on the figure revealed the presence of small, bright spots scattered across the surface of the samples. These localized areas of increased brightness are indicative of corrosion products or localized corrosion attack. The occurrence of these spots suggests that the protective passivation layer on the SS304 surface has been compromised, leading to the initiation of corrosion processes. This breach in the passive film allows for localized oxidation, resulting in the formation of bright spots which can be attributed to the accumulation of corrosion products such as iron oxides or hydroxides.

Another significant observation was the presence of black spots on the surface of the samples. These black spots were found to be areas where the surface has been affected and

eroded, likely during the mechanical polishing of the samples. The appearance of these spots indicates areas of severe surface degradation, which could be due to the combined effects of mechanical wear and corrosive attack. The black coloration typically signifies the presence of more severe corrosion products or oxides, which have formed due to the breakdown of the surface under aggressive environmental conditions.

Grain Structure of the samples we can understand that the grain structure of the material was prominently visible in the metallographic images, providing valuable information about the microstructure characteristics of the SS304 samples. The material exhibited a predominantly wide grain surface, indicative of a coarse grain structure. This coarse grain structure can influence the corrosion resistance of the material, as larger grains generally have fewer grain boundaries, which can act as sites for corrosion initiation.

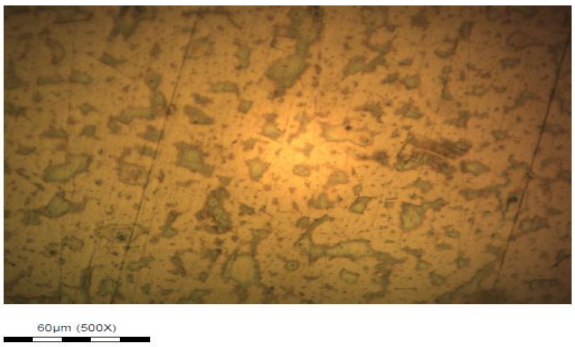

Figure 4.18: OM metallographic microstructure for samples taken from exposed surface of material

Figure 4.19: Samples exposed to 3.5% $NaCl_2$ solution for 168 hours (Foto).

Additionally, the metallographic analysis revealed the presence of twin structures. These features revealed that the microstructure has been undergoes twining to improve the materials mechanical and localized attack. Metallographic analysis highlighted several key features indicative of corrosion and microstructure alterations in the SS304 samples. The presence of small bright spots and black spots on the surface, along with the observed grain

structure and twinning of structure, provides a comprehensive understanding of the material's behavior under corrosive conditions.

Figure 4.19: Image for samples exposed to 3.5%$NaCl_2$ solution for 336 hours(foto).

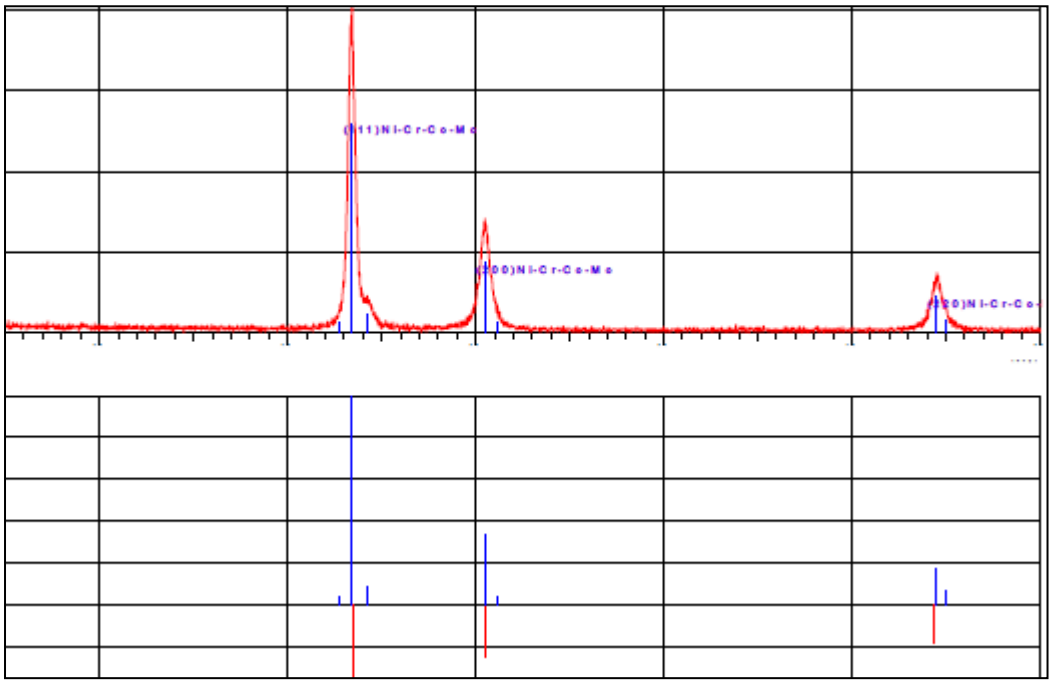

Figure 4.20: XRD data result crystal structure result for samples exposed to 3.5%nacl solution of steam autoclave chamber for 7days.

4.6 Discussion of The Result

4.6.1 Corrosion rate analysis

The investigation into the causes of corrosion on SS304 within a steam autoclave chamber revealed significant differences in corrosion behavior depending on the solution type and exposure conditions. The corrosion rates were assessed by immersing SS304 specimens in pure water, hard water, 0.5% NaCl solution, and 3.5% NaCl solution for durations of 3 days, 5 days, and 7 days at both room temperature and within the steam autoclave.

The corrosion rate analysis indicated minimal weight loss for specimens immersed in pure water and hard water, suggesting these environments are relatively non-aggressive to SS304. In contrast, specimens exposed to NaCl solutions exhibited significantly higher corrosion

rates. This increase was particularly pronounced in the 3.5% NaCl solution, where the corrosive nature of chloride ions accelerated the corrosion process. The immersion time further influenced the corrosion rate, with longer exposure times resulting in greater material loss.

4.6.2 SEM analysis

Surface analysis using Scanning Electron Microscopy (SEM) provided detailed insights into the morphology of the corroded specimens. For samples immersed in the 3.5% NaCl solution, SEM images revealed the initiation of pitting corrosion, characterized by localized pits on the surface. These pits increased in number and depth with prolonged immersion, indicating progressive deterioration of the SS304 surface. Additionally, the formation of a solid surface layer was observed, likely a corrosion product that developed as the immersion time increased.

4.6.3 Microstructure analysis

The microstructure analysis corroborated the SEM findings, showing the presence of pits in the specimens immersed in the 3.5% NaCl solution. The pits were more pronounced after longer immersion times, highlighting the aggressive nature of chloride ions in inducing localized corrosion. The microstructure changes were less significant for specimens exposed to pure water and hard water, consistent with the lower corrosion rates observed in these environments.

4.6.4 XRD analysis

X-ray Diffraction (XRD) analysis was conducted to identify the chemical composition of the corrosion products. The results confirmed the presence of chloride ions (Cl-) in the corrosion oxide layer on specimens immersed in the 3.5% NaCl solution. The hydrous effect, likely due to the steam environment within the autoclave, contributed to the formation of hydrated oxide layers. This finding underscores the role of chloride ions in destabilizing the passive film on SS304, leading to pitting and other forms of localized corrosion.

4.6.5 Analysis of samples from autoclave chamber parts

Additional tests were performed on samples cut from the autoclave chamber body, which had been subjected to operational conditions involving saline solutions. SEM and XRD analyses of these samples revealed the presence of pitting predominantly attributed to chloride ion contamination during the sterilization process. The localized nature of this corrosion suggests that chloride ions were able to penetrate and undermine the protective oxide layer on SS304, facilitating the formation of pits.

4.6.6 Synthesis of findings

The results of this study clearly indicated that chloride ions are a major factor in the corrosion of SS304 within steam autoclave environments. While pure water and hard water exhibit negligible corrosive effects, the presence of $NaCl_2$, especially at higher concentrations, significantly accelerates corrosion. This effect is exacerbated by the high-temperature and high-pressure conditions within the autoclave, which promote the breakdown of the passive film and the formation of localized corrosion sites.

The study's findings have important implications for the use of SS304 in environments where exposure to saline solutions and autoclave conditions is common. To mitigate the risk of corrosion, it is essential to control the chemical composition of the autoclave environment, particularly by minimizing the presence of chloride ions. Implementing regular maintenance and inspection protocols to detect and address early signs of corrosion can further enhance the longevity and reliability of SS304 components in industrial applications.

CHAPTER FIVE:

CONCLUSION AND RECOMMENDATION

5.1 Conclusion

This research investigated the causes of corrosion in 304 stainless steels within a steam autoclave chamber, with a specific focus on the machine at National Veterinary Institute. The study aimed to identify the key factors contributing to corrosion initiation and progression in SS304 under steam autoclave conditions when exposed to various working solution and sodium chloride concentration.

The experimental results demonstrated that chloride ions play a significant role in the corrosion of SS304. Immersion tests in various environments, including pure water, hard water, 0.5% sodium chloride ($NaCl_2$) solution, and 3.5% $NaCl_2$ solution, revealed that the presence of chloride ions notably accelerates the corrosion process. The corrosion rate was found to increase with higher $NaCl_2$ concentrations and longer exposure times at steam autoclave. According to the result from weight loss analysis at higher salinity, such as in a 3.5% NaCl solution, results in increased susceptibility, with a average corrosion rate of 0.0256872 mm/year and a weight loss of 4.32333 mg.

Scanning Electron Microscopy (SEM) and X-ray Diffraction (XRD) analyses provided further insights into the corrosion mechanisms. SEM images showed the initiation and progression of pitting corrosion in samples immersed in 3.5% $NaCl_2$ solution, with more pronounced pits forming over extended immersion periods and exposed to steam conditions in the autoclave chamber. The formation of a solid surface layer on the samples indicated the accumulation of corrosion products due to reaction of chlorine with iron and chromium at the SS304 surface. Microstructures analysis confirmed the presence of pitting corrosion and alterations in the grain structure, while XRD analysis identified the presence of chloride ions, hydrated oxides and carbides6 in the corrosion products.

Additionally, tests on samples cut from the autoclave chamber body revealed evidence of pitting and crevice corrosion due to exposure to saline solutions during sterilization processes. These findings underscore the vulnerability of autoclave components to chloride-induced corrosion.

In conclusion, the research highlights the aggressive nature of chloride ions in promoting corrosion of SS304 in steam autoclave environments and formation of localized pitting corrosion. The result from SEM and OM revealed that localized corrosion affect the surface and form highly depicted pits and trans granular corrosion To mitigate corrosion and

enhance the longevity and reliability of autoclave systems, the following recommendations are proposed; minimize the Use of Chloride-Containing Solutions, Reduce or eliminate the use of saline solutions during sterilization processes to limit chloride ion exposure, Implement Regular Cleaning and Maintenance, Establish routine cleaning protocols to remove chloride residues and other corrosive contaminants from autoclave components, Use of Corrosion Inhibitors, Consider the application of corrosion inhibitors to protect SS304 surfaces from chloride-induced corrosion.

Generally, this study provides valuable insights into the mechanisms and factors influencing corrosion in SS304, offering practical guidance for preventing and mitigating corrosion in steam autoclave systems at the National Veterinary Institute and similar industrial settings.

5.2 Recommendations

Based on the findings of this research, the following recommendations are made for preventing and mitigating corrosion in SS304 within steam autoclave environments:

1. Environmental Control: Limit the use of saline solutions and ensure thorough rinsing and cleaning to remove chloride residues after sterilization processes.
2. Material Selection: Consider using materials with higher corrosion resistance for components exposed to aggressive environments.
3. Protective Coatings: Apply corrosion-resistant coatings to SS304 surfaces to provide an additional barrier against chloride ion penetration.
4. Regular Monitoring: Implement regular monitoring and maintenance schedules to detect early signs of corrosion and perform timely interventions.
5. Water Treatment: Use treated water with low chloride content for steam generation to reduce the risk of chloride-induced corrosion. By adopting these strategies, industries can enhance the durability and safety of their equipment, ensuring reliable operation and compliance with regulatory standards.

REFERENCE

Abdelfatah, A., Raslan, A. M., & Mohamed, L. Z. (2022). Corrosion characteristics of 304 stainless steel in sodium chloride and sulfuric acid solutions. *International Journal of Electrochemical Science*, *17*(4), 220417.

Adeniyi, A. G., Ogunleye, O., Durowoju, M., & Odeyemi, S. (2019). Damaging Profile of SS-304 Crevice Corrosion in Chloride Environments. ABUAD Journal of Engineering Research and Development, 2, 11-9.

Ahmad, Z. (2006). Introduction to corrosion. *Principles of corrosion engineering and corrosion control. Oxford: Butterworth-Heinemann*, *1*, 1-8.

Ajay, A. V., Mohan, S., & Sivapirakasam, S. P. (2021, August). Corrosion behavior of Zn-doped ZrO2 coated AISI 304 stainless steel under simulated marine environment. In AIP Conference Proceedings (Vol. 2352, No. 1, p. 020078). AIP Publishing LLC.

Al Ansari, Dr. Mohammed Saleh. (2023). A Study on Crevice Corrosion on Stainless Steel: Detecting Methods. 911-927.

Alharbi, S. O., Ahmad, S., Gul, T., Ali, I., &Bariq, A. (2024). The corrosion behavior of low carbon steel (AISI 1010) influenced by grain size through microstructural mechanical.Scientific Reports, 14(1), 5098.

Ali, S.; Irfan, M.; Niazi,U.M.; Rani, A.M.A.; Rashedi, A.;Rahman, S.; Khan, M.K.A; Alsaiari,M.A.; Legutko, S.; Petr ˚u, J.; et al.Microstructure and MechanicalProperties of Modified 316L Stainless Steel Alloy for Biomedical Applications Using PowderMetallurgy. Materials 2022, 15, 2822.

Al-Taher, S. A., Ghayad, I. M., Ibrahim, K. M., &Barakat, Y. E. (2014). The effect of pitting corrosion on the fatigue strength of 304 and 316 stainless steel alloys. *Journal of Metallurgical Engineering (ME)*, *3*(1).

Aslam, R., Mobin, M., Zehra, S., &Aslam, J. (2022). A comprehensive review of corrosion inhibitors employed to mitigate stainless steel corrosion in different environments. *Journal of Molecular Liquids*, *364*, 119992.

Aslani, F. and Dehestani, M. (2020). Probabilistic impacts of corrosion on structural failure and performance limits of reinforced concrete beams. Construction and Building Materials, 265, 120316.

BahmaniOskooee, M., HosseinNedjad, S., &Samadi, A. (2018).Effect of copper addition on the microstructure, hardness and antibacterial properties of martensitic stainless steel (410s). Journal of Advanced Materials and Technologies, 7(1), 35-44.

Bansod, A. V., Patil, A. P., Moon, A. P., &Khobragade, N. N. (2016). Intergranular corrosion behavior of low-nickel and 304 austenitic stainless steels. *Journal of Materials Engineering and Performance*, *25*, 3615-3626.

Bearss, J. J., Honnold, S. P., Picado, E. S., Davis, N. M., & Lackemeyer, J. R. (2017). Validation and verification of steam sterilization procedures for the decontamination of biological waste in a biocontainment laboratory. *Applied Biosafety*, *22*(1), 33-37.

Bearss, J. J., Honnold, S. P., Picado, E. S., Davis, N. M., & Lackemeyer, J. R. (2017). Validation and verification of steam sterilization procedures for the decontamination of biological waste in a biocontainment laboratory. *Applied Biosafety*, *22*(1), 33-37.

Boniardi, M. V., &Casaroli, A. (2014). Stainless steels. LucefinSpA.

Cladera, Antoni& Weber, Benedikt&Leinenbach, Christian &Czaderski, Christoph&Shahverdi, Moslem &Motavalli, Masoud. (2014). Iron-based shape memory alloys for civil engineering structures: An overview. Construction and Building Materials. 2014. 281-293. 10.1016/j.conbuildmat.2014.04.032.

Della Rovere, C. A., Alano, J. H., Silva, R., Nascente, P. A. P., Otubo, J., &Kuri, S. E. (2012). Influence of alloying elements on the corrosion properties of shape memory stainless steels. *Materials Chemistry and Physics*, *133*(2-3), 668-673.

Design Guidelines for the Selection and Use of Stainless Steel.Specialty Steel Industry of the United States.Washington, D.C., USA

Dion, M., & Parker, W. (2013). Steam sterilization principles.Pharmaceutical engineering, 33(6), 1-8

Duan, Jiaqi&Farrugia, Didier & Davis, Claire & Li, Zushu. (2021). Effect of impurities on the microstructure and mechanical properties of a low carbon steel.Ironmaking& Steelmaking. 49. 1-7. 10.1080/03019233.2021.1972270.

EchCharqy, Y., Radouani, R., &Essahli, M. (2023). FE modeling of the effect of conductivity in galvanic corrosion between different types of stainless steel and carbon steel in a structure bolted joint. *International Journal of Building Pathology and Adaptation*, *41*(3), 574-587.

Elmquist, R. E., & Hartland, A. (2016). Reference Module in Materials Science and Materials Engineering MATS 01908.

Evaluation of Physico Chemical Water Quality of Bishoftu and Dukam Towns,Ada'a and Sebeta Hawas Districts, Oromia Regional State, EthiopiaDaniel Balcha and Tsehaye Doja

Fayomi, O. S. I., Akande, I. G., & Odigie, S. (2019, December). Economic impact of corrosion in oil sectors and prevention: An overview. In Journal of Physics: Conference Series (Vol. 1378, No. 2, p. 022037). IOP Publishing.

Firmanto, H., &Budhyantoro, A. (2023). Surface Quality And Corrosion Resistance Of 316l Stainless Steel Electropolished Using Phosphoric–Sulfuric Acids. *JurnalRekayasaMesin*, *14*(3), 823-834.

Folkhard, E. (2012). Welding metallurgy of stainless steels.Springer Science & Business Media.

Fontana, M. G., & Greene, N. D. (1967). Corrosion Engineering.

Fontana, Mars G., and Norbert D. Greene (1967). Corrosion Engineering, New York: McGraw-Hill,

Fouda, A. S., Diab, M. A., El-Sonbati, A. Z., & Hassan, S. A. (2017). Evaluation of some organic compounds containing O, N and S atoms as corrosion inhibitors for stainless steel 304 in acid solutions. Int. J. Electrochem. Sci., 12, 5072-5091.

Freire, L., Carmezim, M. J., Ferreira, M. G. S., &Montemor, M. F. (2011). The electrochemical behaviour of stainless steel AISI 304 in alkaline solutions with different pH in the presence of chlorides. *ElectrochimicaActa*, *56*(14), 5280-5289.

Galan, F. L. O. R. E. N. T. I. N. A., Ducu, M. C., Fulger, M. A. N. U. E. L. A., & Negrea, D. A. (2020). Investigation of oxidation behavior of 304l and 310s steels with potential application in supercritical water-cooled nuclear reactors. Rev. Chim, 71, 98-105.

Gardner, L. (2019). Stability and design of stainless steel structures – Review and outlook.Thin-Walled Structures, 141(December 2018), 208–216.

Guide, S. D. (2013). Structural Stainless Steel. American Institute of Steel Construction: Chicago, IL, USA.

Guo, C., Shi, S., Dai, H. *et al.* Effect of Chloride Ion on the Corrosion Behavior of 316L Stainless Steels in Hydrofluoric Acid Solution. *J. of MateriEng and Perform* **33**, 3207–3220 (2024).

Ha, H. Y., Jang, J. H., Lee, T. H., Kim, S. D., Lee, C. H., & Moon, J. (2021). Enhancement of the resistance to localized corrosion of type 304 borated stainless steels through hot rolling. *Corrosion Science*, *192*, 109798.

Han, X., Wei, P., Zhao, Y., Wang, Z., Li, C., Wu, X., & Zhang, H. (2023). Enhanced pitting corrosion resistance of nanostructured AISI 304 stainless steel via pipe inner surface grinding treatment. *Nanomaterials*, *13*(2), 318.

Harsimran, et, al. (2021). Overview of Corrosion and Its Control: a Critical Review. Proceedings on Engineering Sciences, 3(1), 13–24.

Hauser, M., Nitzsche, P., Weidner, A., Henkel, S., Biermann, H., Volkova, O., &Wendler, M. (2023). Effect of Cu addition on solidification, precipitation behavior and mechanical

properties in austenitic CrNi–N stainless steel. Materials Science and Engineering: A, 862, 144422.

He, R. R., Li, M. F., Malomo, B., & Yang, L. (2020). Enhancing corrosion and mechanical properties of 304 stainless steel by depositing and annealing Zr75Cu25 thin-film metallic glass. *Surface and Coatings Technology*, *400*, 126221.

Herath, I., Davies, J., Will, G., Tran, P. A., Velic, A., Sarvghad, M., ...&Yarlagadda, P. K. (2022). Anodization of medical grade stainless steel for improved corrosion resistance and nanostructure formation targeting biomedical applications. *ElectrochimicaActa*, *416*, 140274

Huang, A., Wang, K., Zhao, Y. et al. Effect of Copper Addition on the Formability of 304L Austenitic Stainless Steel. J. of MateriEng and Perform 32, 3563–3570 (2023).

Jian, L., Huanjun, Z., Ke, W., & Xuehui, W. (2015). Corrosion behavior of SS-304 in NaCl solution at different temperatures using electrochemical noise technique. Int. J. Electrochem. Sci, 10, 931-937.

Jian, L., Huanjun, Z., Ke, W., & Xuehui, W. (2015). Corrosion behavior of SS-304 in NaCl solution at different temperatures using electrochemical noise technique. *International Journal of Electrochemical Science*, *10*(1), 931-937.

Jinlei Li, Meihang Du, GuangxinLv, Lin Zhou, Xiuqiang Li, Luca Bertoluzzi, Changhong Liu, Shining Zhu, and Jia Zhu,2018. Interfacial Solar Steam Generation Enables Fast Responsive, Energy-Efficient, and Low-Cost Off-Grid Sterilization, advanced science news

Kamaraj, A., &Erning, J. W. (2020). Susceptibility of 304 stainless steel to crevice corrosion in electrochemically active fluids. *Corrosion*, *76*(4), 424-435.

Karafyllias, G. (2017). The effect of acidity and salinity level in erosion-corrosion performance of metals.

Karki, V. & Singh, M. (2017). Investigation of corrosion mechanism in Type 304 stainless steel under different corrosive environments: A SIMS study. International Journal of Mass Spectrometry, 421, 51–60.

Khalifeh, A. (2020). Stress Corrosion Cracking Behavior of Materials. IntechOpen. doi: 10.5772/intechopen.90893.

Kim, H. P., & Kim, D. J. (2018). Intergranular corrosion of stainless steel. *Corrosion Science and Technology*, *17*(4), 183-192.

Lakkam, K., Kerur, S. M., &Shirahatti, A. (2019, October). Experimental investigation of effect of pitting corrosion on the mechanical properties of 304 grade stainless steel without heat treatment. In *AIP Conference Proceedings* (Vol. 2166, No. 1). AIP Publishing.

Li, H., Yang, X., Yin, X., Wang, X., Tang, J., & Gong, J. (2021). Effect of chloride impurity on corrosion kinetics of stainless steels in molten solar salt for CSP application: experiments and modeling. *Oxidation of Metals*, *95*, 311-332.

Li, K., Sun, L., Cao, W., Chen, S., Chen, Z., Wang, Y., & Li, W. (2022). Pitting corrosion of 304 stainless steel in secondary water supply system. *Corrosion Communications*, *7*, 43-50.

Li, L., Yan, J., Xiao, J., Sun, L., Fan, H., & Wang, J. (2021). A comparative study of corrosion behavior of S-phase with AISI 304 austenitic stainless steel in H2S/CO2/Cl-media. *Corrosion Science*, *187*, 109472.

Liao, J., Tan, J., Wu, X., Ning, D., Xue, G., & Yao, W. (2019). Corrosion fatigue behavior of 304 stainless steel notched specimen in high-temperature pressurized water. Materials Science and Engineering: A, 748, 137-145.

Lin, M. T., Wan, C. H., & Wu, W. (2017). Characterization and corrosion resistance of TiZr coating on SS304 stainless steel using cathodic arc evaporation techniques. *Surface and Coatings Technology*, *320*, 217-225.

Lindell, D., &Pettersson, R. (2015). Crystallographic effects in corrosion of austenitic stainless steel 316L. *Materials and Corrosion*, *66*(8), 727-732.

Liou, H. Y., Tsai, W. T., Pan, Y. T., & Hsieh, R. I. (2001). Effects of alloying elements on the mechanical properties and corrosion behaviors of 2205 duplex stainless steels. Journal of Materials Engineering and performance, 10, 231-241.

Liu, R., Ivanovich, N., Zhu, C., Yeo, Y. P., Wang, X., Seita, M., &Lauro, F. M. (2023). Influence of grain size and crystallographic orientation on microbially influenced corrosion of low-carbon steel in artificial seawater. Materials & Design, 234, 112353.

LP. Karjalainen, T. Taulavuorl, M. Sellman, A. Kyrolainen. (2008). Some Strengthening Methods for Austenitic Stainless Steels.material technology.

Maher, M., Iraola-Arregui, I., Youcef, H. B., Rhouta, B., &Trabadelo, V. (2022). The synergistic effect of wear-corrosion in stainless steels: A review. *Materials Today: Proceedings*, *51*, 1975-1990.

Malik, A. U., Kutty, P. M., Siddiqi, N. A., Andijani, I. N., & Ahmed, S. (1992). The influence of pH and chloride concentration on the corrosion behaviour of AISI 316L steel in aqueous solutions. *Corrosion science*, *33*(11), 1809-1827.

Marcus, P., &Oudar, J. (Eds.). (2002). *Corrosion mechanisms in theory and practice* (pp. 243-286). New York: Marcel Dekker.

Mariani, F. E., Takeya, G. S., Casteletti, L. C., Neto, A. L., & Totten, G. E. (2016). Heat treatment of precipitation-hardening stainless steels alloyed with niobium. *Materials Performance and Characterization*, *5*(1), 38-46.

Marsh, G. N. and Chew, C. (1984). Well man clinic in general practice. In British Medical Journal (Vol. 288, Issue 6412).

McGuire, M. F (2008). Stainless steels for design engineers. Asm International

Md.SohrabHossain, N.N. NikAb.Rahman, V. Balakrishnan, Z.A. Rajion, d.O. Ab.Kadir, Mathematical modeling of Enterococcus faecalis, Escherichia coli, and Bacillus sphaericus inactivation in infectious clinical solid waste by using steam autoclaving and supercritical fluid carbon dioxide sterilization, Chemical Engineering Journal (2014)

Meguid, E. A. E., Mahmoud, N. A., & Gouda, V. K. (1998). Pitting corrosion behaviour of AISI 316L steel in chloride containing solutions. *British corrosion journal*, *33*(1), 42-48

Mohammed Ali, H. B. (2016). *Atmospheric pitting corrosion of stainless steel* (Doctoral dissertation, University of Birmingham).

Mohanty, C. P. (2022). *Corrosion interactions between stainless steel and borosilicate glasses* (Doctoral dissertation, The Ohio State University).

Momeni, M., Esfandiari, M., &Moayed, M. H. (2012). Improving pitting corrosion of 304 stainless steel by electropolishing technique. *Iranian Journal of Materials Science and Engineering*, *9*(4), 34-42.

Montoya, T., Katona, R. M., Karasz, E. K., Taylor, J. M., Snow, J., Bryan, C. R., ...& Schaller, R. F. (2023). Influence of realistic, cyclic atmospheric cycles on the pitting corrosion of austenitic stainless steels. *Journal of The Electrochemical Society*, *170*(4), 041502.

Nair, A. P., Arafat, S., & Vincent, S. (2020). Corrosion characteristics of zinc coated SS304 stainless steel. Materials Today: Proceedings, 28, 1210-1215.

Nele, L., Caggiano, A., & Teti, R. (2016). Autoclave cycle optimization for high performance composite parts manufacturing. *Procedia CIRP*, *57*, 241-246.

Nuthalapati, S., Kee, K., Pedapati, S. R., &Jumbri, K. (2024). A review of chloride induced stress corrosion cracking characterization in austenitic stainless steels using acoustic emission technique. *Nuclear Engineering and Technology*, *56*(2), 688-706.

Oyawale, F.A. and A.E. Olaoye. 2007. “Design and Construction of an Autoclave”. Pacific Journal of Science and Technology. 8(2):224-230.

Painkra, T. K., Naik, K. S., Nishad, R. K., Sen, P. K., &Bohidar, S. K. (2014). Review about high performance of Austenitic Stainless Steel. Int. J. Innov. Res. Sci. Technol, 1, 93-99.

Palanisamy, D., Senthil, P., &Senthilkumar, V. (2016). The effect of aging on machinability of 15Cr-5Ni precipitation hardened stainless steel. *Archives of Civil and Mechanical Engineering*, *16*, 53-63.

Parangusan, H., Bhadra, J., & Al-Thani, N. (2021). A review of passivity breakdown on metal surfaces: Influence of chloride-and sulfide-ion concentrations, temperature, and pH. *Emergent Materials*, *4*(5), 1187-1203.

Pedapati, S. R. I. N. I. V. A. S. A. R. A. O., Nuthalapati, S. U. R. E. S. H., & KEE, K. Detection and characterization of chloride induced stress corrosion cracking on SS304 under perlite thermal insulation. *Materials Research Foundations*, *29*.

PER HAMLIN,2012. Modeling of Generation and Distribution of Steam in an Autoclave, Department of Chemical and Biological Engineering Chalmers University of Technology SE-412 96 Göteborg, Sweden

Piere, R. R. (2008). Corrosion Engineering-Principles and Practice.

Practical Guidelines for the Fabrication of Austenitic Stainless Steels, e International Molybdenum Association (IMOA),2020, London, UK

Puspalata, R., Chandran, S., Veena, S., & Krishna Mohan, T. V. (2022). Chemistry conditions and corrosion behaviour in simulated crevices of alloy steel. *Corrosion Engineering, Science and Technology*.

Raghavan, V., & Antia, D. P. (1994). The chromium equivalents of selected elements in austenitic stainless steels. *Metallurgical and Materials transactions A*, *25*, 2675-2681.

Rahman, T., Ebert, W. L., & Indacochea, J. E. (2018). Effect of molybdenum additions on the microstructures and corrosion behaviours of 316L stainless steel-based alloys. *Corrosion Engineering, Science and Technology*, *53*(3), 226-233.

Ravitej, S. V., Murthy, M., &Krishnappa, M. (2018). Review paper on optimization of process parameters in turning Custom 465® precipitation hardened stainless steel. Materials Today: Proceedings, 5(1), 2787-2794.

Raymond G. Lewis, 2002. Practical Guide to Autoclave Validation, pharmaceutical engineering

Ress, J., Monrrabal, G., Díaz, A., Pérez-Pérez, J., Bastidas, J. M., & Bastidas, D. M. (2020). Microbiologically influenced corrosion of welded AISI 304 stainless steel pipe in well water. *Engineering Failure Analysis*, *116*, 104734.

Revie, R. W. (2008). *Corrosion and corrosion control: an introduction to corrosion science and engineering*. John Wiley & Sons.

Rosidah, A. A., Setyowati, V. A., Suheni, S., & Rijayanto, R. (2021). The effect of time variation on the steels corrosion rate in 0.5 M H2SO4 solution. Journal of Mechanical Engineering, Science, and Innovation, 1(2), 49-55.

Rutala, W.A., & Weber, D. J. (2019).Guideline for disinfection and sterilization in healthcare facilities, 2008. Update: May 2019

Saefuloh, I., Kanani, N., Ramadhan, F. G., Rukmayadi, Y., Yusuf, Y., Abdullah, S., &Susilo, S. (2020, March). The study of corrosion behavior and hardness of AISI stainless steel 304 in concentration of chloride acid solution and temperature variations. In *Journal of Physics: Conference Series* (Vol. 1477, No. 5, p. 052058). IOP Publishing.

Saefuloh, I., Kanani, N., Ramadhan, F. G., Rukmayadi, Y., Yusuf, Y., Abdullah, S., & Susilo, S. (2020, March). The study of corrosion behavior and hardness of AISI stainless steel 304 in concentration of chloride acid solution and temperature variations. In Journal of Physics: Conference Series (Vol. 1477, No. 5, p. 052058). IOP Publishing.

Saefuloh, Iman, Nufus Kanani, F. Gumelar Ramadhan, Y. Rukmayadi, Y. Yusuf, Syarif Abdullah, and Sidik Susilo. "The study of corrosion behavior and hardness of AISI stainless steel 304 in concentration of chloride acid solution and temperature variations." In *Journal of Physics: Conference Series*, vol. 1477, no. 5, p. 052058. IOP Publishing, 2020.

Salas, B. V., & Wiener, M. S. (2009). Corrosion engineering: principles and practice. *Corrosion Engineering, Science, and Technology*, *44*(1), 8.

Salimon, A. I., Statnik, E. S., Kan, Y., Yanushevich, O. O., Tsarev, V. N., Podporin, M. S., ... &Korsunsky, A. M. (2022). Comparative study of biomaterial surface modification due to subcritical CO2 and autoclave disinfection treatments.The Journal of Supercritical Fluids, 191, 105789.

Sanchez, R. G., Huang, X., & Liu, P. (2018). Effect of water density/pressure on the corrosion behavior of 304 and 310 stainless steels. Oxidation of Metals, 89(1), 165-182.

Sandle, T. (2013). Sterility, sterilisation and sterility assurance for pharmaceuticals: technology, validation and current regulations. Elsevier

Schweitzer, P. A (1996). Corrosion engineering handbook.

Schweitzer, P. A. (2013). Fundamentals of Corrosion-Mechanisms, Causes, and Preventative Methods.In Journal of Chemical Information and Modeling (Vol. 53, Issue 9).

Schweitzer, P.E.,.P.A.(2009).Fundamentals of Corrosion: Mechanisms, Causes, and Preventative Methods (1st ed.). CRC Press. https://doi.org/10.1201/9781420067712

Shit, G., Mariappan, K., &Ningshen, S. (2023). Improvement of sensitization and intergranular corrosion of AISI type 304L stainless steel through thermo-mechanical treatment. *Corrosion Science*, *213*, 110975.

Shit, G., Mariappan, K., &Ningshen, S. (2023). Improvement of sensitization and intergranular corrosion of AISI type 304L stainless steel through thermo-mechanical treatment. *Corrosion Science*, *213*, 110975.

Shoemaker, L. E., & Crum, J. R. (2000). Nickel-chromium-molybdenum superalloys: the solution to corrosion problems in wet limestone FGD air pollution control systems. Special Metals Corporation, 3200.

ShovaNeupane et al 2022. Can We Enhance Passivity with a Surface Finish? Spectroscopic and Electrochemical Analysis on 316L Stainless Steel, J. Electrochem. Soc. 169 011505

Simionescu, N. L., &Benea, L. (2017). The corrosion behavior of 316L stainless steel in different simulated body fluids solutions. *International Multidisciplinary Scientific GeoConference: SGEM*, *17*, 353-360.

Singh, A. K. (2020). Microbially Induced Corrosion and its Mitigation.

Singh, R., Chattoraj, I., Kumar, A. *et al.* The effects of cold working on sensitization and intergranular corrosion behavior of AISI 304 stainless steel. *Metall Mater Trans A* **34**, 2441–2447 (2003).

Soleimani, M., Mirzadeh, H., &Dehghanian, C. (2020). Effect of grain size on the corrosion resistance of low carbon steel. Materials Research Express, 7(1), 016522.

Spisák, Bernadett&Szávai, Szabolcs. (2019). Mechanisms of Stress Corrosion Cracking. 10.26649/musci.2019.052.

Tan, J., Zhang, Z., Zheng, H., Wang, X., Gao, J., Wu, X., ... & Huang, P. (2020). Corrosion fatigue model of austenitic stainless steels used in pressurized water reactor nuclear power plants. Journal of Nuclear Materials, 541, 152407.

Tuthill, A. H., & Covert, R. A. (2000). Stainless steels: an introduction to their metallurgy and corrosion resistance. *Dairy Food Environ San*, *20*, 506-517.

Ul-Hamid A, Saricimen H, Quddus A, Mohammed AI, Al-Hems LM. Corrosion study of SS304 and SS316 alloys in atmospheric, underground and seawater splash zone in the Arabian Gulf. *Corrosion Engineering, Science and Technology*. 2017;52(2):134-140.

Ul-Hamid, A., Saricimen, H., Quddus, A., Mohammed, A. I., & Al-Hems, L. M. (2017). Corrosion study of SS304 and SS316 alloys in atmospheric, underground and seawater splash zone in the Arabian Gulf. Corrosion Engineering, Science and Technology, 52(2), 134-140.

Users guide stainless steel, steel and tube.newzland stainless steel development association(2013).Retrived from www.steelandtube.co.nz

Villegas-Tovar, J., Gaona-Tiburcio, C., Lara-Banda, M., Maldonado-Bandala, E., Baltazar-Zamora, M. A., Cabral-Miramontes, J., ... & Almeraya-Calderón, F. (2023). Electrochemical corrosion behavior of passivated precipitation hardening stainless steels for aerospace applications. *Metals*, *13*(5), 835.

Wang, S. G., Sun, M., & Long, K. (2012). The enhanced even and pitting corrosion resistances of bulk nanocrystalline steel in HCl solution. *steel research international*, *83*(8), 800-807.

Wang, Z., Li, H., Shen, Q., Liu, W., & Wang, Z. (2018). Nano-precipitates evolution and their effects on mechanical properties of 17-4 precipitation-hardening stainless steel.ActaMaterialia, 156, 158-171.

Was, G. S., &Ukai, S. (2019). Austenitic stainless steels.Structural alloys for nuclear energy applications, 293-347

Weidmann, E., Guesnier, A., & Taylor, B. (2005). Metallographic preparation of stainless steel.

Xiaojia Yang, M. L. (2020). Failure analysis of a 304 stainless steel heat exchanger in liquid sulfur recovery units.

Xiong, Y., Yue, Y., Lu, Y., He, T., Fan, M., Ren, F., & Cao, W. (2018). Cryorolling impacts on microstructure and mechanical properties of AISI 316 LN austenitic stainless steel. *Materials Science and Engineering: A*, *709*, 270-276.

Ye, D., Li, J., Jiang, W., Su, J., & Zhao, K. (2012). Effect of Cu addition on microstructure and mechanical properties of 15% Cr super martensitic stainless steel. Materials & Design, 41, 16-22.

Yuan, J., Huang, M., Li, Y., Wang, L., Li, H., & Xu, W. (2023). Revealing the grain size-dependent twinning variants and the associated strengthening mechanisms in a carbon-free austenitic steel. *Materials Science and Engineering: A*, *864*, 144577.

Zaffora, A., Di Franco, F., & Santamaria, M. (2021). Corrosion of stainless steel in food and pharmaceutical industry. *Current Opinion in Electrochemistry*, *29*, 100760.

Zeng, Q., Khanlari, K., & Lin, N. (2021). An investigation on the possibility to improve the corrosion and cavitation resistance of SS304 steel by NiTi coatings. *International Journal of Modern Physics B*, *35*(04), 2150057.

Zhang, J., Ju, P., Wang, C., Dun, Y., Zhao, X., Zuo, Y., & Tang, Y. (2019). Corrosion Behaviour of 316L Stainless Steel in Hot Dilute Sulphuric Acid Solution with Sulphate and NaCl. *Protection of Metals and Physical Chemistry of Surfaces*, *55*, 148-156.

Zhou, T., Babu, R. P., Odqvist, J., Yu, H., &Hedström, P. (2018). Quantitative electron microscopy and physically based modelling of Cu precipitation in precipitation-hardening martensitic stainless steel 15-5 PH. Materials & Design, 143, 141-149.

APPENDICES:

APPENDICES 1: SAS Software ANOVA Tables for Corrosion Rate

1. ANOVA for effect of Solution Type, Condition and Exposure Time on the on the Weight loss of SS304

SV	DF	SS	MS	F	Pr > F
Model	23	374.9081715	16.3003553	430.80	<.0001
Error	48	1.8162015	0.0378375		
Corrected Total	71	376.7243730			

2. ANOVA for interaction effect of Solution Type, Condition and Exposure Time on the Weight loss of SS304

SV	DF	SS	MS	F	Pr > F
Condition	1	58.8205695	58.8205695	1554.56	<.0001
Exposure Time	2	5.8742217	2.9371108	77.62	<.0001
Solution Type	3	215.0275508	71.6758503	1894.31	<.0001
Condition* Exposure Time	2	2.5991423	1.2995712	34.35	<.0001
Solution_T*Condition	3	84.6778096	28.2259365	745.98	<.0001
Solution_*Exposure_T	6	6.1057078	1.0176180	26.89	<.0001
Soluti*Condit*Exposu	6	1.8031697	0.3005283	7.94	<.0001

3. ANOVA for effect of Solution Type, Condition and Exposure Time on the on the Corrosion rate of SS304

SV	DF	SS	MS	F	Pr > F
Model	23	0.01336705	0.00058118	492.65	<.0001
Error	48	0.00005663	0.00000118		
Corrected Total	71	0.01342368			

\

4. ANOVA for interaction effect of Solution Type, Condition and Exposure Time on the Corrosion rate of SS304

SV	DF	SS	MS	F	Pr > F
Condition	1	0.00205301	0.00205301	1740.28	<.0001
Exposure Time	2	0.00014003	0.00007002	59.35	<.0001
Solution Type	3	0.00761622	0.00253874	2152.02	<.0001
Condition* Exposure Time	2	0.00004927	0.00002464	20.88	<.0001
Solution_T*Condition	3	0.00304451	0.00101484	860.25	<.0001
Solution Type*Exposure_T	6	0.00028709	0.00004785	40.56	<.0001
Soluti*Condit*Exposu	6	0.00017692	0.00003832	24.99	<.0001

APPENDIX 2. Samples Elemental Compositions

1 Result of element composition analysis for samples employed in immersion and exposed to steam autoclave conditions.

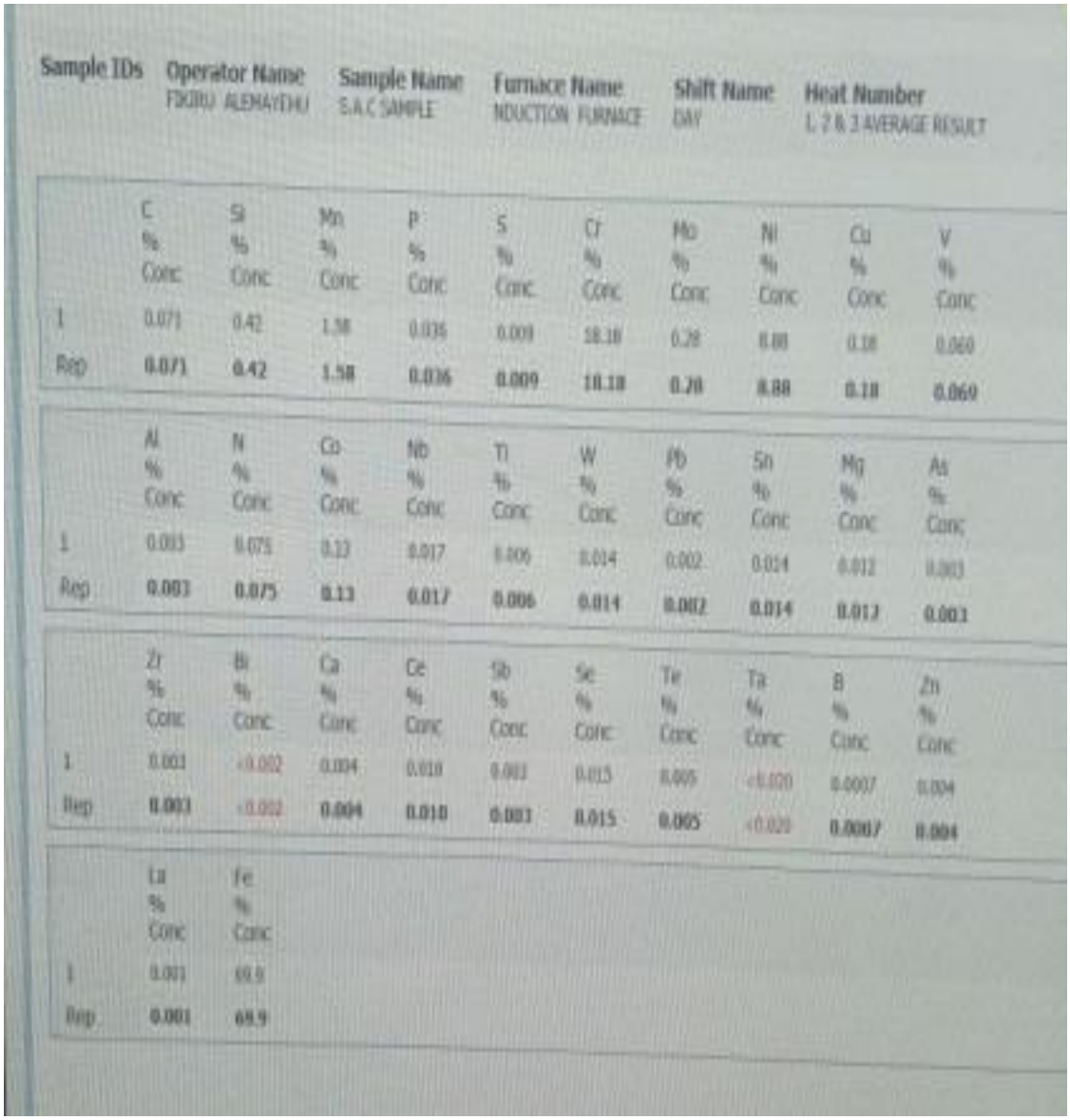

Sample IDs	Operator Name	Sample Name	Furnace Name	Shift Name	Heat Number
	FIKIRU ALEMAYEHU	S.A.C SAMPLE	INDUCTION FURNACE	DAY	1, 2 & 3 AVERAGE RESULT

	C % Conc	Si % Conc	Mn % Conc	P % Conc	S % Conc	Cr % Conc	Mo % Conc	Ni % Conc	Cu % Conc	V % Conc
1	0.071	0.42	1.58	0.036	0.009	18.18	0.28	0.88	0.18	0.060
Rep	**0.071**	**0.42**	**1.58**	**0.036**	**0.009**	**18.18**	**0.28**	**0.88**	**0.18**	**0.060**

	Al % Conc	N % Conc	Co % Conc	Nb % Conc	Ti % Conc	W % Conc	Pb % Conc	Sn % Conc	Mg % Conc	As % Conc
1	0.003	0.075	0.13	0.017	0.006	0.014	0.002	0.014	0.012	0.003
Rep	**0.003**	**0.075**	**0.13**	**0.017**	**0.006**	**0.014**	**0.002**	**0.014**	**0.013**	**0.003**

	Zr % Conc	Bi % Conc	Ca % Conc	Ce % Conc	Sb % Conc	Se % Conc	Te % Conc	Ta % Conc	B % Conc	Zn % Conc
1	0.003	<0.002	0.004	0.010	0.003	0.015	0.005	<0.020	0.0007	0.004
Rep	**0.003**	<0.002	**0.004**	**0.010**	**0.003**	**0.015**	**0.005**	<0.020	**0.0007**	**0.004**

	La % Conc	Fe % Conc
1	0.001	69.9
Rep	**0.001**	**69.9**

2. Element composition of materials cutout of steam autoclave chamber component

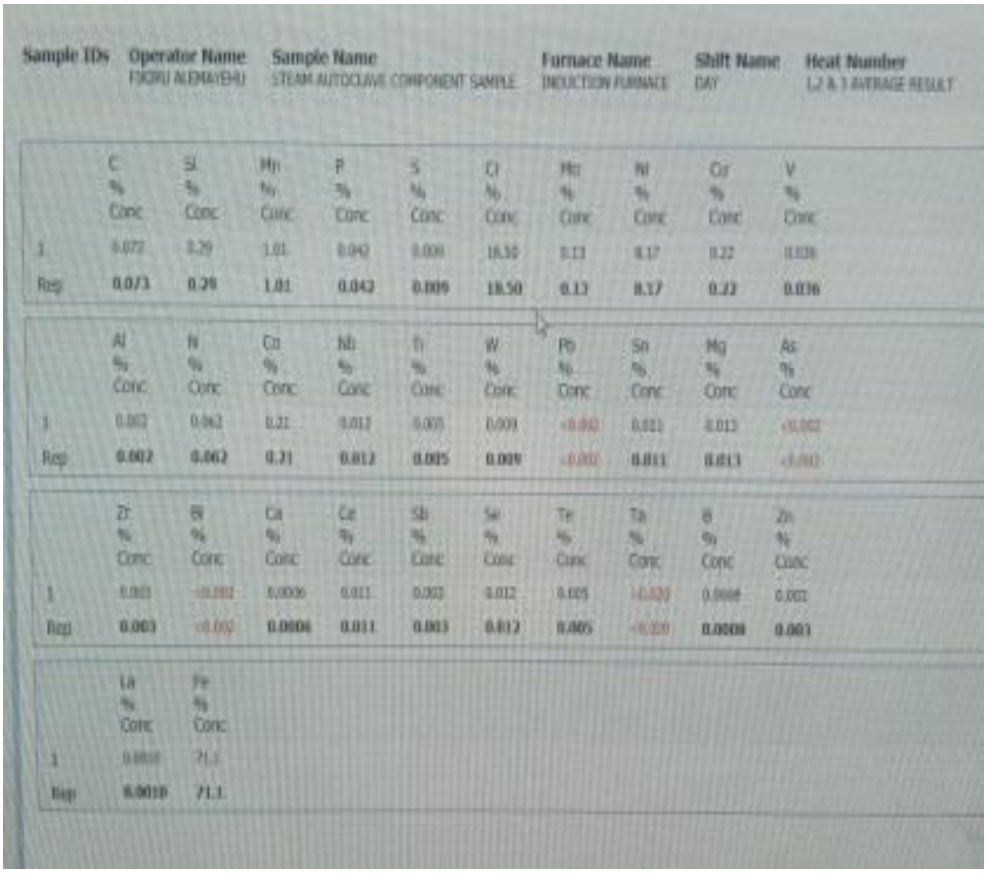

Sample IDs	Operator Name	Sample Name	Furnace Name	Shift Name	Heat Number
	FIDORU ALEMAYEHU	STEAM AUTOCLAVE COMPONENT SAMPLE	INDUCTION FURNACE	DAY	L2 & 3 AVERAGE RESULT

	C % Conc	Si % Conc	Mn % Conc	P % Conc	S % Conc	Cr % Conc	Mo % Conc	Ni % Conc	Cu % Conc	V % Conc
1	0.072	0.29	1.01	0.040	0.009	18.50	0.13	0.17	0.22	0.038
Rep	**0.073**	**0.29**	**1.01**	**0.042**	**0.009**	**18.50**	**0.13**	**0.17**	**0.22**	**0.036**

	Al % Conc	N % Conc	Co % Conc	Nb % Conc	Ti % Conc	W % Conc	Pb % Conc	Sn % Conc	Mg % Conc	As % Conc
1	0.002	0.062	0.21	0.012	0.005	0.009	<0.002	0.011	0.013	<0.002
Rep	**0.002**	**0.062**	**0.21**	**0.012**	**0.005**	**0.009**	<0.002	**0.011**	**0.013**	<0.002

	Zr % Conc	Bi % Conc	Ca % Conc	Ce % Conc	Sb % Conc	Se % Conc	Te % Conc	Ta % Conc	B % Conc	Zn % Conc
1	0.003	<0.002	0.0006	0.011	0.003	0.012	0.005	<0.020	0.0008	0.002
Rep	**0.003**	<0.002	**0.0006**	**0.011**	**0.003**	**0.012**	**0.005**	<0.020	**0.0008**	**0.003**

	La % Conc	Fe % Conc
1	0.0010	71.1
Rep	**0.0010**	**71.1**

APPENDIX 3: Samples Hardness Test Results

1.

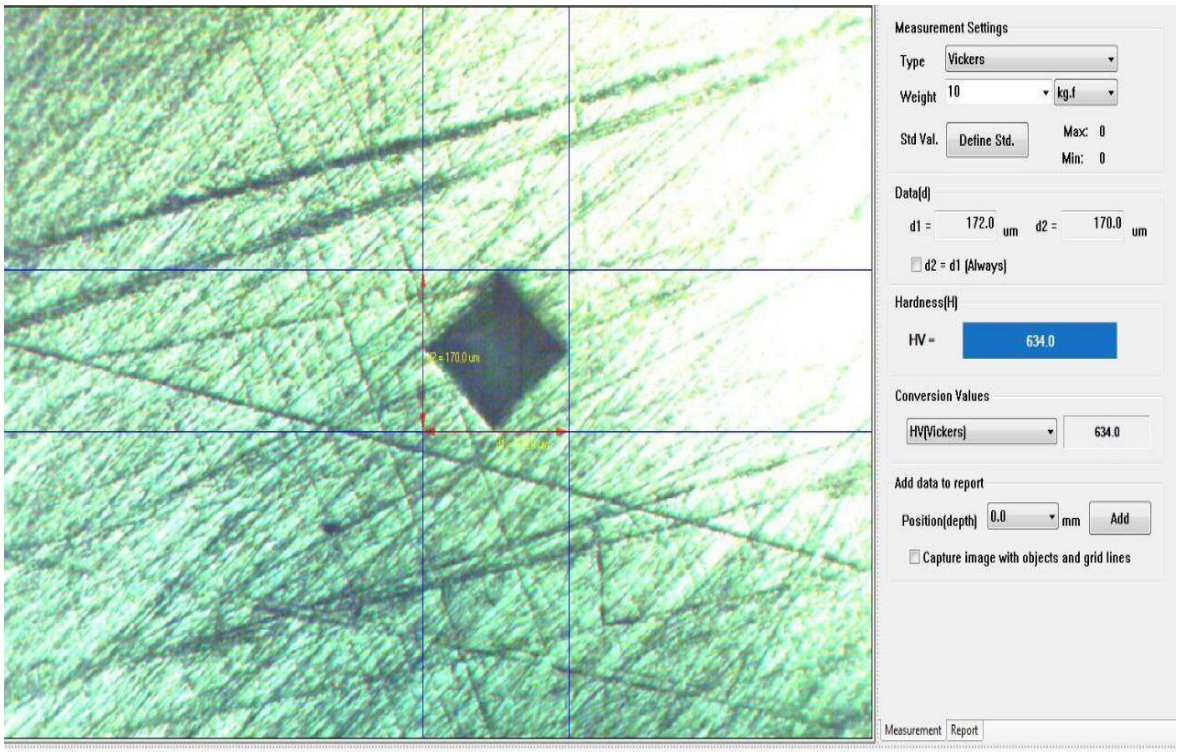

2.

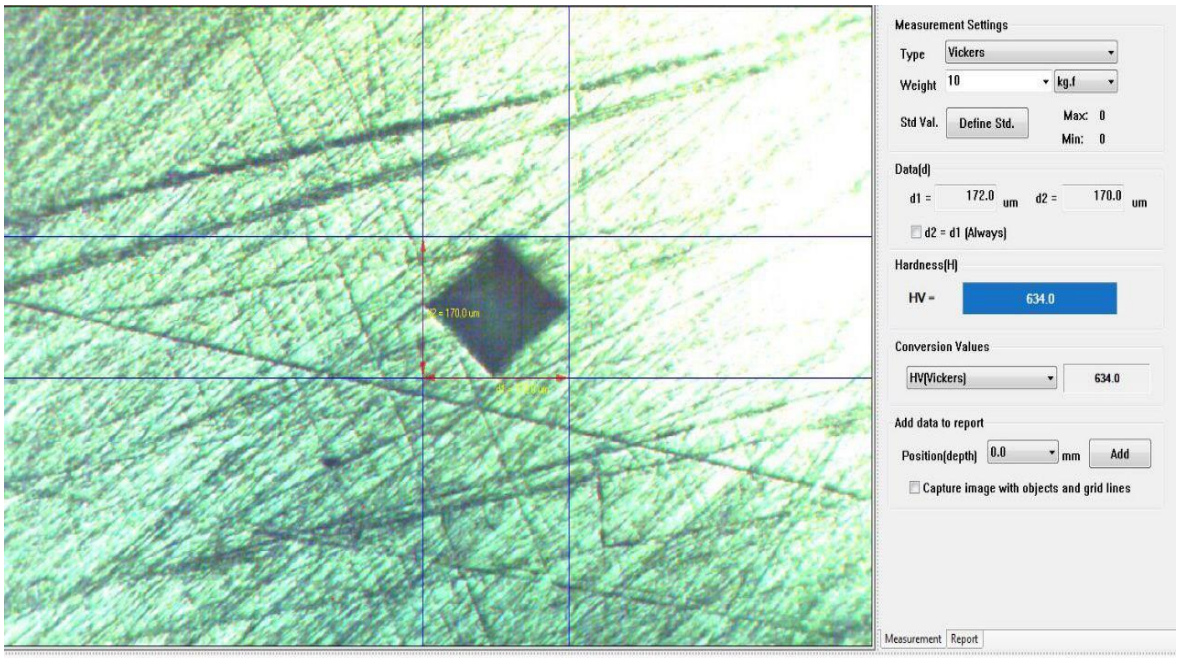

3.

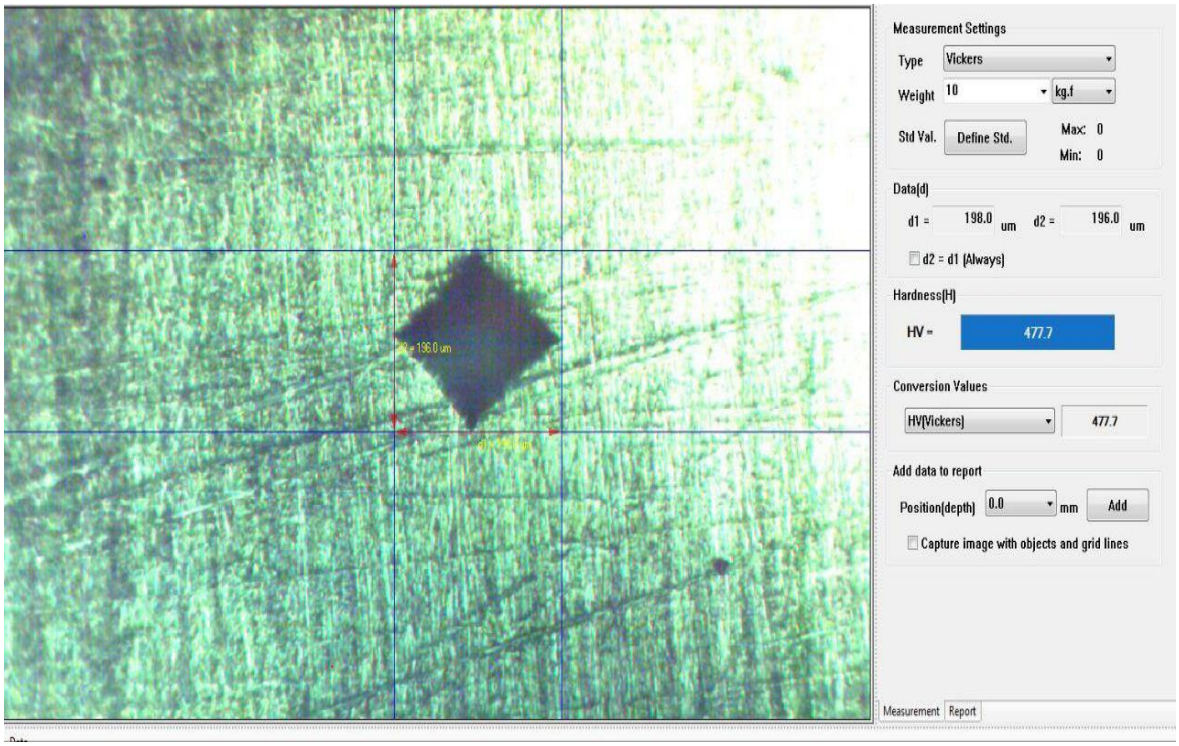
Measurement Settings
Type
Vickers
Weight
10
kg.f
Std Val.
Define Std.
Max: 0
Min: 0
Data[d]
d1 = 198.0 um
d2 = 196.0 um
d2 = d1 (Always)
Hardness[H]
HV =
477.7
Conversion Values
HV(Vickers)
477.7
Add data to report
Position(depth)
0.0
mm
Add
Capture image with objects and grid lines
Measurement
Report

5.

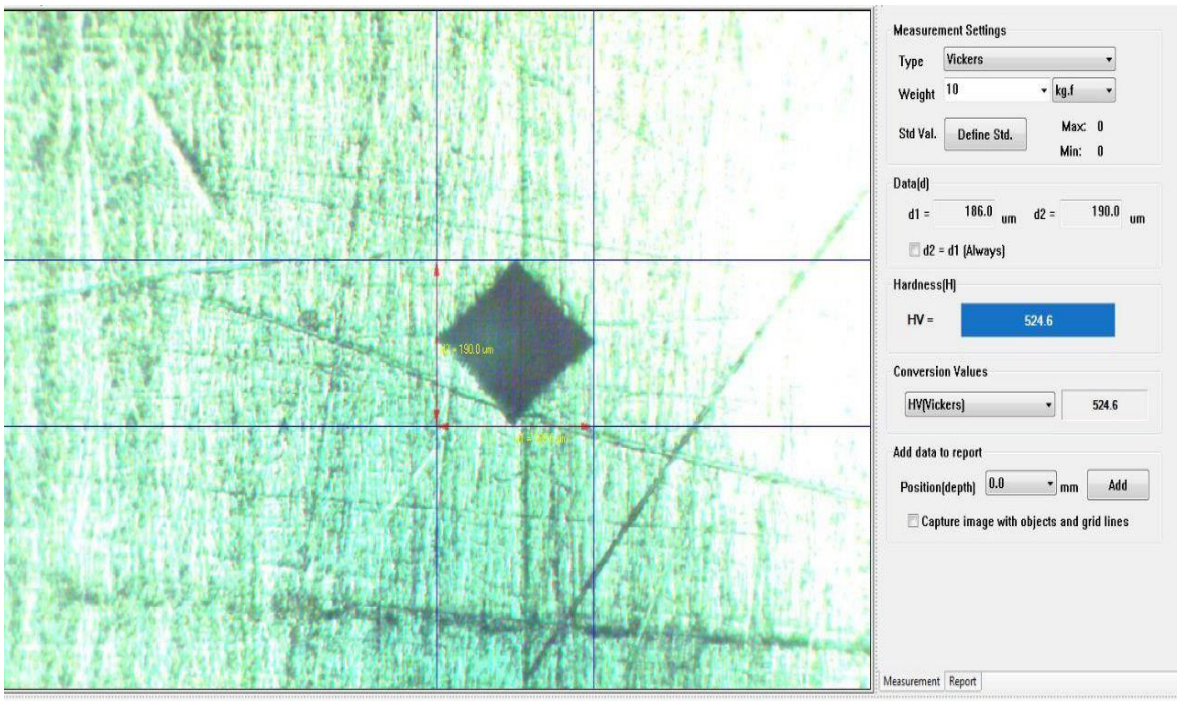
Measurement Settings
Type
Vickers
Weight
10
kg.f
Std Val.
Define Std.
Max: 0
Min: 0
Data[d]
d1 = 186.0 um
d2 = 190.0 um
d2 = d1 (Always)
Hardness[H]
HV =
524.6
Conversion Values
HV(Vickers)
524.6
Add data to report
Position(depth)
0.0
mm
Add
Capture image with objects and grid lines
Measurement
Report

APPENDIX 4: Microstructure Images

1.

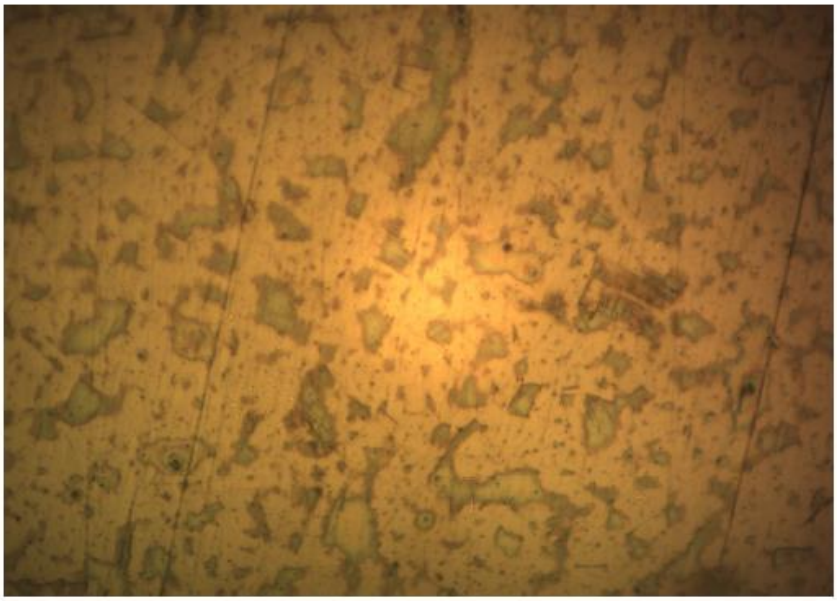

2.

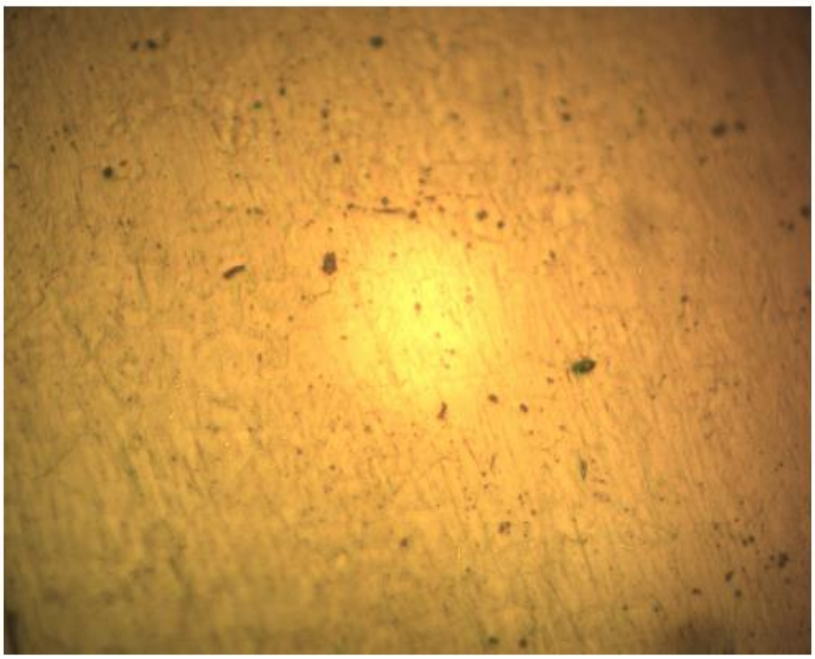

3.

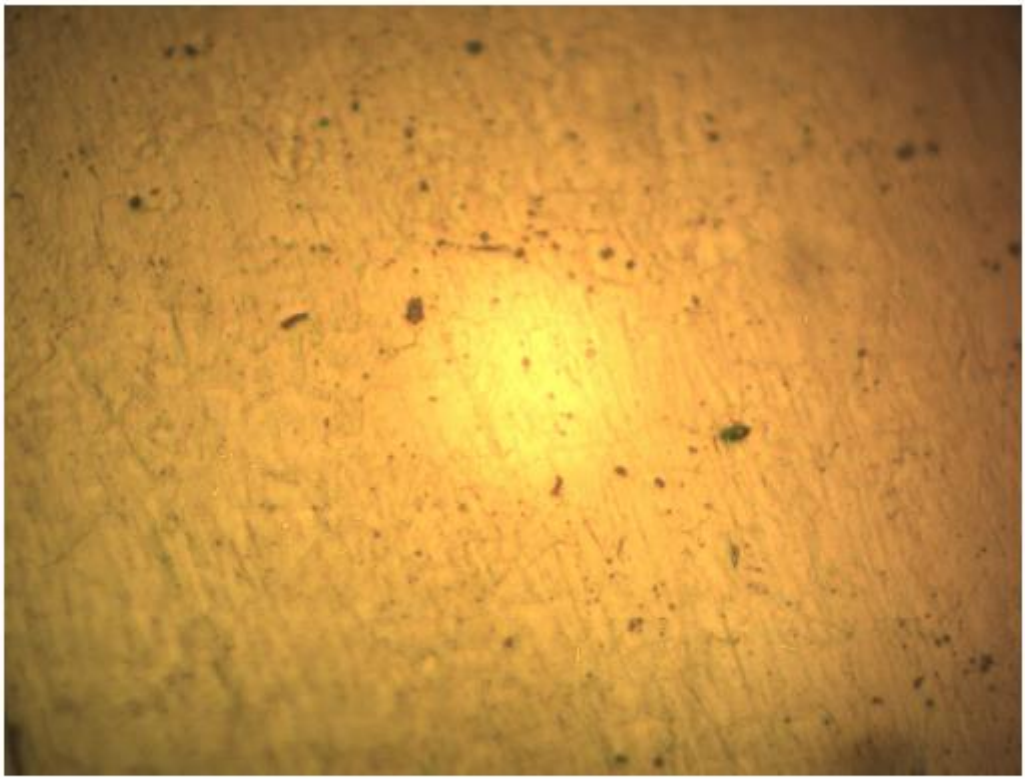

60µm (500X)

APPENDIX 5: SEM Image

1. Samples taken from the corroded surface of autoclave chamber

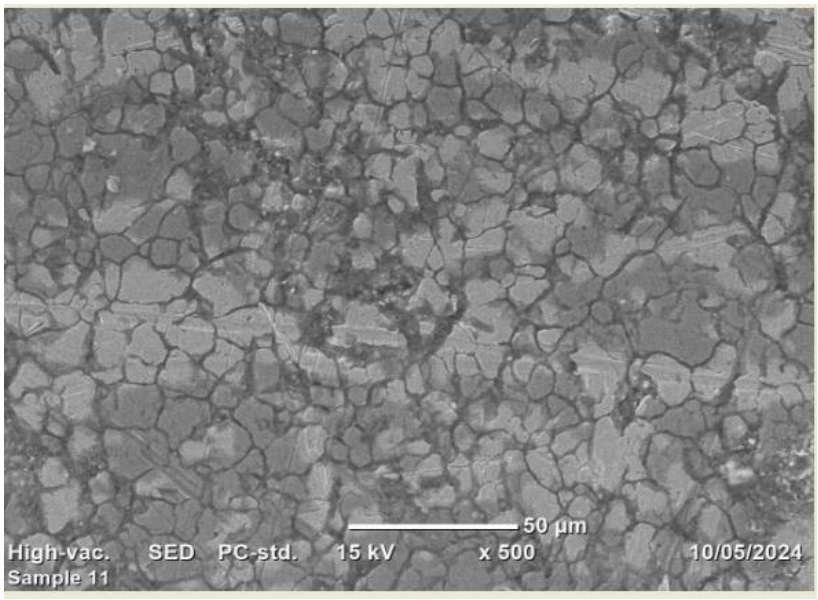

4. Immersion in 3.5%nacl for 168hours at room conditions

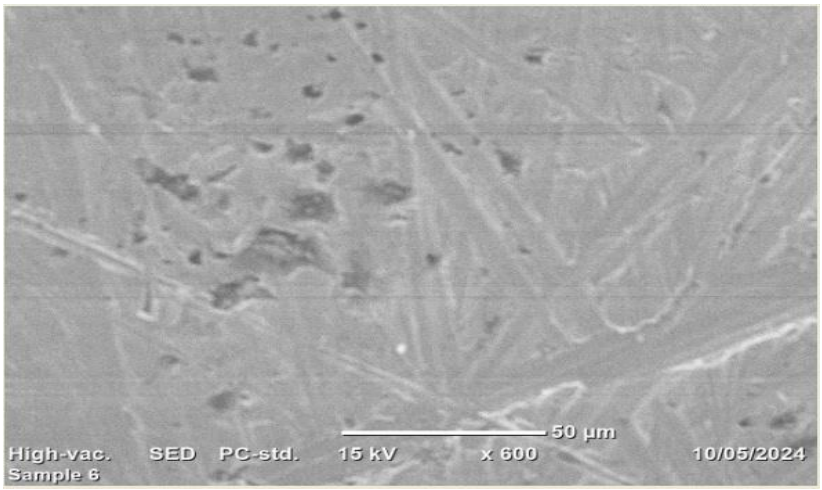

3. Samples exposed to 3.5% nacl solution for 168 hours at steam autoclave